

SpiderFab™ : Process for On-Orbit Construction of Kilometer-Scale Apertures

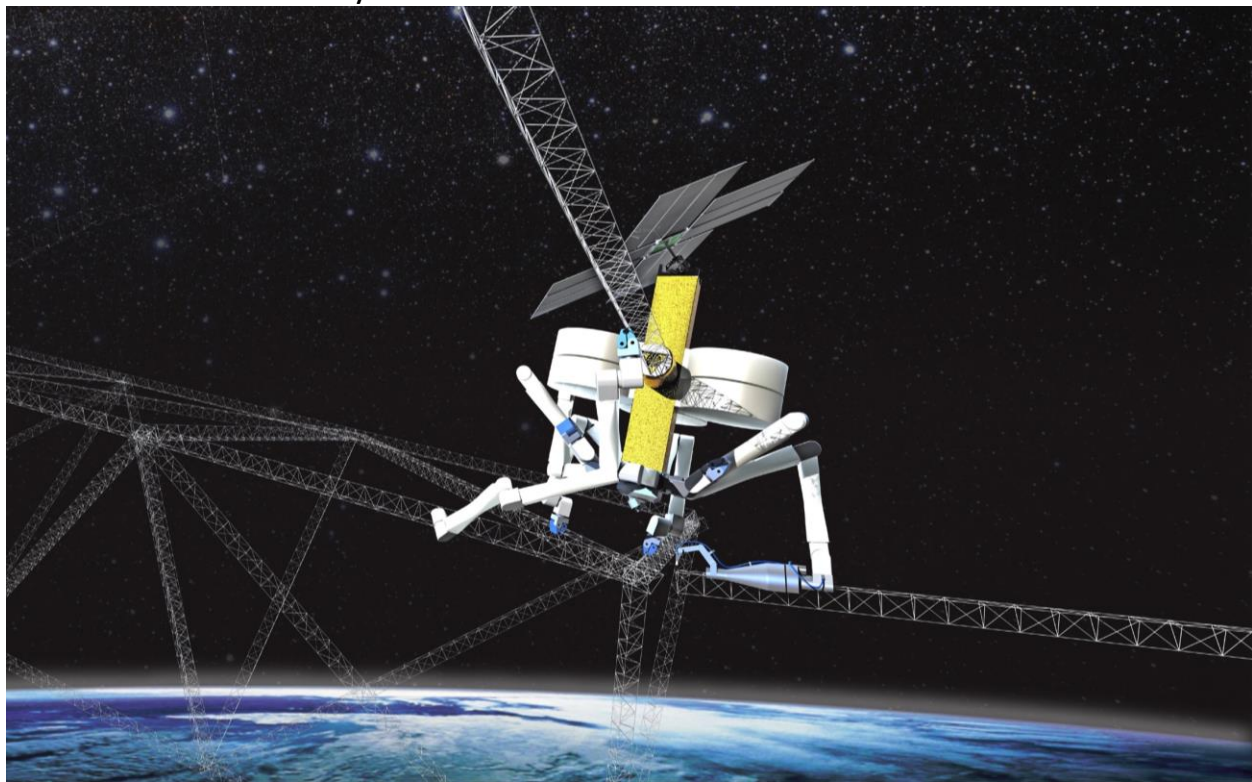
Authors: Robert Hoyt, Jesse Cushing, Greg Jimmerson, Jeffrey Slostad, Robert Dyer, Steve Alvarado

Tethers Unlimited, Inc.
11711 N. Creek Pkwy S., Suite D113
Bothell, WA 98011

Final Report
Report Date:
29 February 2016

Period of Performance:
1 Oct 2013 – 30 January 2016

Grant # NNX13AR26G



Sponsored By:



NASA Innovative Advanced Concepts (NIAC)
NASA Goddard Space Flight Center
8800 Greenbelt Road
Greenbelt, MD 20771

TABLE OF CONTENTS

SF 298 ERROR! BOOKMARK NOT DEFINED.

TABLE OF CONTENTS 2

1. INTRODUCTION 3

1.1 SUMMARY 3

1.2 BACKGROUND: SPIDERFAB PHASE I RESULTS 3

 1.2.1 *SpiderFab Architecture*..... 3

 1.2.2 *SpiderFab Technology Maturation Plan* 4

1.3 BACKGROUND: TRUSSELATOR SBIR..... 5

1.4 SPIDERFAB PHASE II WORK PLAN 6

2. PHASE II ACCOMPLISHMENTS 7

2.1 DEVELOPMENT OF TOOLS FOR IN-SPACE MANUFACTURE AND ASSEMBLY OF STRUCTURES 7

 2.1.1 *SpiderFab Joiner Spinneret Process Development* 7

 2.1.2 *SpiderFab Joiner Spinneret Prototype Development* 14

 2.1.3 *SpiderFab Joiner Spinneret Prototype Vacuum Testing*..... 15

 2.1.4 *SpiderFab Joiner Spinneret Engineering Model* 16

 2.1.5 *SpiderFab Pultrusion Spinneret Tool*..... 18

 2.1.6 *2nd Order Truss Assembly Demonstration*..... 19

2.2 DEVELOPMENT OF ROBOTICS METHODS FOR ASSEMBLY OF SPACE STRUCTURES 21

 2.2.1 *Overview* 21

 2.2.2 *Baxter Robot* 21

 2.2.3 *SpiderFab Robotic Vision System* 21

 2.2.4 *SpiderFab Robotics Testing Software Platform* 33

 2.2.5 *Custom End Effector*..... 37

 2.2.6 *Truss Assembly Demonstrations* 38

2.3 DEMONSTRATION MISSION CONCEPT DESIGNS 45

 2.3.1 *MakerSat-I: Long-Baseline Sensor Mission Concept*..... 45

 2.3.2 *MakerSat-II: Constructable™ Antenna Demonstration Mission* 47

3. OUTREACH AND TRANSITION EFFORTS 48

3.1 OUTREACH 48

3.2 TRANSITION SUCCESSES 49

CONCLUSIONS 49

Appendix A – Spiderfab Joiner Head Configuration Trade Study A1

Appendix B – Spiderfab: An Architecture For Self-Fabricating Space Systems B1

Appendix C – Makersat: In-Space Additive Manufacturing Of Constructable™ Long-Baseline Sensors C1

Appendix C – Spiderfab Presentation D1

1. INTRODUCTION

1.1 SUMMARY

The SpiderFab effort has investigated the value proposition and feasibility of radically changing the way we build and deploy spacecraft by enabling space systems to fabricate and integrate key components on-orbit. In this Phase II effort, we have focused on developing and demonstrating tools and processes to enable robotic systems to manufacture and assemble high-performance structural elements that will serve as the support structures for components such as antennas and solar arrays. Through testing of these technologies in the laboratory environment, these efforts have established the technical feasibility of the key capabilities required for in-space manufacture of large apertures such as antennas, solar arrays, and optical systems, maturing prototype technical solutions for these capabilities to TRL-4. The SpiderFab effort has resulted in **successful post-NIAC transition** of the technology, first to SBIR-funded development of a technology for in-space manufacture (ISM) of truss structures, and then to a NASA/STMD-Tipping Point Technologies funded effort to prepare a flight demonstration of ISM of a structure for a GEO communications satellite.

1.2 BACKGROUND: SPIDERFAB PHASE I RESULTS

1.2.1 SpiderFab Architecture

In the Phase I we developed an architecture for a “SpiderFab” system that integrates additive manufacturing techniques with robotic assembly to enable in-space manufacturing of large apertures. We identified the key capabilities required to implement this architecture and detailed two concept implementations of this architecture, one a mobile robotic system, illustrated in Figure 1, capable of manufacturing spacecraft components such as antenna reflectors, and the second a palletized payload designed to assemble large solar arrays, as illustrated in Figure 2.

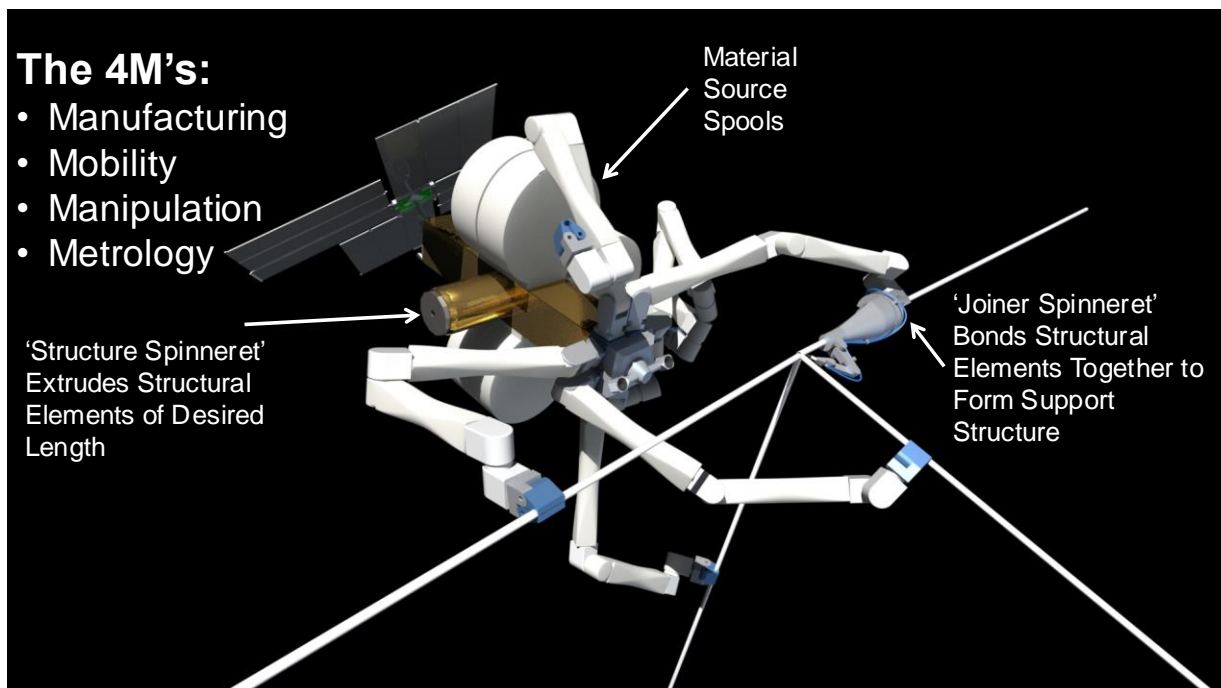


Figure 1. Concept for a 'SpiderFab Bot' for in-space manufacture of large support structures.

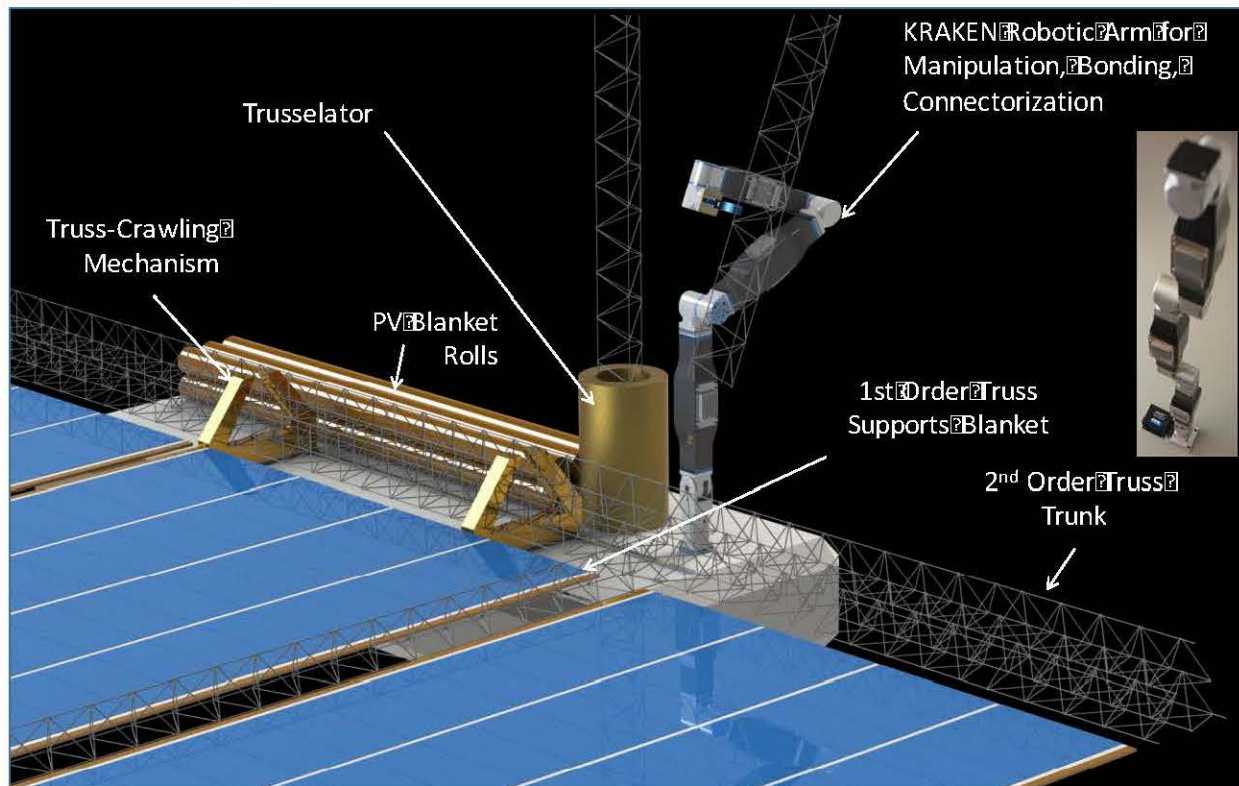


Figure 2. Concept for a palletized SpiderFab payload for in-space manufacture of large solar arrays.

We then investigated the value proposition for on-orbit fabrication of several different kinds of large space system components, and in each case found that the dramatic improvements in structural performance and packing efficiency enabled by on-orbit fabrication can provide order-of-magnitude improvements in key system metrics. For phased-array radars, SpiderFab enables order-of-magnitude increases in gain-per-stowed-volume. For the New Worlds Observer mission, SpiderFab construction of a starshade can provide a ten-fold increase in the number of Earth-like planets discovered per dollar. For communications systems, SpiderFab can change the cost equation for large antenna reflectors, enabling affordable deployment of much larger apertures than feasible with current deployable technologies. To establish the technical feasibility, we identified methods for combining several additive manufacturing techniques with robotic assembly technologies, metrology sensors, and thermal control techniques to provide the capabilities required to implement a SpiderFab system. We performed proof-of-concept level testing of these approaches, in each case demonstrating that the proposed solutions are feasible. These Phase I efforts established the SpiderFab architecture at TRL-3.

1.2.2 SpiderFab Technology Maturation Plan

Figure 3 illustrates an incremental technology maturation plan in which a sequence of flight missions will demonstrate increasingly capable in-space manufacturing solutions, starting with a nanosat-scale demonstration of ISM of a long linear truss for long-baseline sensing applications, progressing to demonstration of ISM of a 2D RF aperture, and then graduating to an operational capability for ISM of very large space systems.

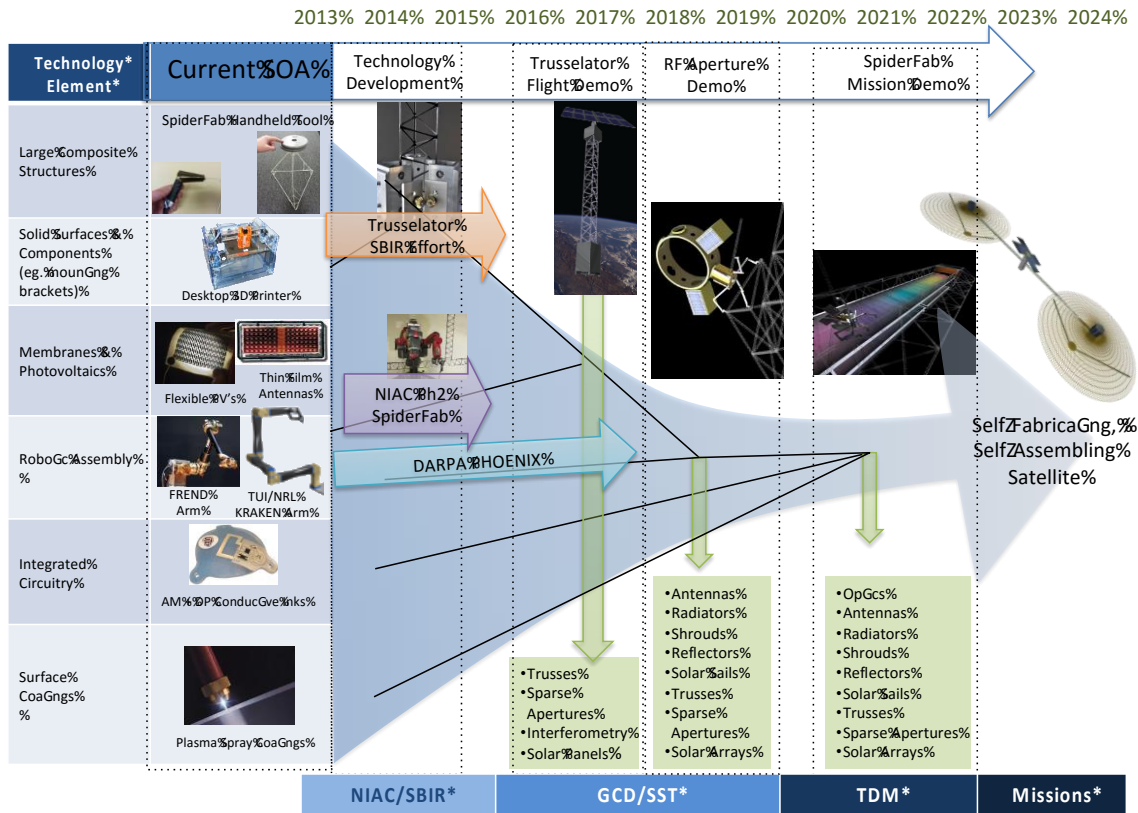


Figure 3. SpiderFab Technology Maturation Plan.

1.3 BACKGROUND: TRUSSELATOR SBIR

In addition to the NIAC SpiderFab effort, TUI is also performing a parallel Phase II SBIR titled “Trusselator”, in which we are developing a key initial component of the SpiderFab architecture, a device that converts spools of carbon fiber feedstock into high-performance carbon fiber trusses. The preliminary Trusselator prototype developed in the Phase I SBIR effort is shown in Figure 4 through Figure 7 along with examples of trusses fabricated by the device. Figure 8 shows a 16-m truss sample fabricated with this prototype. This truss sample is light enough yet strong enough to be self-supporting in 1 gee. In the Phase II SBIR effort, TUI is refining the device design to reduce its size, weight, and power (SWaP) and enable it to operate reliably in a vacuum environment. Our goal for this Phase II prototype is to fit the mechanism within a 3U (30x10x10cm) volume to enable affordable flight validation on a CubeSat platform.

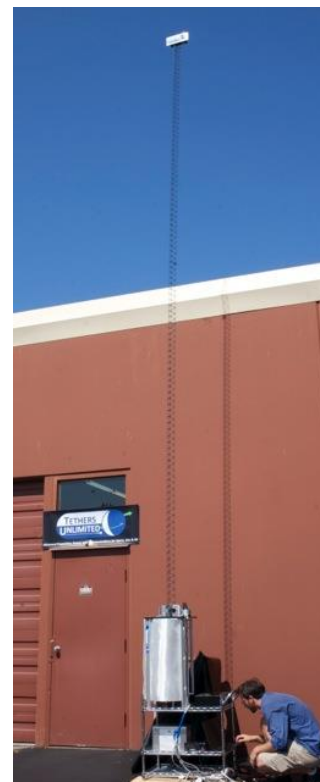


Figure 4. Truss Fabrication demonstration.



Figure 5. Close-up of the carbon-fiber truss exiting the Trusselator prototype.

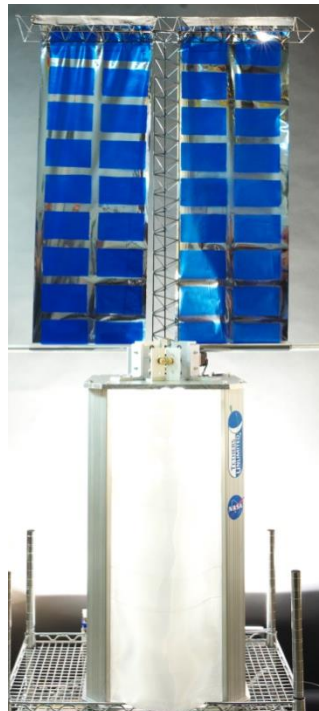


Figure 6. Proof-of-concept demonstration of deploying mock solar panels using the Trusselator.

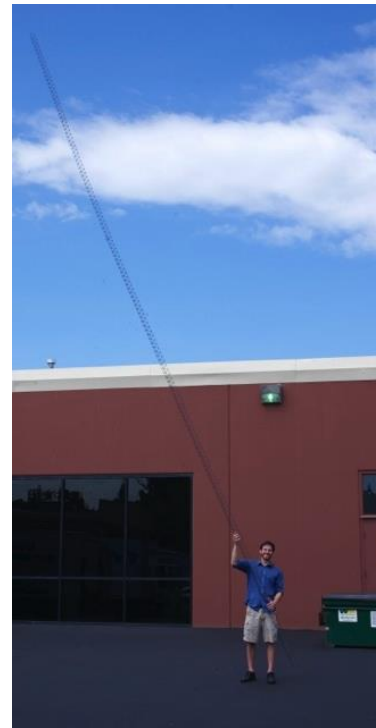


Figure 7. Carbon-Fiber Truss fabricated by the Phase I Trusselator prototype.



Figure 8. 16m Truss sample, with semi trailer shown for scale.

1.4 SPIDERFAB PHASE II WORK PLAN

The objective of the Phase II effort was to develop key technologies and mission analyses to mature the SpiderFab architecture to a level where it is suitable for NASA GCD and SST programs to build and fly affordable flight demonstrations. To accomplish this objective, we proposed to (1) design methods to enable in-space manufacture and assembly of structures in the space environment; (2) build and test prototypes implementing these methods in a vacuum environment; (3) develop a concept for a mission to demonstrate in-space manufacture of a large RF aperture; and (4) evaluate the performance, cost, and risk tradeoffs between in-space manufacture and traditional ‘deployable’ approaches for large apertures.

2. PHASE II ACCOMPLISHMENTS

2.1 DEVELOPMENT OF TOOLS FOR IN-SPACE MANUFACTURE AND ASSEMBLY OF STRUCTURES

One of the objectives of this Phase II effort was to design and test methods to enable robotic systems to assemble the 1st-order truss elements fabricated by the Trusselator into 2D and 3D ‘truss-of-trusses’ structures to create support structures for satellite components such as antennas and arrays. We chose to focus our efforts on enabling creation of such 2nd-order truss structures, rather than simpler approaches such as joining rods together to create a 1st order truss structure (as was illustrated in Figure 1) because 2nd order truss structures can achieve 30X improvements in structural efficiency relative to 1st-order structures.¹ This enhanced structural efficiency is necessary to allow very large (100m-1km) apertures to be built with viable launch masses while achieving the structural stiffness needed to enable attitude and dynamical control of such large structures.

In order to make progress towards the capability to assemble 2nd order truss structures, we designed, prototyped, and demonstrated a SpiderFab “spinneret” tool that a robotic system can use to bond the carbon fiber composite truss segments together. We also prototyped a spinneret tool for free-form extrusion of composite rod segments.

2.1.1 SpiderFab Joiner Spinneret Process Development

To kick off the Phase II effort, TUI performed an in-depth trade study of the key variables that drive the SpiderFab process for fabricating truss-based structures, with the purpose of narrowing down the array of options for development. The complete trade study can be found in Appendix A. The following list of variables was identified, and the noted options selected as being most promising and/or necessary for successful development of the SpiderFab Phase II effort.

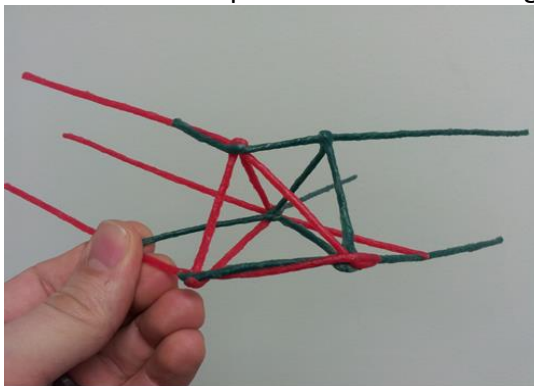
- A) Feedstock Composition – Carbon Fiber composite with thermoplastic matrix composed of Polyetheretherkeytone (CF/PEEK) was selected as the baseline material for use in development of SpiderFab processes, based upon its combination of high strength, high stiffness, low-outgassing, and high operating temperature capability.
- B) Feedstock Format – We selected pre-consolidated CF/PEEK tapes and rods as our feedstock format. This form of feedstock can be stored compactly. Relative to a process that uses separate fiber and thermoplastic as feedstock, using a pre-consolidated composite reduces the mechanical force, power, and system complexity required to achieve high consolidation of the material in the on-orbit processes.
- C) Heating Method – We evaluated several different methods for thermally processing and bonding the CF/PEEK materials, including contact heating, ultrasonic welding, and laser heating, and chose contact heating as our baseline approach due to its significantly lower power requirements and lower system complexity.
- D) Compaction Method – To ensure high bond strength between joined elements in a structure, we chose mechanical compression techniques.

1. Murphey, T.W., Hinkle, J.D., "Some Performance Trends in Hierarchical Truss Structures," AIAA-2--3-1903.

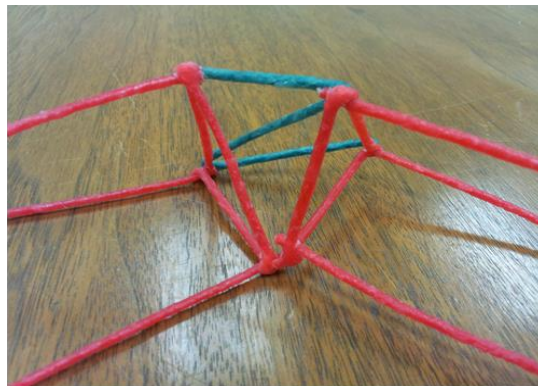
- E) Joint Geometry Scheme – To enable high-strength joints between two or more linear truss elements at arbitrary angles, we investigated several concepts, including tapered truss termination and attachment ('point joint'), attachment of directly-contacting existing truss nodes ('butt joint'), and "bridging-the-gap" attachment of non-contacting nodes ('spanner joint'). Based upon our testing with SpiderFab tools, we selected the gap-bridging concept because it achieved high joint strengths with acceptable complexity for forming the joints.
- F) Gripping Mechanisms – To enable a robotic system to manipulate truss elements, we developed several gripper mechanism designs to enable precise and repeatable manipulation and positioning of trusses. These end-effector tools must incorporate compliance and/or sensing to prevent damage to the structure.

2.1.1.1 Joint Geometry Development

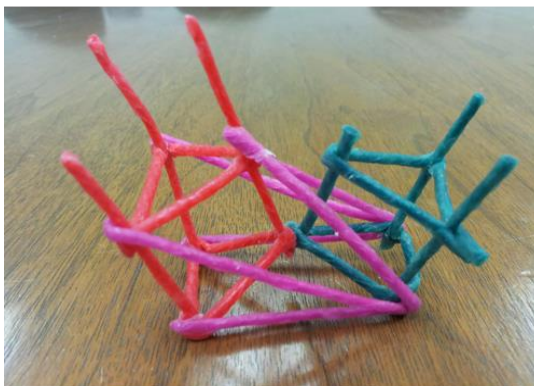
Because the geometry of joints between truss-based structural element is a strong driver of the requirements for a number of the other technical aspects of the assembly process, we investigated several candidate schemes for constructing joints between truss elements. For ease of visualization and manipulation, we used colored flexible composite rods to depict the geometry possibilities, which are many. These colored models were created to simulate some of the recurring types of attachment, including point joints, butt joints, and spanner joints. Figure 9 shows a handful of the possibilities for creating a structure of trusses.



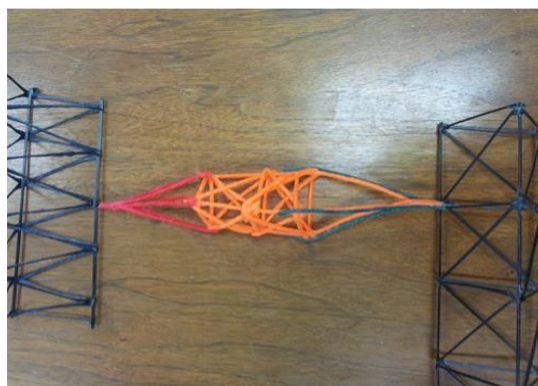
A. Laminate Longeron Excess



B. Join one node directly, add a Z to triangulate the 4 other nodes



C. High Angle, Join one node directly, brace across prior bay(s)



D. Terminate at points, single node joints

Figure 9. Truss-to-truss joint geometry candidates.

After our initial investigation, we performed additional modeling using sections of truss that were fabricated using the Trusselator prototype constructed in our Phase I SBIR effort. Some of these assemblies were single intersections (connection of 2 discrete trusses), and others were multiple intersections (connection of 3 or more discrete trusses in the same area). Each of the assemblies included both butt joint attachments and spanner joint attachments. These models, shown Figure 10, further illustrate the complex geometry possibilities, and the challenge of designing and building a SpiderFab tool which can accomplish this task.

These geometries illustrate the butt joint and spanner joint methods of attachment using CF/PEEK rod or tape segments for the attachment material. Where two nodes have physical contact there would be a single segment that bonds the two together, whereas for the spanner joints, two or three discrete segments would proceed to the nearest nodes, forming a triangulated structure. A “longeron lamination” method, depicted in Figure 10, is used to affix the connecting member onto the longeron of the pre-existing truss structures.

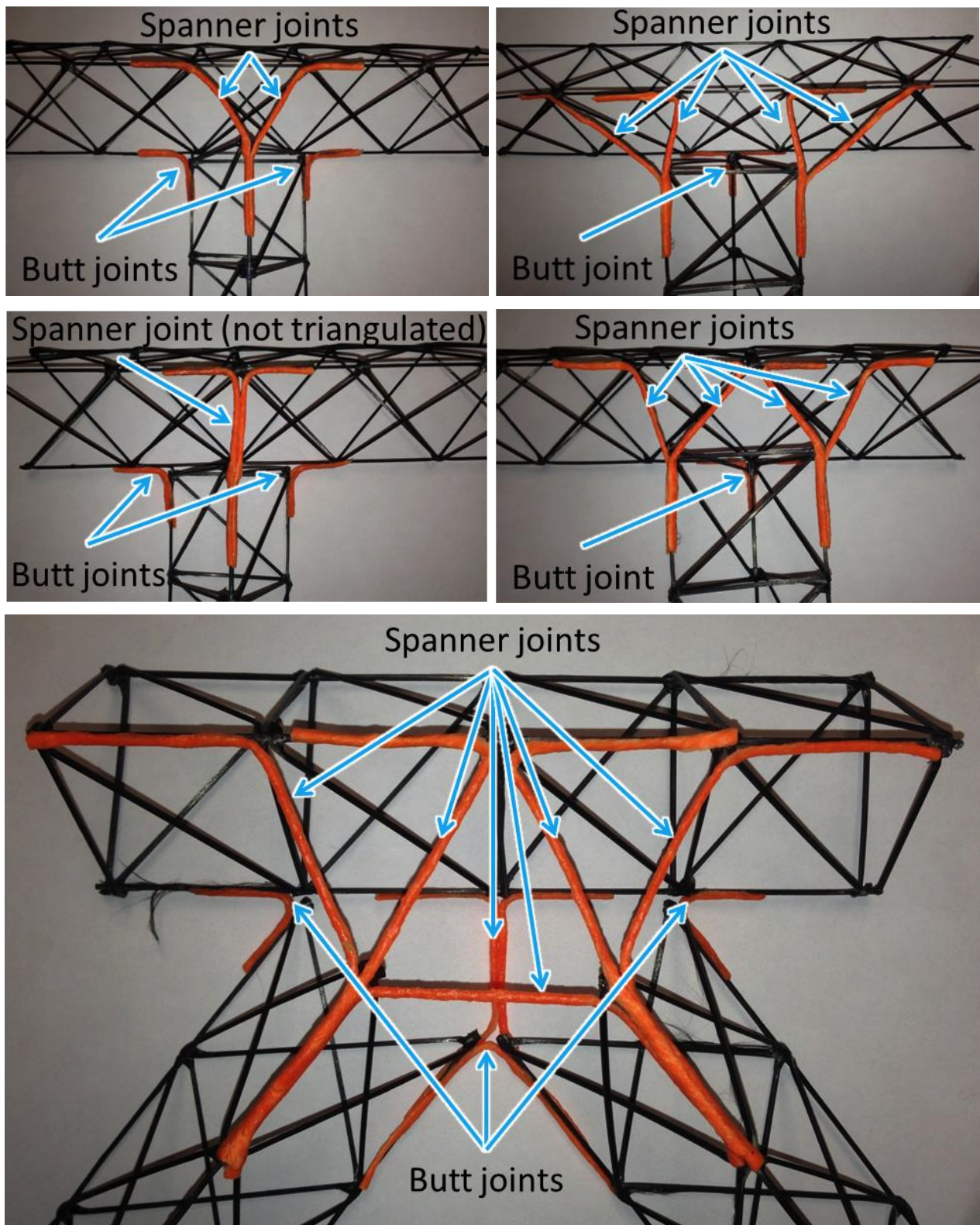


Figure 10. Additional Joint Geometry Concepts. Models of single intersections (top) and multiple intersections (bottom) using CF/PEEK trusses and flexible rods representing CF/PEEK joining members.

2.1.1.2 Joint Geometry Fabrication Tests (Butt Joints)

Next we began testing our geometries using CF/PEEK rods and tapes to join pre-made trusses. In the process we tested several of our previously identified critical variables, including feed-stock format (tape and rod), heating method (contact heating), and compaction method (stationary, rolling, and sliding compression). For creating a butt joint assembly, we placed CF/PEEK ribbons across the nodes to be joined, and then pressed a heated metallic block onto them to melt and fuse the PEEK resin. Because the joining material was in ribbon form, these joints relied upon the physical contact of the trusses for compressive stiffness. Figure 11 shows two joints accomplished by this method.

One of the main challenges with this approach was getting the ribbons to adhere to the truss rather than the heated iron. Because of this issue, our compression method transitioned to something more akin to sliding or laminating with a brush-like stroke along the length of the ribbon. This achieved fairly strong bonds, but soon led to build-up of matrix material on the hot iron. Tapes were also added to bridge between bays farther away from the butt joint to act as tension members for additional stiffness. This had a moderate benefit, but it was clear that using pure tension members had limitations. It is clear that with the current truss design, we cannot rely on butt joints alone, as it puts severe restrictions on the location and angle at which the trusses can be joined, which is an unacceptable limitation for long-term goal of the SpiderFab process to be capable of fabricating structures with geometry varied throughout their extent in order to optimize their performance.

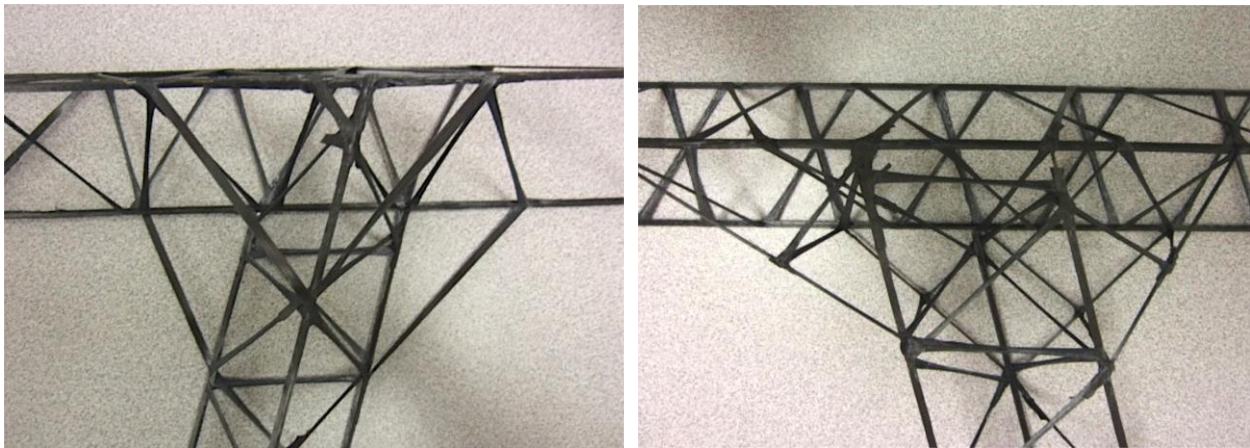


Figure 11. Butt Joint Geometry. *Joining was done using a heated iron to attach CF/PEEK ribbons (left) and rods (right) from the nodes of one truss to the nearest nodes of the other. Note the angle of attachment determined by the location of the nodes, illustrating a severe limitation of using only butt joints.*

2.1.1.3 Joint Geometry Fabrication Tests (Spanner Joints)

To create an assembly in which the two trusses can be joined at any angle or orientation, they must be separated by a gap and a spanner joint method employed. This necessitates members with compressive strength, so CF/PEEK rods were used rather than tapes. Figure 12 shows a top and bottom view of an assembly of two trusses utilizing the spanner joint method.

The same hot iron was used for heating and joining the spanning segments. Using CF/PEEK in the rod form had the advantage of not adhering to the hot iron as much as the ribbons, but after the initial fusing of the joint, some “brush stroke” motion was helpful for getting all the fibers to lay down neatly and forming a strong bond. This spanner joining method showed considerable improvement over the previously tested butt joint method with ribbon material.



Figure 12. Spanner Joint Geometry. *Joining trusses with a separation distance was accomplished using a heated iron to attach CF/PEEK rods from the nodes of one truss to the nodes of the other (spanner joint).*

2.1.1.4 Joint Geometry Fabrication Tests (Splice Joints)

After experimenting with making assemblies of trusses, we experimented with several other applications of the contact welding method using the hot iron. Two important uses are for the repair of broken joints within a truss, and for splicing of segments together. To test the capability of the contact welding approach for these needs, we cut one longeron of a truss in multiple places along its length. Using heat and compression we were able to make lap joints to repair the longeron in a shortened state, resulting in a curved truss, shown in Figure 13. This

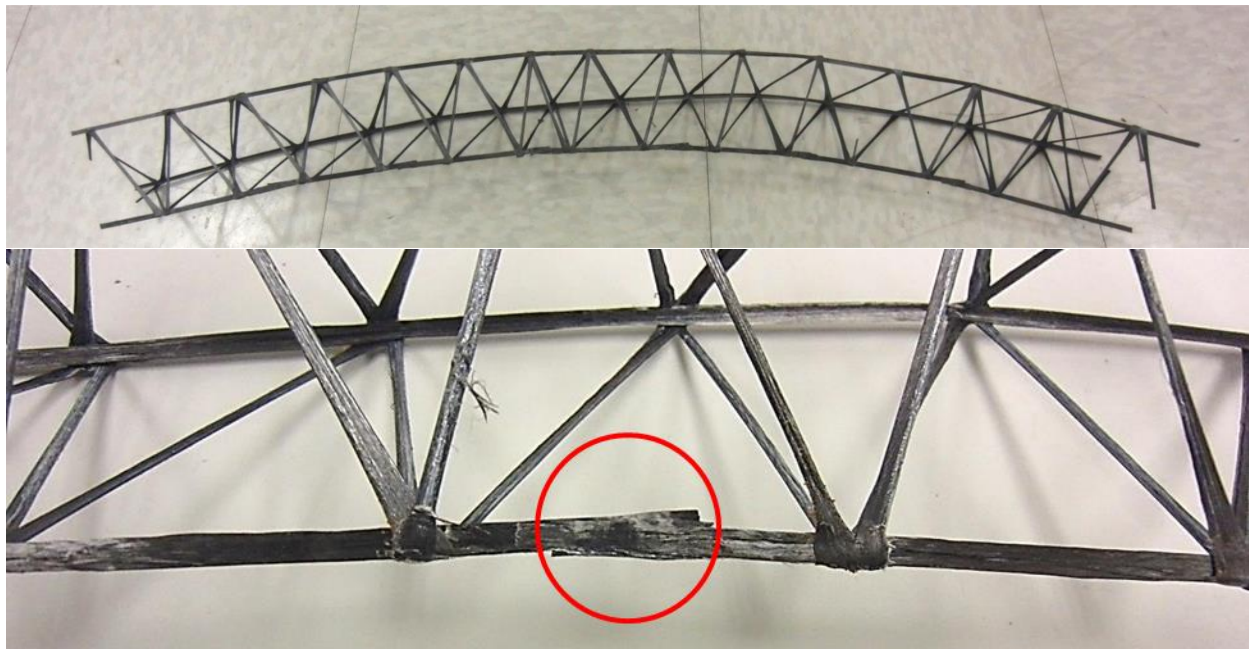


Figure 13. Curved truss-making concept. *Curved truss formed by cutting every other bay of one of the longerons, and rejoining it in a shortened state (circled). Rejoining was done using a heated iron.*

could be a useful method for creating structures with organic shapes or complex geometries.

2.1.1.5 Joint Geometry Fabrication Tests (Point Joints)

After achieving encouraging results with the previous tests, we evaluated the capability of our process to form tapered ends onto pre-existing trusses. Tapering the ends of the trusses would enable truss elements to be connected with point joints, which have the advantage of transmitting only tension and compression, thereby simplifying structural analysis. On one end of the truss we clipped off the diagonals and bent the now unsupported longerons radially inward until they met in a point. Bending the longerons required heating at the last remaining node to soften the material. The three were joined in a point by heated contact using the soldering iron in similar fashion to the previously performed tests. Pre-formed CF/PEEK rods were attached between the tapered longerons to provide additional bracing of the structure. Figure 14 (left) shows this tapered longeron point design.

On the other end of the truss we used three longeron sections that had been cut out of another truss, attached one end of each to the final truss node, and joined the other ends to each other at a point on the neutral axis of the truss. This section was also buttressed by additional rods. We also experimented with adding PEEK resin via a manual fused filament fabrication technique, as reinforcement for the joints. Figure 14 (center) shows the resulting termination.

Finally, this truss was placed in TUI's Instron Machine for compressive strength testing, shown on the right of Figure 14. Each time the truss reached its limit and broke, we repaired and reinforced it for further testing, resulting in 18 successive compression tests, with a maximum load measurement of 208 lbs. The capability of the SpiderFab methods to repair and reinforce weak or broken segments will be a major factor for risk reduction for future flight opportunities.



Figure 14. Point Joint Geometry Fabrication and Testing. *Using SpiderFab techniques, we formed pointed tips on the ends of a truss (left), reinforced them with PEEK resin (center), and performed compression to evaluate their structural integrity (right).*

2.1.2 SpiderFab Joiner Spinneret Prototype Development

Having observed and evaluated some of the significant variables for successful manual application of the SpiderFab processes, we were ready to begin designing and building hardware to perform these processes using robotic automation. We started by sketching out several design concepts for a SpiderFab tool which would do one or more of these things: feed material into a processing zone, form tape into rods, hold the material against the application surface, heat it to above the melting temperature of PEEK (380C), cool it to below the service temperature of PEEK (250C) under compaction, cut the feedstock, and restart another segment of feedstock.

One of the problems that we hoped to solve in the development of a SpiderFab Joiner Spinneret was the adhesion of matrix material to any surface other than the intended truss joint. This would include the heated contact welder as well as any heated forming elements such as those for transitioning tape into rods. An idea was generated that we could perform both heating and cooling with the same compression block if we could dump heat quickly with active cooling. This method is fairly inefficient from a total power perspective, but it has the potential to solve one of the major issues that we had previously encountered.

We quickly sketched out a simple concept and made a prototype to test, as shown in Figure 15, which included a heated block that would melt the PEEK, and an actively cooled plate that would be brought to bear on the heated block for quick cooling and solidification of the matrix, and a conical spring to separate the two except under sufficient compression. Along with a strategic heating and cooling routine, this has enabled removal of the contact surface without adhesion of material.

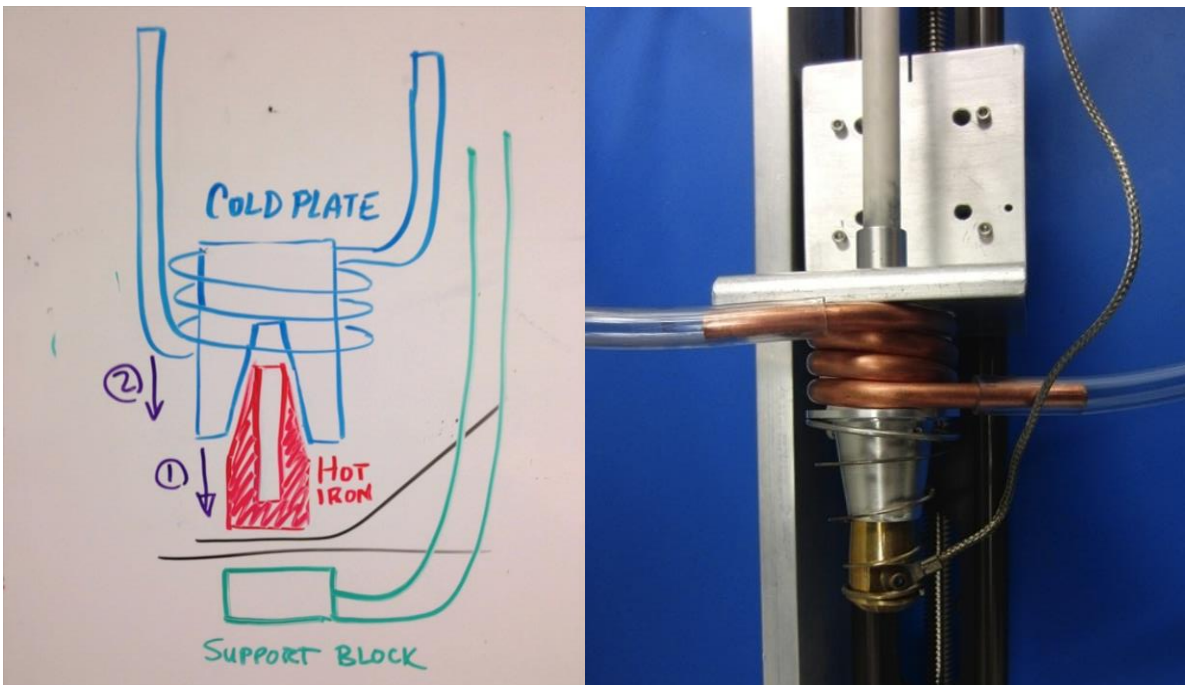


Figure 15. Hot / Cold Welder Concept (left) and Prototype (right). *This contact welder heats the material to the melting point, shuts off the heater, applies the cold block to draw away heat, and retracts from the joint with little to no adhesion of matrix on the welder head.*

Error! Reference source not found. shows preliminary testing (left) and the resultant joints formed with consolidated rod stock (right). The resulting joints seem to have excellent consolidation, and more-than-sufficient strength. The rod flattens out with heated compression, resulting in a larger surface area for good cohesion with the truss.

2.1.3 SpiderFab Joiner Spinneret Prototype Vacuum Testing

The objective of this test was to investigate the ability of the SpiderFab Joiner Spinneret to rapidly form a weld between CF/PEEK materials and then release the tool from the composite material without accumulating PEEK on the tool, all while under vacuum. For expediency, these tests were not performed with water-cooling to eliminate the need to make water pass-throughs in and out of the chamber. For automation, the tool was mounted to a lead screw actuator controlled via laptop from outside the chamber. The actuator forced the welding head against a fixtured CF/PEEK truss, with a rod of CF/PEEK situated in between. A test stand was setup in the vacuum chamber with integrated lighting and video camera, as shown in Figure 17.

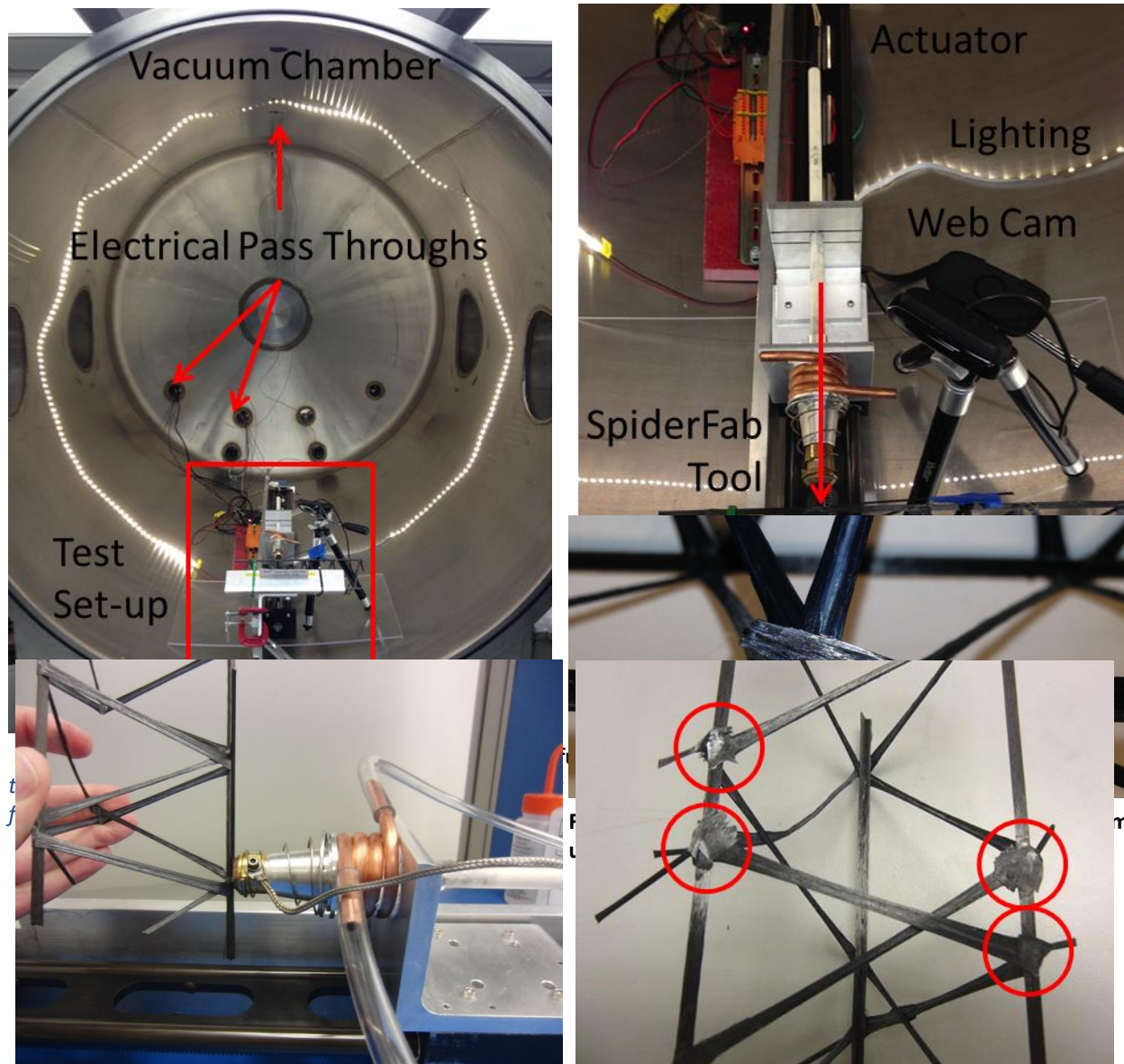


Figure 16. Joiner Spinneret (left) welding CF/PEEK rods to the nodes of a truss (right).

Several test welds were made at atmosphere to verify operation of the tool and to calibrate the actuator. After successfully proving the system in atmosphere, the same test was performed in vacuum of 300 mtorr. The entire welding process at atmosphere with no water cooling was approximately 2 minutes, while the time in vacuum was approximately 5 minutes, due to the lack of convective air cooling. The addition of liquid cooling for vacuum testing will significantly reduce cycle time. The joints formed in vacuum were visually of equal quality to those formed in atmosphere, achieving good consolidation with the truss, as shown in Figure 18.

2.1.4 SpiderFab Joiner Spinneret Engineering Model

After the success of the first generation prototype, we decided to build a second Joiner Spinneret, integrating improvements based upon our results testing the first prototype. The new tool operates in the same manner as the previous one, but with some improvements for performance and automation. For one, the weld head mass has been reduced from 80g to 30g, which allows it to thermally cycle much more quickly and power-efficiently. The new design has a small linear stage and 12V linear actuator for driving the motion of the weld head against the substrate. Lastly, the new design has a prong which extends from the base of the tool out in front of the weld head to provide a support structure against which the mechanism can push to compact the joint. This prevents any sagging or collapsing of the truss due to imbalanced forces while it is in a softened state. The new design can be attached to a pistol grip handle for hand-held operation, or to a mounting plate for a robotic arm. Figure 19 shows a cross-section view of the new design.

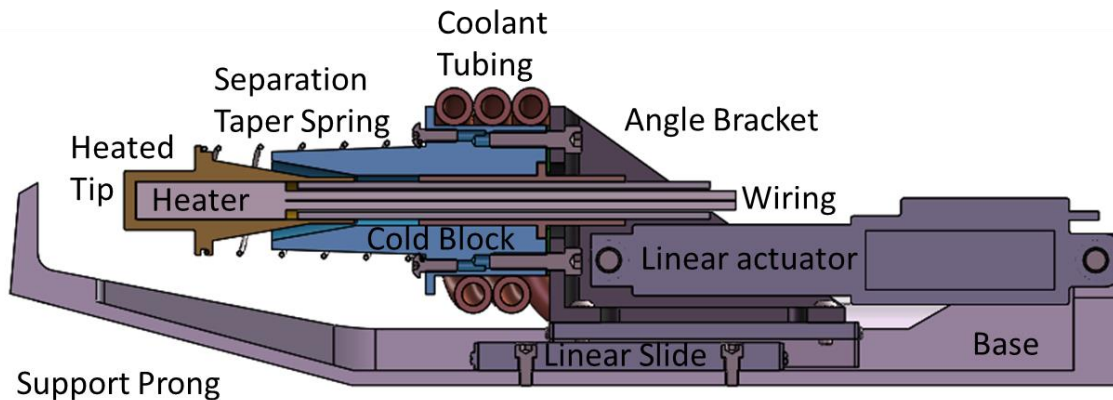


Figure 19. Cross-Section of the new Joiner Spinneret with Linear Actuator and Support Prong.

This version is electronically controlled by an Arduino microcontroller, which is programmed to govern the staged operation of the system:

- 1) Fully retract the linear actuator
- 2) Turn on heater (temperature controller set to 400°C, measured by a thermocouple)
- 3) Extend the linear actuator until the tip contacts the elements to be joined
- 4) Hold for 5 seconds to melt the PEEK resin
- 5) Turn off the heater
- 6) Extend the linear actuator until the cold block seats against the back of the heated tip
- 7) Cool tip for solidification of PEEK
- 8) Loop back to step 1

When the tip is released from the composite joint, the separation spring returns the heated tip to its fully retracted position, and the tool is ready to perform more joints.

The Arduino interfaces with devices for heating, temperature sensing, linear actuation, and display: 1) a solid state relay turns the cartridge heater on and off during various phases of heating and cooling, 2) a thermocouple amplifier breakout board converts the voltage from the thermocouple to a resolution that the Arduino can read, 3) a control board governs the motion of the linear actuator at the direction of the Arduino, and 4) an LCD screen displays the status of the Joiner tool. Power comes from a standard wall outlet through a 9 Volt DC adapter.

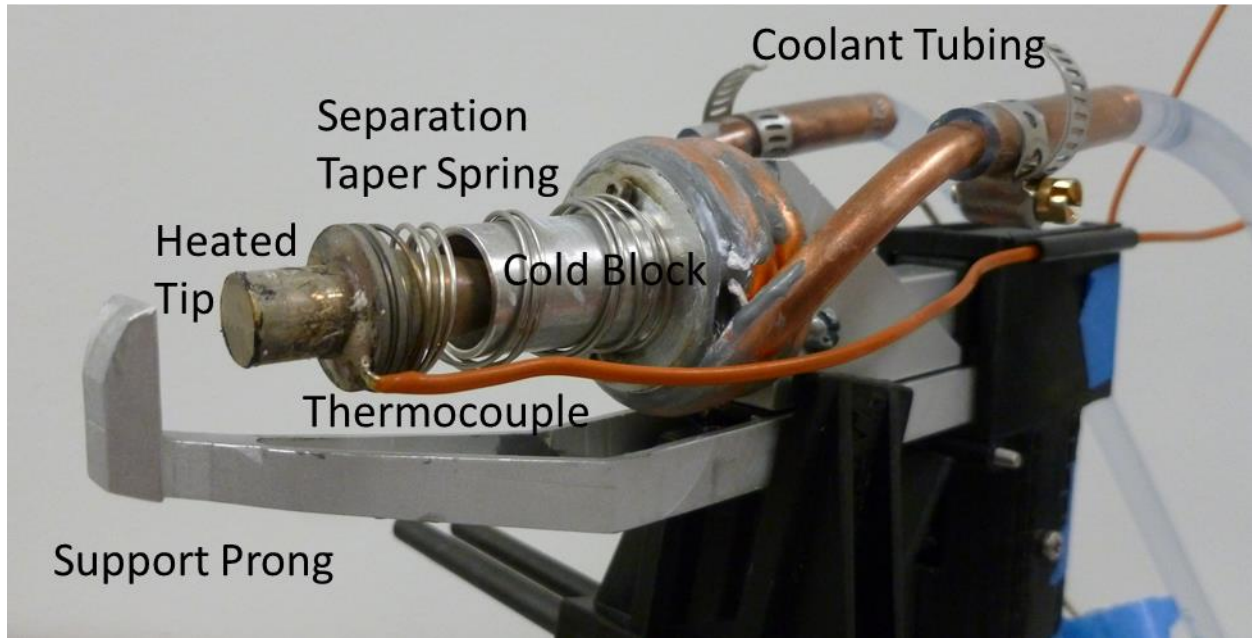


Figure 20. SpiderFab Joiner Spinneret. *TUI developed a custom contact welder which can heat and cool the joined substrates under compression, resulting in strong bonds and minimal weld head adhesion.*

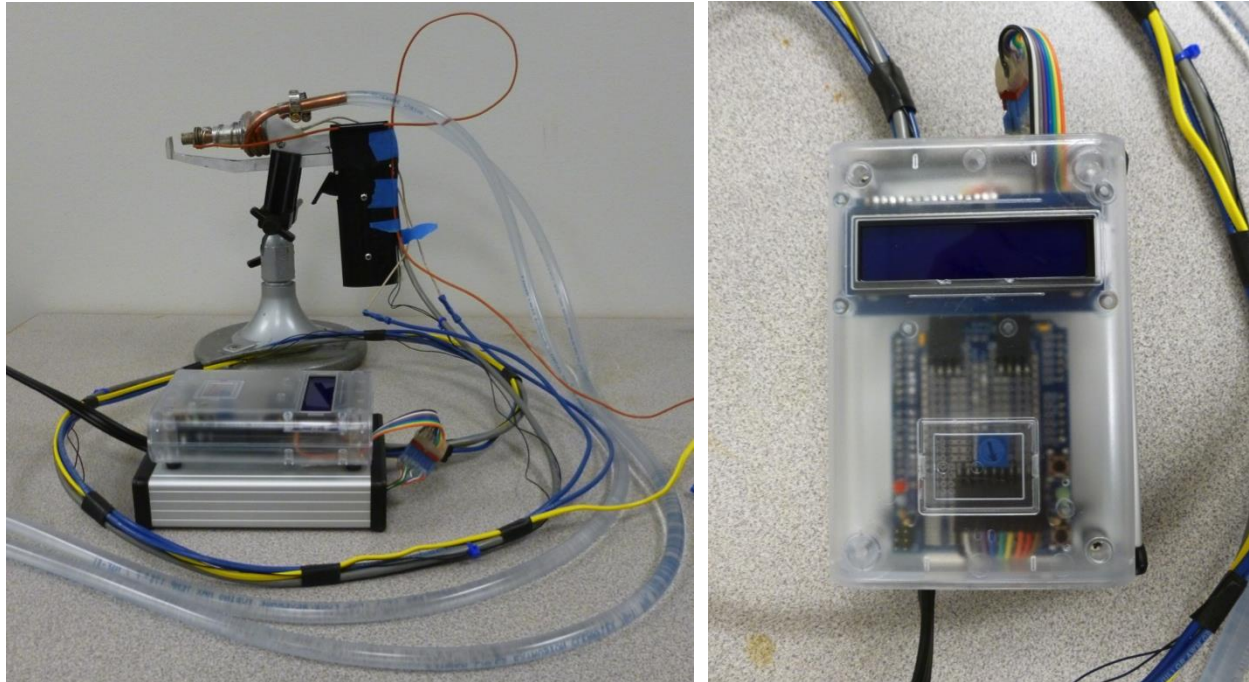


Figure 21. SpiderFab Joiner Spinneret Tool with Water Cooling Lines and Control Electronics. *The water lines draw heat away from the contact welder for re-solidification of the PEEK matrix. The Joiner Spinneret has three phases of operation, governed by an Arduino microcontroller.*

2.1.5 SpiderFab Pultrusion Spinneret Tool

We also prototyped a pultrusion tool to form tension members and extrude free-form rigid members. The 3D-printed prototype pultrusion ‘spinneret’ end effector is shown in Figure 22. This tool forces co-mingled glass fibers and ABS through a heated die to form a consolidated extrusion with round cross-section. Figure 23 shows a ‘fractal pyramid’ structure fabricated using this tool, and Figure 24 shows a test in which this tool was used as an end-effector on the Baxter robot.

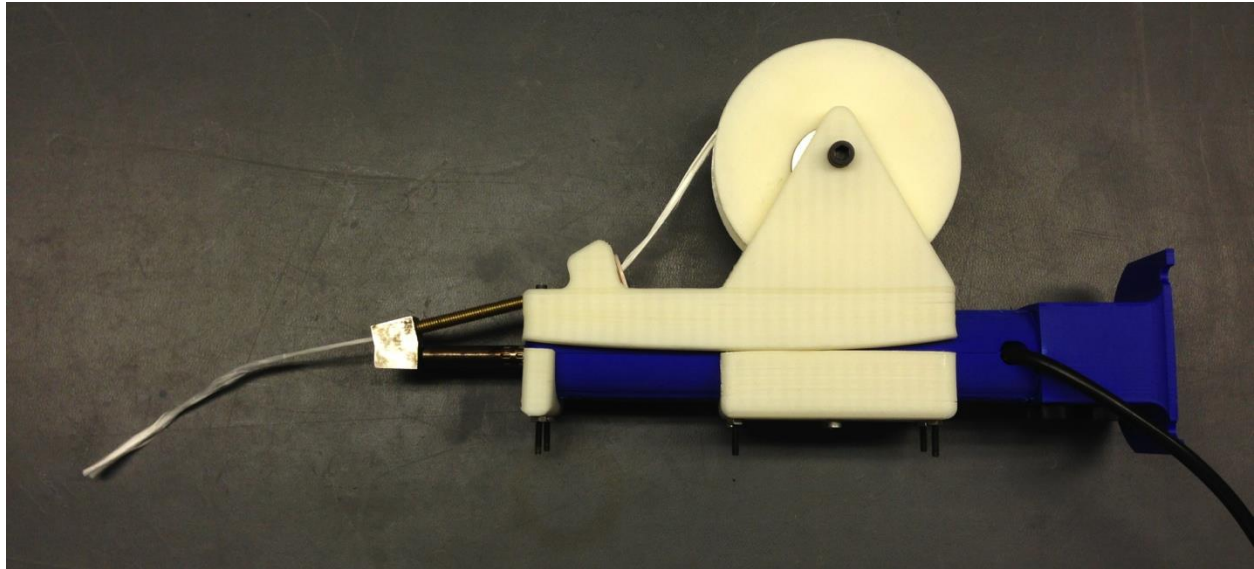


Figure 22. SpiderFab Pultrusion Spinneret Tool. *A spool of flexible co-mingled glass and plastic fibers get pulled through a heated die for melting and consolidation into stiff members for tension and moderate compression.*

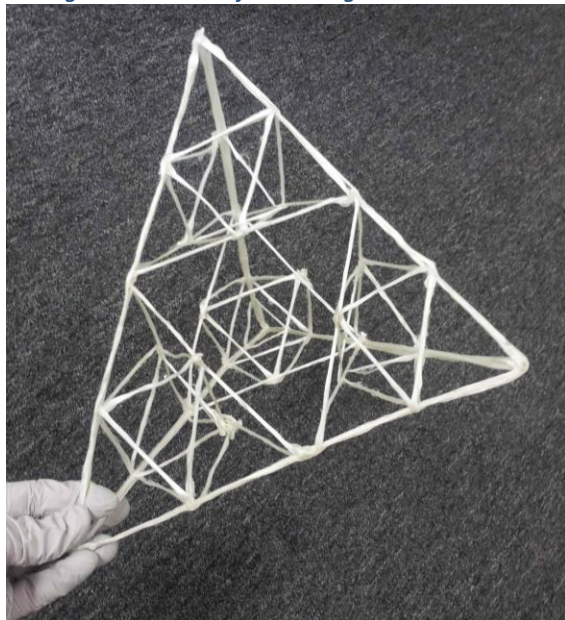


Figure 23. A 'fractal pyramid' constructed of Twintex material using the SpiderFab pultrusion spinneret.



Figure 24. Test of pultrusion of long elements using the SpiderFab spinneret as an end-effector on the Baxter robot.

2.1.6 2nd Order Truss Assembly Demonstration

In order to scope the challenges that must be addressed to enable robotic assembly of 2nd order truss structures, we fabricated multiple segments of truss with our Trusselator prototype and then manually assembled a truss-of-trusses structure using an assembly jig constructed of 80:20 components, shown in Figure 25 and Figure 26, the Joiner Spinneret prototype shown in Figure 20, and the Pultrusion Spinneret shown in Figure 22. The purpose of this exercise was to characterize the dexterity, reach, and range that a robotic manipulator will require to enable

such an assembly. Figure 27 shows the 3-m long 2nd-order truss sample, which masses just 620 grams.

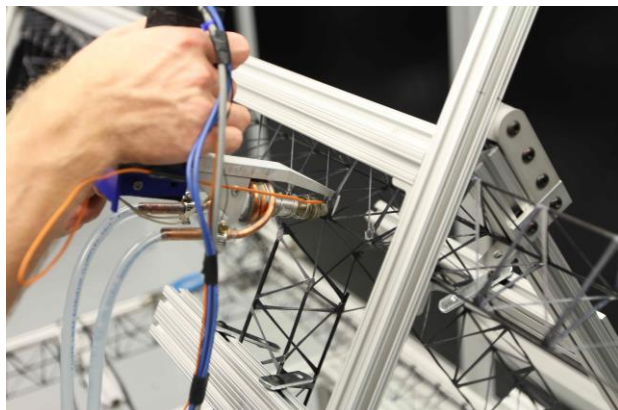


Figure 25. 2nd-Order Truss Assembly. *The Joiner Spinneret was used to join longeron and batten 1st order truss elements, and a Pultrusion Spinneret used to create diagonal tension elements.*

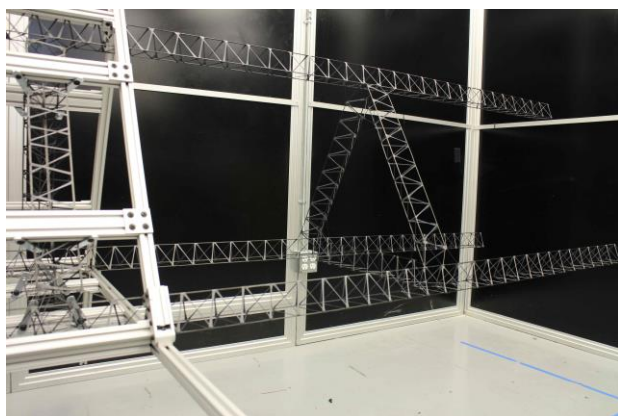


Figure 26. A jig was used to position the elements for welding.

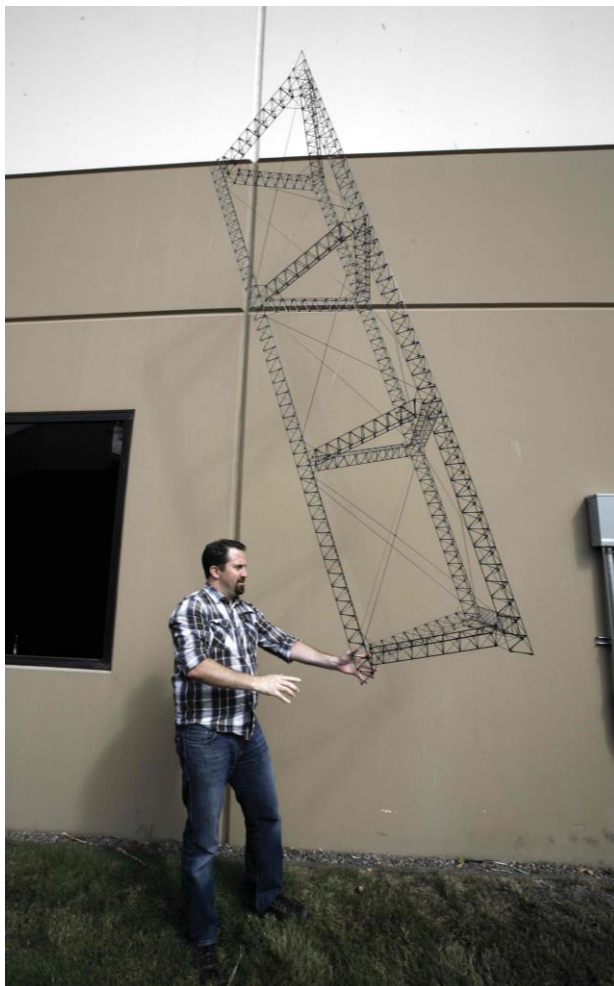


Figure 27. Truss-of-trusses sample. *The 2nd order truss sample is 3m long and masses just 620 grams.*

2.2 DEVELOPMENT OF ROBOTICS METHODS FOR ASSEMBLY OF SPACE STRUCTURES

Having demonstrated the feasibility of assembling composite truss based structures using relatively simple tools employing thermal processes, we turned our focus to developing methods to enable robotic systems to perform assembly of these structures in a highly automated manner.

2.2.1 Overview

The focus of this effort was on performing proof of concept demonstrations that verified the ability for an autonomous robot to grasp, manipulate, and join trusses. To complete these demonstrations, we developed a fast and efficient robotic vision system to enable closed-loop control of the robotic assembly, developed a robust software framework to provide support for these and future robotic demonstrations, designed, fabricated, and tested custom robot end-effectors and truss joints.

2.2.2 Baxter Robot

To support these demonstrations, TUI acquired, under company investment funds, a Baxter robot from Rethink Robotics. The Baxter, shown in Figure 28, is a robotic platform combining two 7DOF, 1.2m reach robotic arms and a vision system that includes both head-mounted and arm-mounted boresight cameras. While the Baxter would not be suitable for use in a space environment, it provided a very capable and affordable platform for developing and validating end-effector tools, vision-based software algorithms, and assembly CONOPS.

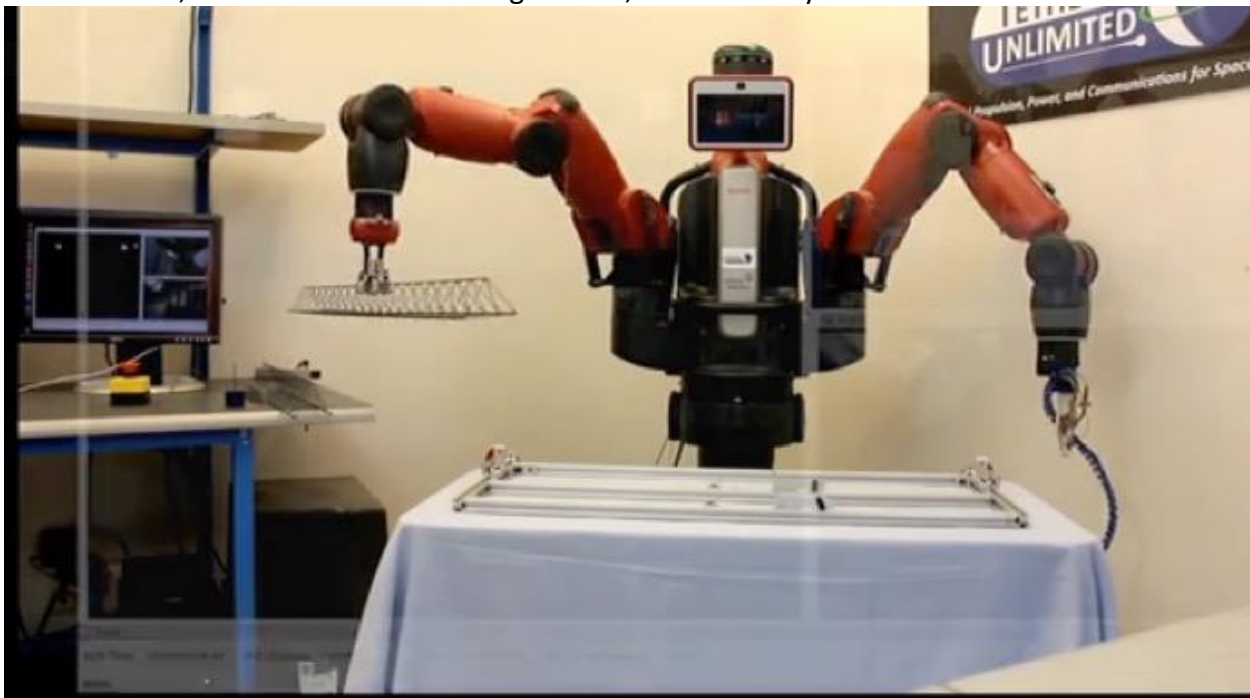


Figure 28. TUI's Baxter robot performing a truss assembly demonstration.

2.2.3 SpiderFab Robotic Vision System

To perform autonomous on-orbit truss assembly and construction, a robotic system will need a sensing system that will enable it to precisely grasp, position, and join truss elements. For this effort, we chose to demonstrate the feasibility of using vision-based software methods to pro-

vide this sensing capability. Working with the Baxter robot as a test platform, we developed a custom SpiderFab image processing framework incorporating the following capabilities:

1. Truss detection and location approximation.
2. Reliable closed-loop truss manipulation.
3. Guided truss manipulation.
4. Real-time image processing.

2.2.3.1 Truss Detection

The first step in the development of the robotic vision system was being able to reliably identify a truss in a variety of different environments. Object recognition is a vital component for any machine vision system and recent advances in this field have resulted in a number of popular algorithms and image processing methods being introduced to aid in this task. However, there is no one-size-fits-all algorithm and each object presents a unique and non-trivial challenge when trying to formulate the correct algorithms to identify it within images of near-arbitrary environments.

One method that many contemporary machine vision systems choose to identify objects in non-predetermined environments is by *feature detection* and *feature descriptor matching*. That is, several key visual features of an object (which are ideally unique to that object) are identified using one or more detection algorithms and the resulting feature descriptors are then used to determine if the object is likely present within an image. Color, shape, edges and prominent markings, tags or logos are all commonly used features used by feature detection algorithms. Examples of object detection by feature detection and matching algorithms are illustrated in Figure 29.

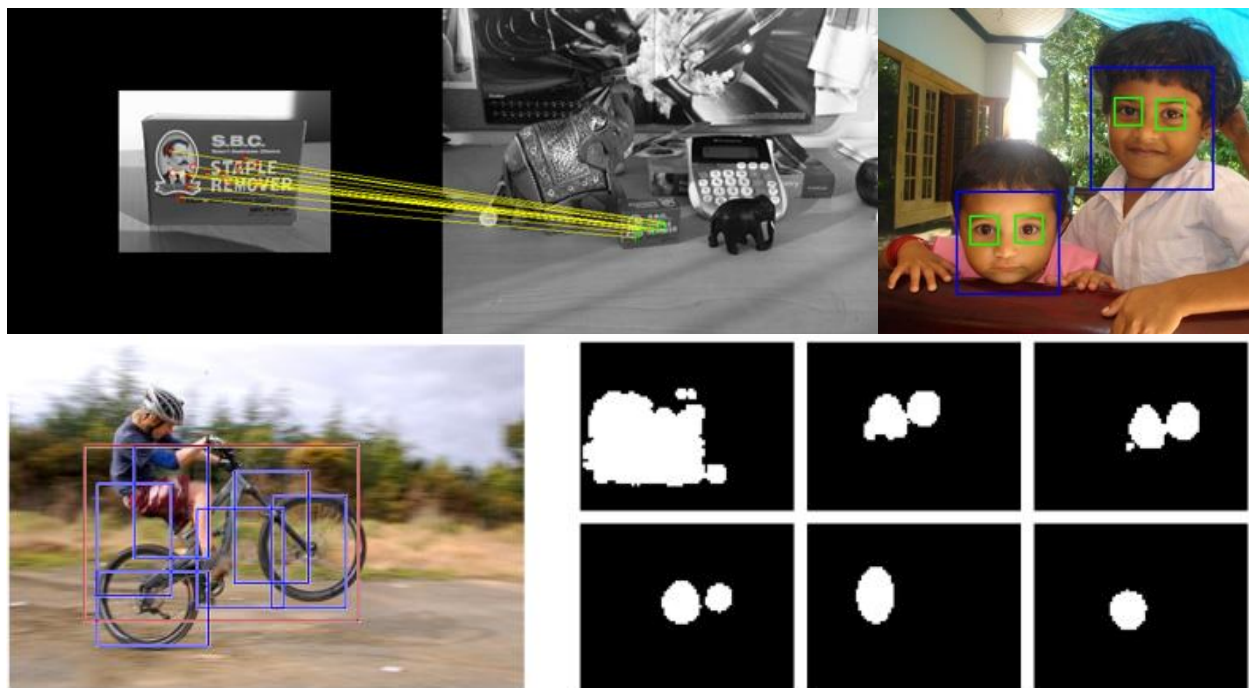


Figure 29. Examples of object detection by Feature Detection and Matching.

Mathematically, there is no universal definition as to what constitutes an image “feature” and calculation time requirements can differ vastly depending on the application. Thus, object detection using feature matching is done in a variety of ways.

To start, we identify the key features of our trusses that can be detected using common image processing techniques. Note that the Python version of OpenCV was used for image processing implementations. Additionally, since the cameras on our current robot platform are limited to monocular vision, algorithms are only performed with respect to 2-dimensional space.

At quick glance, the most prominent features of the truss are the multiple straight-edge longerons that make up the core construction. Out of necessity, the truss segments are arranged in fixed patterns. Currently, they are also uniform in color (dark shade of grey). An example is shown in Figure 30.



Figure 30. Example truss sample.

Unfortunately, our trusses also have several undesirable properties for many image processing object detection algorithms which would prove challenging to overcome. These include:

- Color – The trusses we used for testing are a very dark shade of grey. To ensure research into this matter was both insightful and realistic, we chose not to change the color our trusses for testing. For image processing applications, this is a notoriously difficult color to work with—particularly in environments with poor lighting or a dark background. Even in properly lit environments, shadows present additional problems and can partially obscure a truss within an image or even be mistaken for the truss itself when using object detection algorithms.
- Lack of 2-D surfaces – Although the truss is unique in shape, the lack of flat, 2-dimensional surfaces means that many feature descriptor matching algorithms may have difficulty identifying a truss unless viewed at the exact same angle, with the same background. That is, the gaps between the truss longerons allows the background environment to appear as part of the truss when viewed in a 2-D image—therefore changes in background environments and even viewing the truss from a slightly different angle can alter the appearance of the truss.

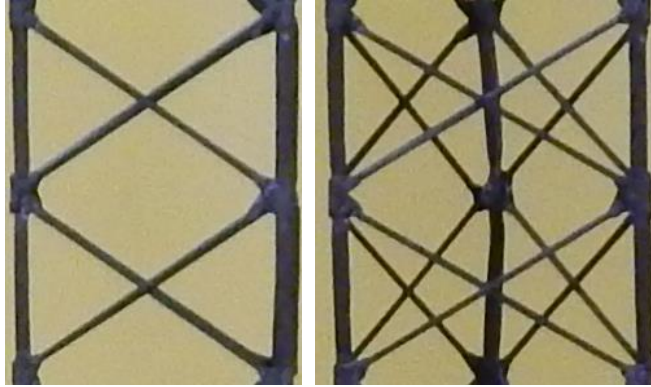


Figure 31. Images of a truss segment viewed from different angles 60 degrees apart.

- Manufacturing imperfections – Despite improvements in the construction and fabrication, trusses will not be identical in appearance.

Despite these disadvantages, significant progress was still made in truss detection using image processing using the algorithms described below.

2.2.3.2 Line Detection Algorithms

The longeron edges can be viewed as individual line segments, which should allow for the use of line detection algorithms. The Hough Line Transform is a simple and popular technique to detect lines within an image. It works on the principle that any line in an image can be represented mathematically as:

$$\rho = x \cos\theta + y \sin\theta$$

Where ρ is the perpendicular distance from the origin to the line. The algorithm uses a two-dimensional array, called an accumulator, of (ρ, θ) pairs to determine which pixels (or subset of pixels) in the image are likely to be associated with a straight line. The accumulator forms a sample-space of possible lines (or a random subset in the case of the probabilistic Hough Transform) within an image and each bin in the sample-space with values (or votes) greater than a preset threshold are determined to be lines.

Figure 32 shows the output image of performing a Probabilistic Hough Line transform on an image containing a truss.

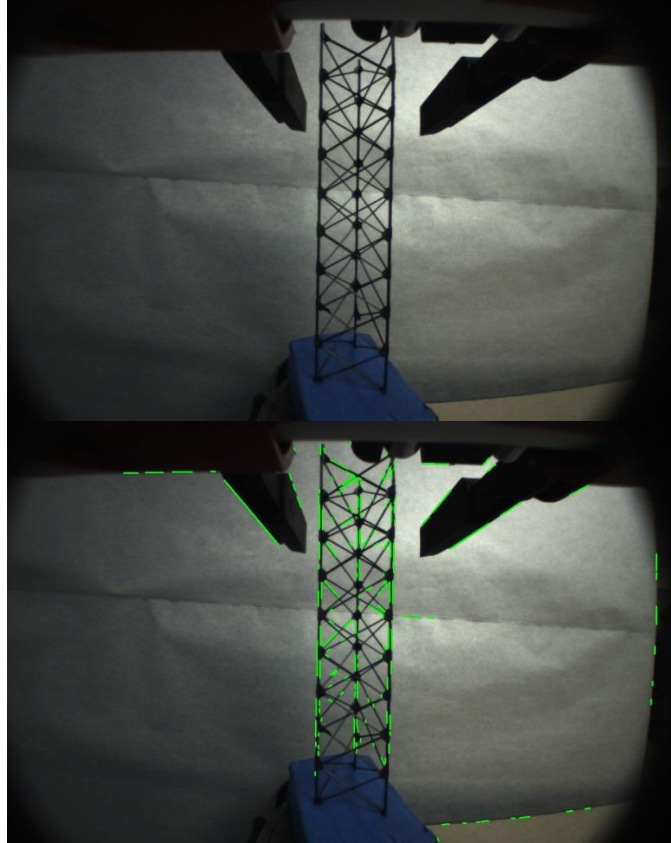


Figure 32. Finding line segments in image using Canny Edge Detection and Hough Line Transform algorithms.

Note that the algorithm successfully detected the edges of the truss, but also picked up considerable noise from lines in the surrounding environment. To filter out the unwanted lines, the inherent properties of the truss must be considered. The three main supporting longerons are paramount to this filtering attempt as they are both the easiest feature of the truss to detect and can also greatly speed up computation time by localizing line segments within a discrete proximity.

To find these longerons, we can perform a histogram of the angles associated with each detected line segment to identify the lines that run parallel with each other. Three (or two) distinct parallel lines of similar length are good indicators of the supporting longerons.

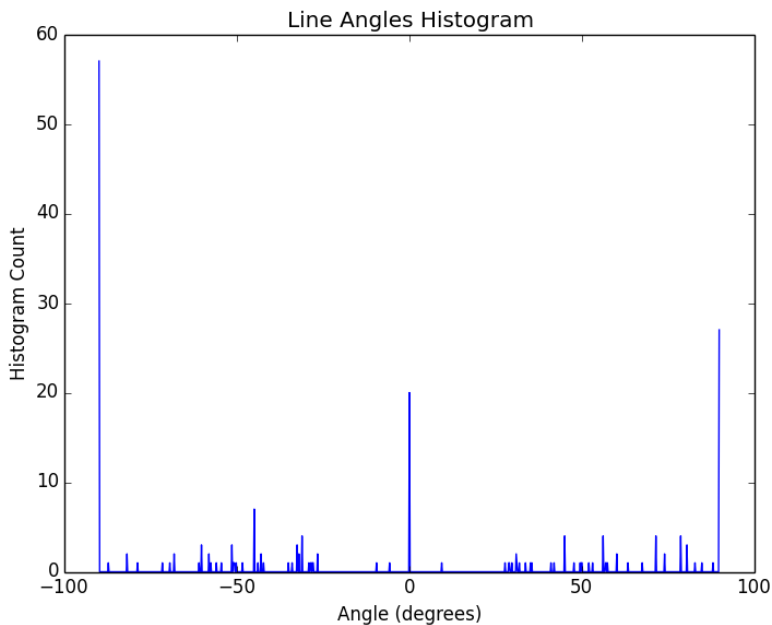


Figure 33 Histogram of Line Segment Angles.

Performing an interpolation algorithm to combine the line segments gives us a better estimate of the longeron lengths and also provides a reduced sample space when attempting to identify the smaller, crossed longerons of the truss.

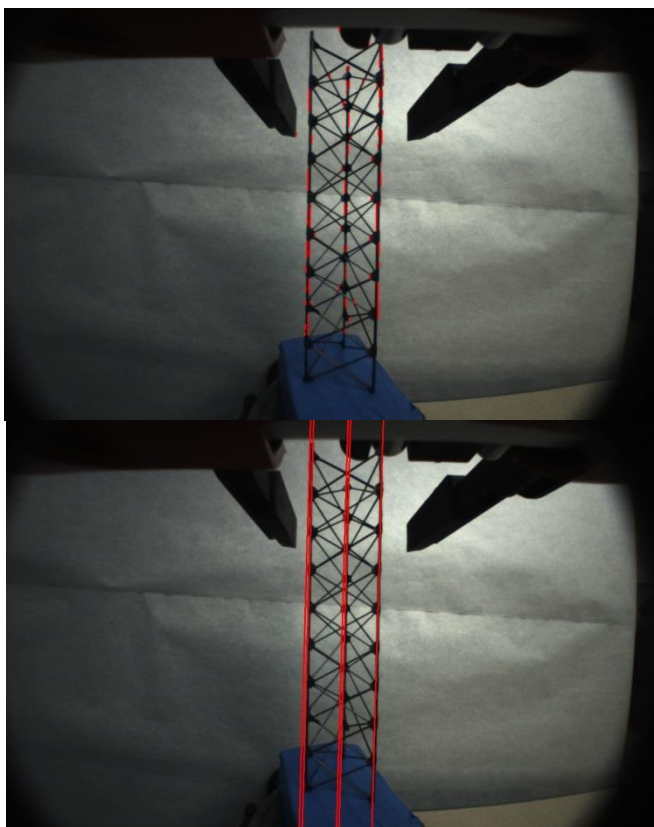


Figure 34. Detecting main longeron supports.

If we examine the region in the image between our newly detected supporting longerons, the smaller longerons of the truss should create a high density of detected line segments. Additionally, these line segments, when taken in parametric equation form, should create several line intersections within our truss region—providing further evidence that what we are looking at is indeed a truss. Note that these line segments should not be parallel with our three main support longerons. Line segments meeting all these requirements are identified as line segments representing a smaller truss longeron.

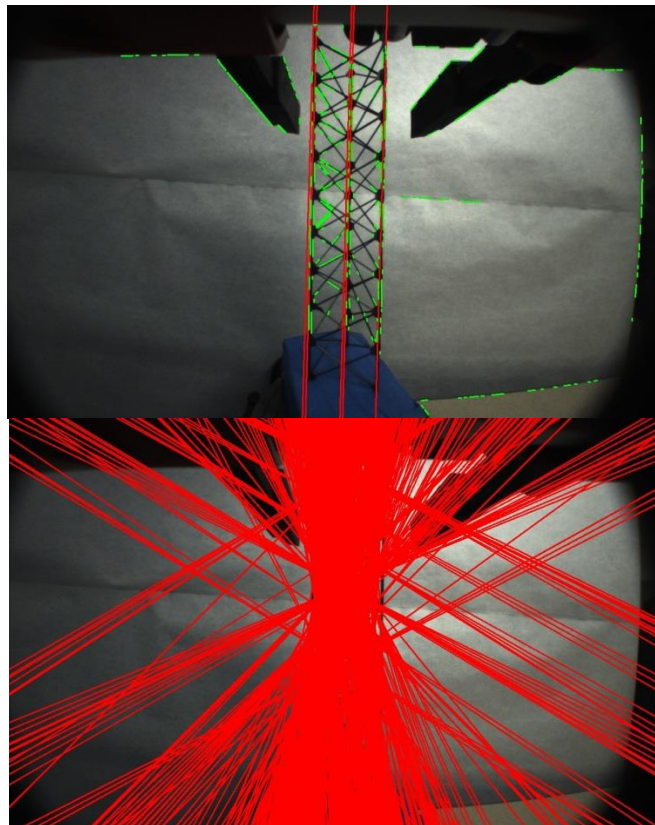


Figure 35. Identifying smaller support longerons. The line segments lying within our truss region and also containing multiple line intersect points within this region are considered part of the smaller support longerons.

Next, we can take all the line segments that we’ve identified as part of the truss and reconstruct the image using only the truss data points.

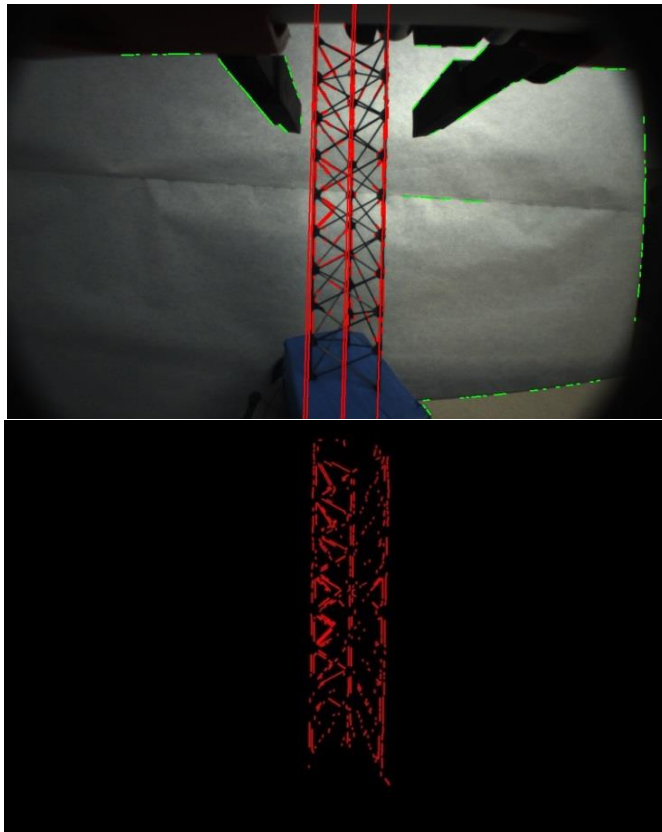


Figure 36. Extracting detected truss line segments from original image.

Finally, applying a Gaussian Blur filter to smooth out the truss line segments gives us our final image.

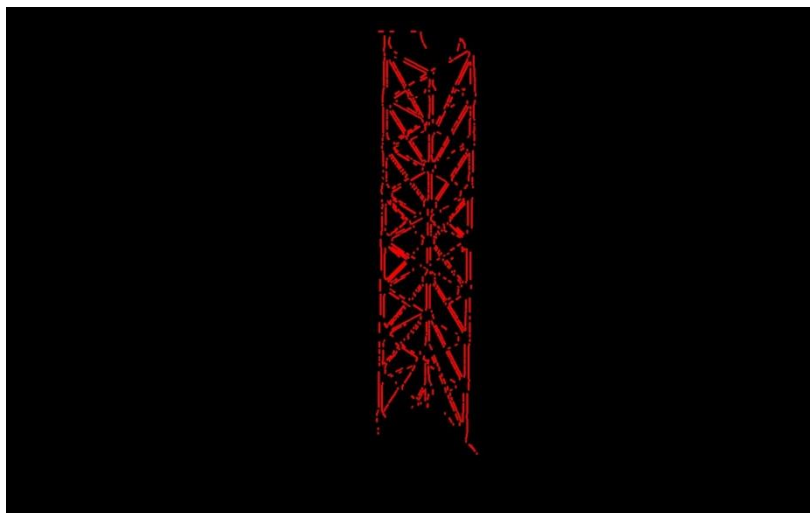


Figure 37. Final image with positive truss identification.

2.2.3.3 Feature Descriptor Matching

Feature descriptor matching is a very popular image processing technique employed by modern machine vision systems. Feature detection algorithms search for prominent or uncommon features within an image using a combination of several advanced image processing techniques.

Information about these detected features is generally stored in *descriptors*—whose size and contents vary according to the feature detection algorithm.

Feature descriptor matching is performed by matching descriptors between two or more images. One image, also called the “query” image, contains the object you are trying to detect. The other image, sometimes called the “train” or “test” image, contains the object within some environment. The feature detection algorithm is run on both images and then a *feature matching* algorithm is used to attempt to match the features shared by the two images—thereby detecting the object in the train image.

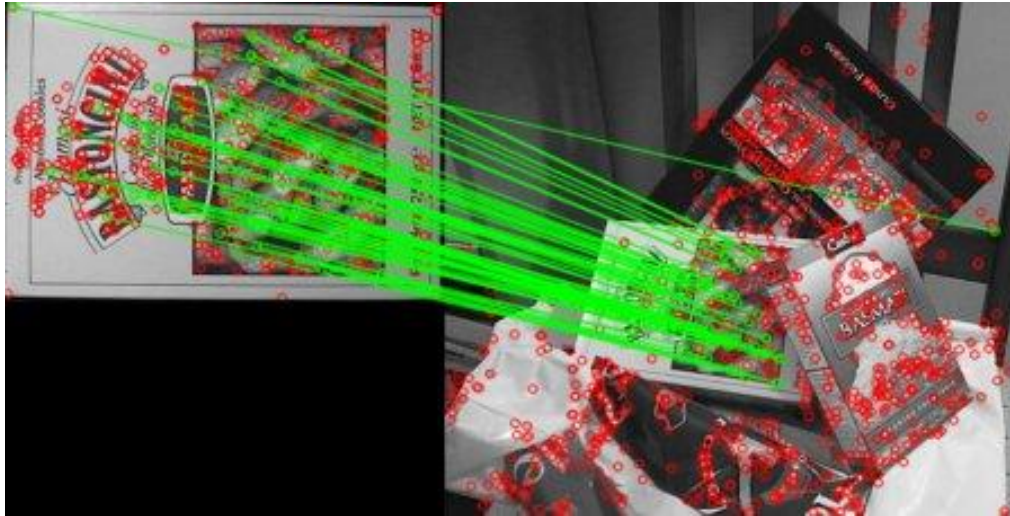


Figure 38. Example of feature descriptor matching.

When choosing feature detection and feature descriptor matching algorithms, it’s important that both algorithms perform well given our expected environments and the features of our object. The algorithms should be able to detect our truss in different lighting conditions as well as varying orientations and distances. Ideally, these algorithms should also be fast to meet our real-time image processing requirements.

Three popular feature detection algorithms excel in most of these areas. All three are scale-invariant so they should detect our object at different distances. They are also rotation invariant and consistent at detecting the same features in different illumination and noisy conditions.

1. Scale Invariant Feature Transforms (SIFT) – A very popular algorithm introduced in 1999. This algorithm is very accurate at detecting features in various conditions. Although this algorithm is likely the most accurate of the three examined here, many of the newer algorithms are faster—making them better suited to real-time applications.
2. Speeded Up Robust Features (SURF) – SURF was introduced as a faster alternative to the SIFT algorithm. In an attempt to appeal to real-time applications, it sacrifices accuracy in favor of speed by significantly reducing a features scale-space information by using a convolutional box filter technique.
3. Oriented FAST and Rotated Brief (ORB) – Uses heavily optimized versions of various algorithms with the goal of creating an algorithm faster than SURF and as accurate as

SIFT in most circumstances. It’s important to mention that, unlike SURF and SIFT, ORB is *not a patented algorithm* and can be used without any royalty costs.

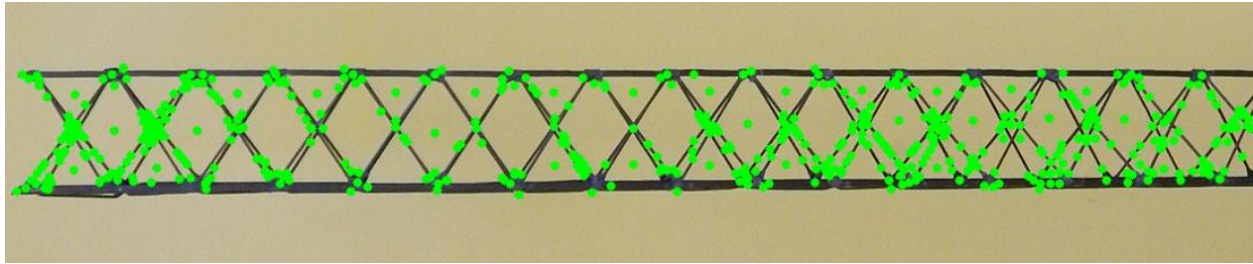


Figure 39. Detecting truss features using SIFT feature detection algorithm. The green circles are features that the algorithm decided are noteworthy and are stored as *keypoint descriptors*.

To perform a more empirical and applicable comparison, each algorithm was used to detect features from a small database of images containing around fifty different truss images. Figure 39 shows an example of the use of the SIFT algorithm on our truss sample. The following graph shows the average computation time of each algorithm when performing feature detection. Note that these tests were performed on a Windows 7 PC with an Intel® Core i7-4770k CPU and 16 GB of memory.

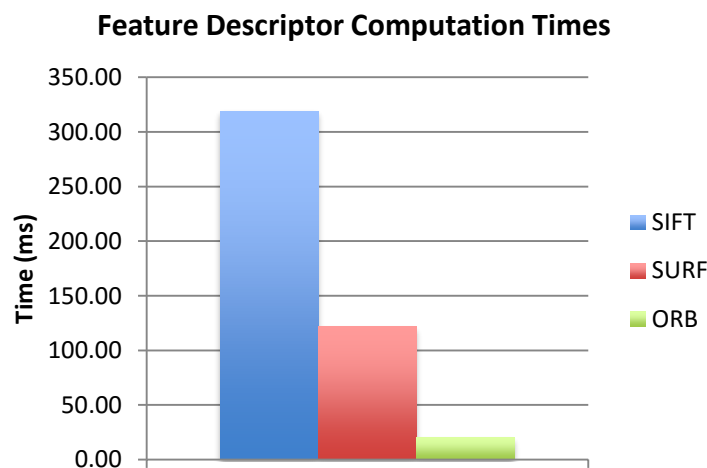


Figure 40. Graph of the computation time of each feature detection algorithm.

As can be seen in Figure 40, ORB was the fastest algorithm by a relatively large margin and SIFT, as expected, was the slowest.

Although speed is an important attribute, we next need to test if the descriptors produced by each algorithm can accurately match objects in different images. Feature matching was tested using two matching algorithms, the Brute-Force Matcher and the FLANN-based matcher. The OpenCV implementations of both algorithms were used for testing purposes.

To continue our comparison testing, we tested different combinations of detection and matching algorithms to attempt to discern which combination would detect our trusses with the most accuracy and which combination would detect them the quickest. Results are compared in Figure 41.

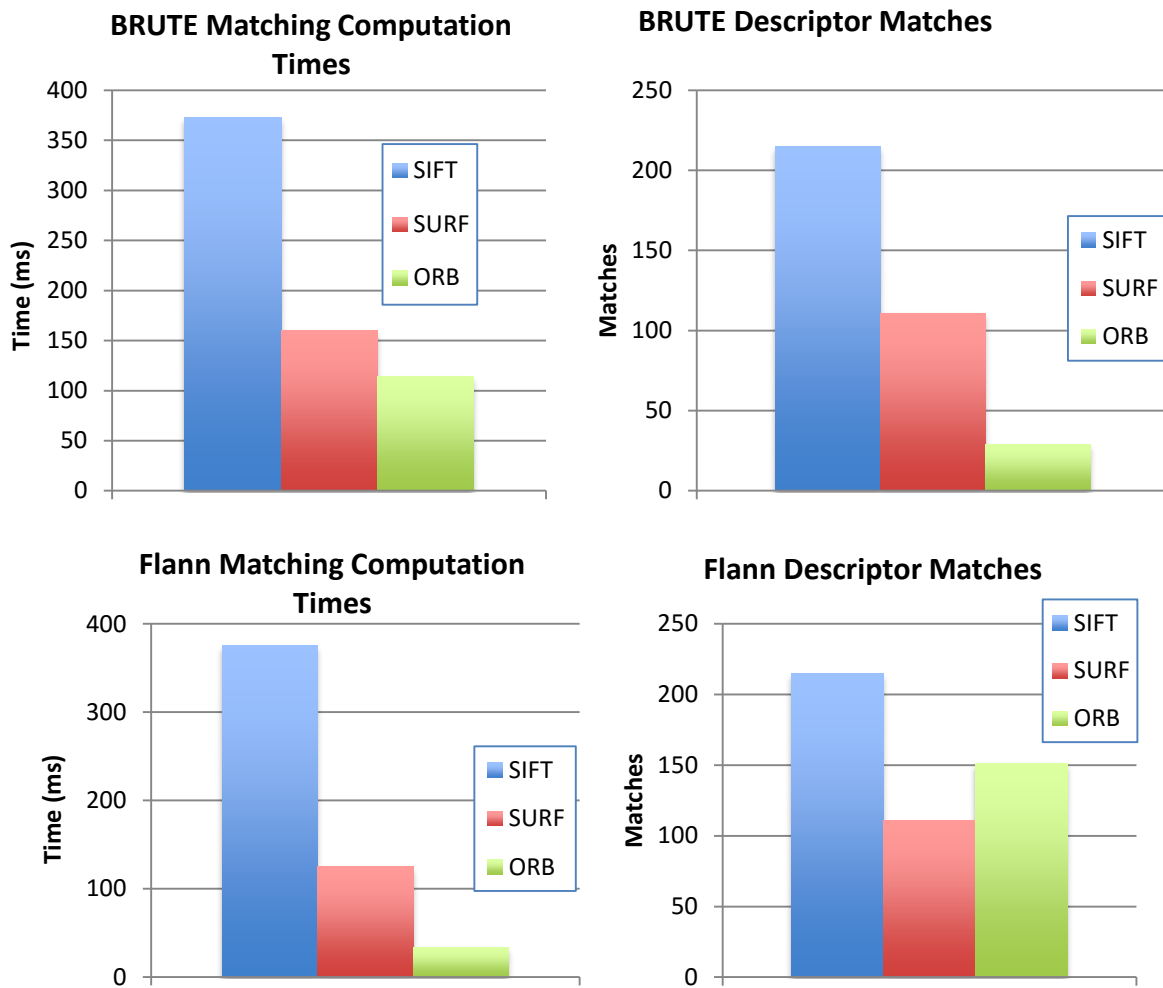


Figure 41. Testing BRUTE and Flann feature matching algorithms with database of truss images.

The resulting data reveals that the ORB feature detector combined with the FLANN Matching algorithm was able to match descriptors between the query and the train images the fastest—with an average computation time of 32.2 milliseconds. ORB-Brute was second-fastest, averaging 111.1 milliseconds and SURF-FLANN was third fastest at 121 milliseconds.

However, despite being among the slowest combinations, the SIFT algorithm with either the FLANN-based or Brute-Force matcher consistently found the most descriptor matches between images--making those combinations the most accurate.

For our application, the ORB-FLANN algorithms were chosen to perform all our descriptor due to the fast computation times and impressive accuracy.

Note that unlike the line detection-based method tested previously, most of the calculations and image processing steps required to perform can potentially be done entirely by the feature detection algorithm—which would greatly speed up calculation time. Unfortunately, feature detection alone is not always reliable given the truss structure. Thus, our final truss detection implementation employs both methods. The line detection method is generally used to find the

entire truss within an environment, and feature descriptor matching is performed to detect finer details of the truss such as truss end points and robot gripper grasping points.

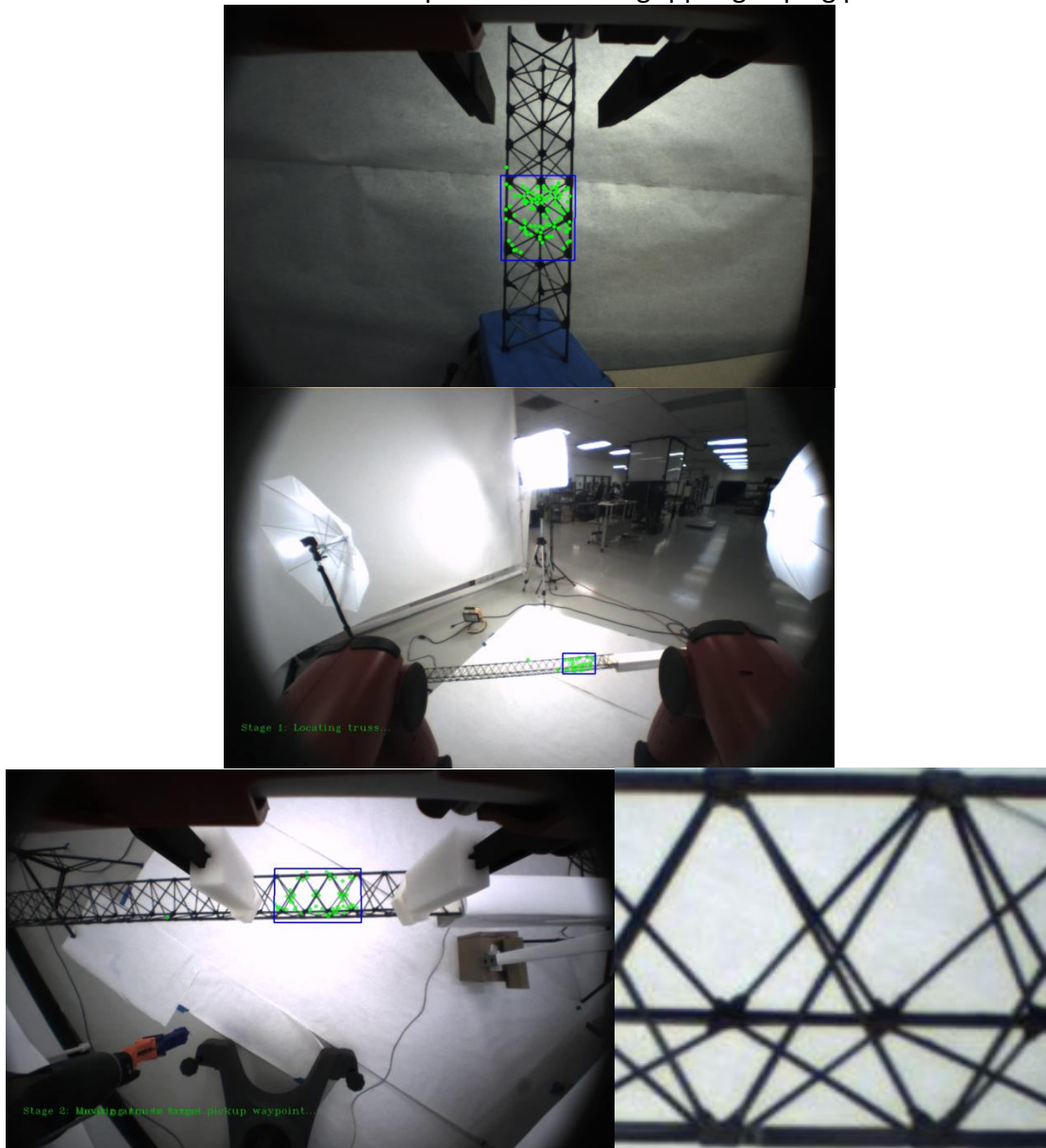


Figure 42. Truss Object Detection using ORB-FLANN Feature Descriptor Matching with a common query image (bottom right).

During our testing, ORB-FLANN feature descriptor matching worked well and generally provided consistent results in various lighting conditions and scales. It did however, struggle when the same query image was used to detect truss at significantly different angles. We chose to compensate for this by using multiple query images of trusses at different angles. If a truss could not be found, we cycled to the next query image until the truss was either identified or presumed absent from the train image.

2.2.4 SpiderFab Robotics Testing Software Platform

To facilitate development and testing of the control algorithms, robotic tools, and assembly CONOPS, we developed a software platform combining GUI, controls, and visualization. Since we expect our robotic software applications will continually evolve as the SpiderFab architecture matures from prototyping stages to final implementation, we decided to structure our software infrastructure to achieve our long-term goals of creating flexible, robust and hardware-agnostic software applications for SpiderFab. This new infrastructure consists of a retooled software version control system, improved coding standards, and a new software architecture that will serve as the foundation upon which all future robotics applications will be constructed.

2.2.4.1 Architecture

The software architecture for our robotics applications serves as both a shared blueprint and accelerated starting point for future applications. Because of this commonality amongst applications, a significant amount of the developed code can be reused, thereby speeding up the development process as well as subjecting the code to rigorous functional testing, making it more robust and reliable in the long term.

Care was taken to establish clear design goals for our new software framework to ensure our resulting implementation remained flexible enough to accommodate a wide range of applications and hardware platforms. After researching preexisting software architectures with similar aims, we ultimately decided that it must have the following characteristics:

1. Hardware Agnosticism – All software applications should be portable across various hardware platforms with minimal effort. An example of such an application would be the control software used for commanding robot movements. This application would ideally be able to run on a PC during early testing phases and then later ported to the final embedded hardware.
2. Reusability/Modularity – The architecture should allow for a significant amount of developed code to be easily reusable across multiple applications. Additionally, software code bases and drivers should be structured in a self-contained manner to allow for applications to be flexible to changes in hardware and software requirements.
3. Scalability – Applications should be allowed to start small and then incrementally scale up as the project matures while minimizing unnecessary complexity.
4. Code Quality/Clarity – The code should be well structured, easily understood by developers and reliable. The minimization of code complexity should always be emphasized during code development.

With our design goals now clearly established, our resulting software architecture was designed using a hierarchical approach commonly used by many middleware web services and cross-platform software frameworks (such as the Android mobile operating system).

The idea is to create a collection of software components organized into “layers” of an overall software stack that provide common or platform-specific services that the application requires but does not necessarily want to handle directly. This adds several layers of abstraction be-

tween the high-level application software, the mid-level software drivers and low-level hardware drivers—making applications flexible to changes in software requirements and reusable across hardware platforms simply by replacing certain layers of the software stack. This manner of structuring code should allow for all of our target goals to be reached. Below is the generic software stack used for SpiderFab software applications.

SpiderFab Robotics Software Architecture

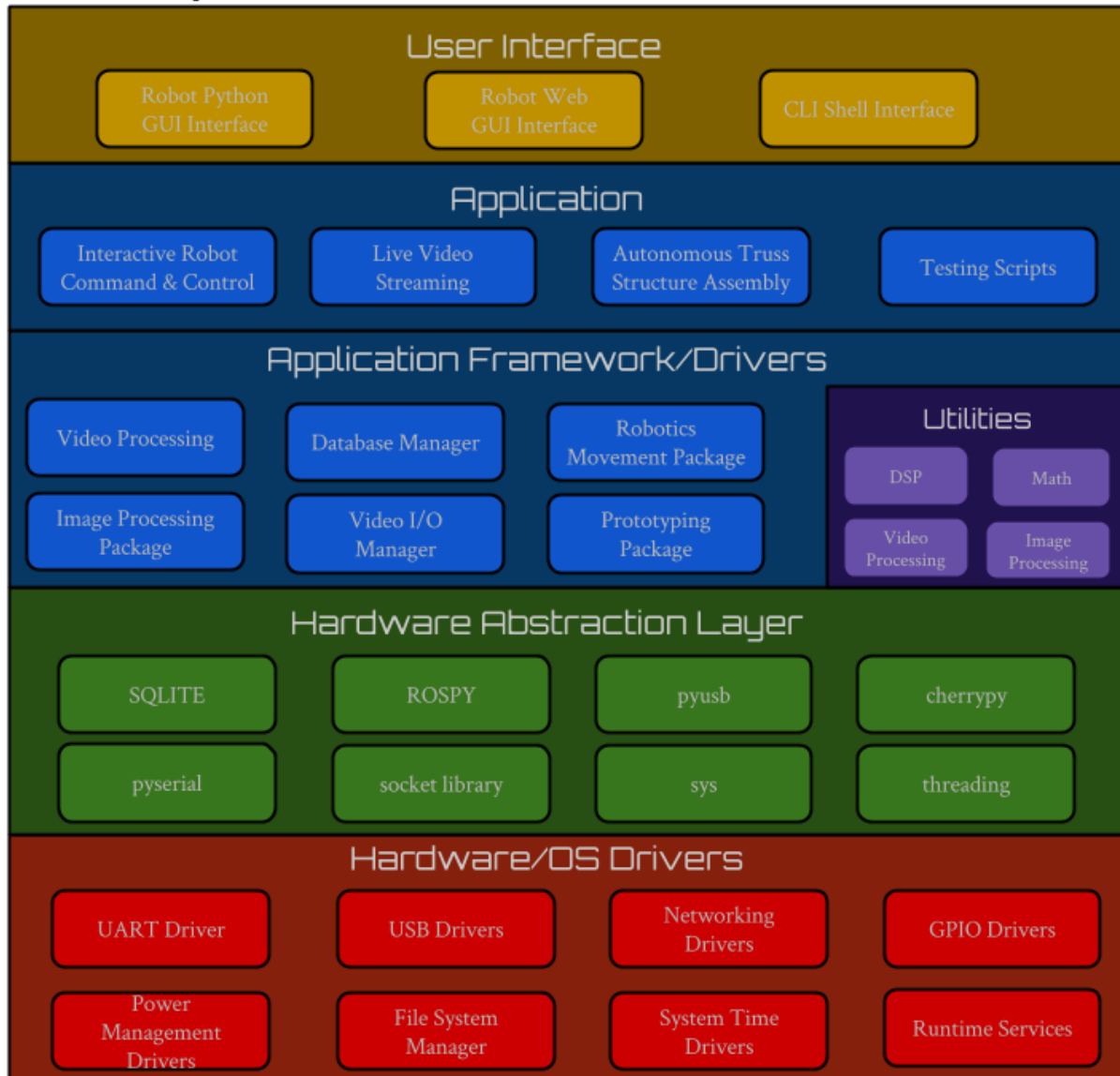


Figure 43. SpiderFab Software Architecture.

1. **User Interface** – Software specifically built to handle the input/output information of the application. A GUI application running on a PC or a command line shell for an embedded device running Linux are common examples. Proper partitioning of user interface code from the application layer should allow applications to run off multiple user interfaces with minimal effort. We developed several user interfaces for our SpiderFab applica-

tions, including Python and web-based GUIs for controlling our robotic test unit Baxter, as shown in Figure 44.

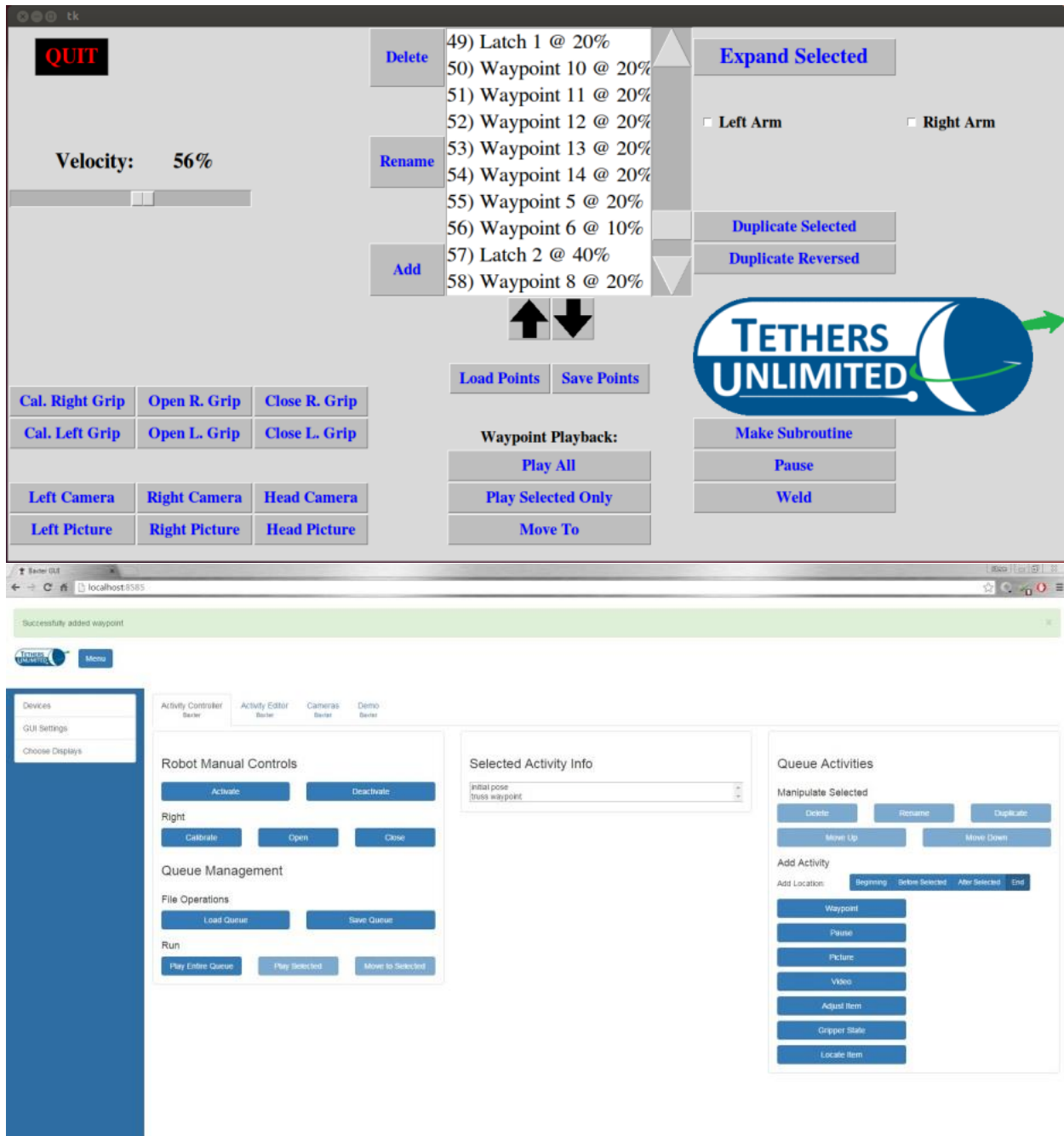


Figure 44. Example of running an application from two different GUI interfaces. The first GUI (top) was quickly built for initial testing using the Python TK library. We later upgraded to a custom HTML-based GUI (bottom) for a cleaner cross-platform interface with more sophisticated controls.

2. **Application** – This layer contains the main application software. Testing scripts, robot control software and video streaming applications are a few applications created for SpiderFab.

3. **Application Framework & Drivers** – Contains generic driver code that applications can access directly to perform a common task. An example is the image processing libraries that both our video streaming and truss assembly applications use for processing photos taken by our robotic cameras.
4. **Hardware Abstraction Layer** – Wraps low level hardware drivers into a common interface that the framework drivers can use. This allows all the upper layers of the software stack to be reused across hardware platforms simply by modifying code at this level.
5. **Hardware/OS Drivers** – Low level software drivers that directly interact with system hardware. These generally come prepackaged with the hardware and do not have to be developed internally.

Figure 45 below illustrates the software stack of our Baxter robot command and control software running on our custom HTML GUI implemented using our SpiderFab architecture.

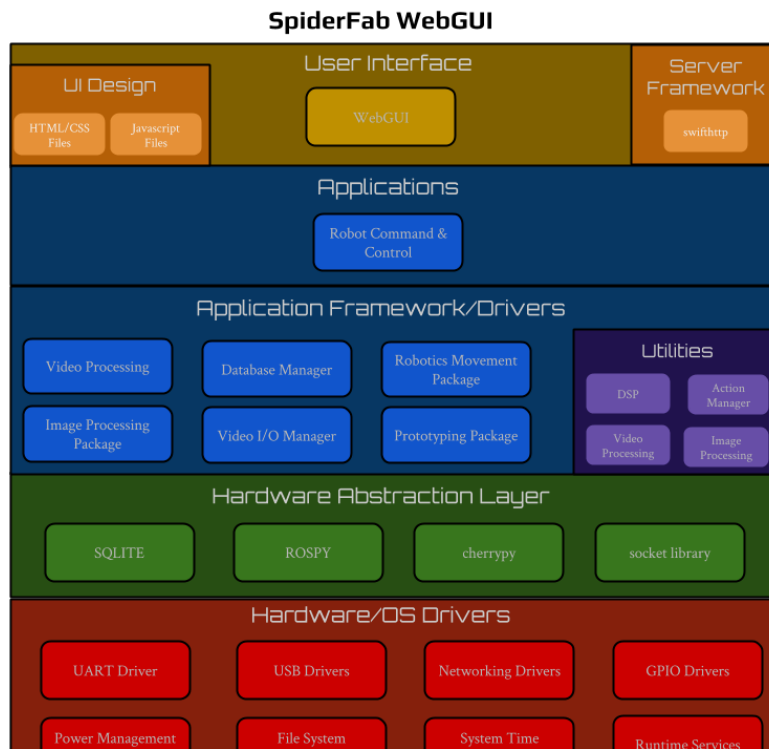


Figure 45. Baxter Command and Control Software Architecture Using Web GUI.

2.2.4.2 Software Infrastructure Upgrades

Once our software architecture was in place, we updated our version control practices to take advantage of this layering separation. Each layer in the SpiderFab Architecture software stack became a separate sub-repository. New applications are built in separate project workspaces, with directories structured in manner similar to our software stack layout. Our coding standards were also optimized to ensure our software applications are of the highest quality. This included the introduction of new tools to facilitate improved code transparency and auto-documentation into our code bases.

2.2.5 Custom End Effector

To enable robotic systems such as the Baxter to grasp and manipulate trusses, we prototyped and evaluated several different gripper designs. The design space looked at trading off compliance, locating features, and size to account for a robotic arm with larger end pose tolerances. It was desired to have a gripper that would locate the truss when the end effector grabbed it and have enough compliance to allow the end effector to be offset from the optimal position.

The base end effector used on the Baxter robot was the parallel gripper, shown in Figure 46. This gripper had 2 fingers that were moved to an open or closed position. There were screw mounts as well as ridges on the fingers to allow for customizing the gripping surface.



Figure 46. An unmodified Rethink Robotics parallel gripper designed for use with the Baxter robot.

Because the Baxter robot's motions had a measured tolerance of approximately $\frac{1}{2}$ centimeter the gripper designs had to be compliant. It was also desired that when the grippers closed, the truss was put into a known and desired orientation. Figure 47 displays some of the gripper fingers that we tested.

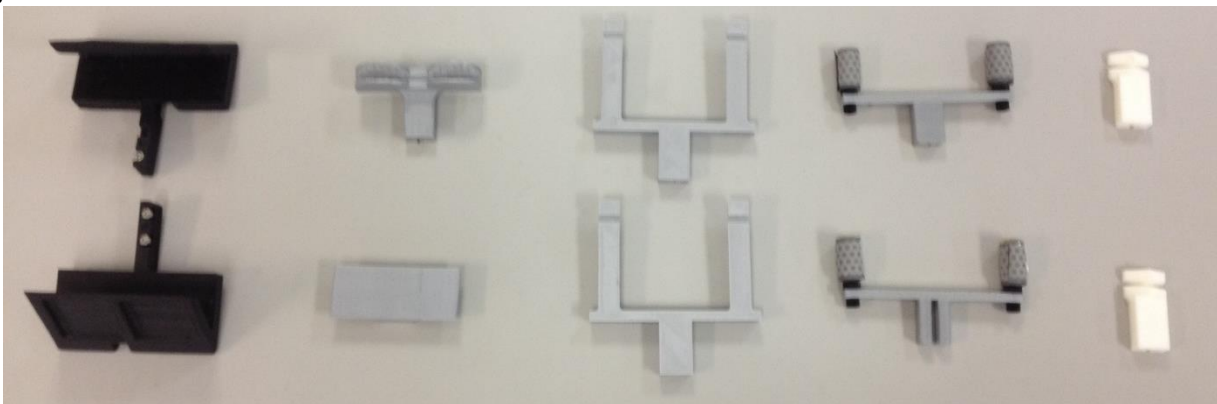


Figure 47. Various designs of gripper fingers.

Initial testing was conducted using an asymmetrical truss and no vision system. To align the truss axially, a set of triangular fingers were tested first. These fingers were bulky and had trouble grabbing the truss off of a flat surface. Another finger design gripped the truss's longe-

ron. This was considerably less bulky than the triangular fingers, but lacked the desired 3 points of contact needed for 6DOF control of the truss. As such, these fingers would often twist the truss into an orientation that was unworkable.

The revised Trusselator we have developed in our Phase II SBIR effort produces trusses that are symmetrical. This enable us to design a finger that gripped the truss on the diagonal members. This provided stability and a compact design. However, these grippers required a much more accurate placement than the previous grippers. To accomplish this precision, we developed the vision system discussed in Section SpiderFab Robotic Vision System. This vision system enabled us to reduce the final position error of the end effector to approximately 3 millimeters. Figure 48 shows one image from the correction algorithm for aligning the fingers to fit between the diagonal members.



Figure 48. Robot identifying truss grasping point and then capturing it with the final gripper design.

2.2.6 Truss Assembly Demonstrations

To test our improved software, gripper design, and new vision system, we developed a proof-of-concept demonstration that required our robot test unit (the Baxter Research Robot), to perform the following actions listed below completely autonomously.

1. Identify and locate the truss in our test environment.
2. Estimate the truss pose in 3D space.
3. Pick up the truss using feature detection algorithms to locate a grasp point on the truss, a closed-loop gripper alignment algorithm and our new gripper design.
4. Manipulate the truss and place it in a custom truss joint attached to the other robot arm.

We broke up the demo into three stages. Action items one and two from the list above were stage one of the demo, and stage two and three were responsible for items three and four respectively.

2.2.6.1 Stage 1 – Truss Object Detection and Location Approximation

For the first stage, a live video stream of 1280x800 frames from Baxter’s head camera was activated. Once the stream settled to our desired frame rate, we used our new line detection image processing algorithms detailed in section 2.2.1 on each frame received from the video stream. Although this slowed the framerate from 30 frames per second (fps) to roughly 7 to 10 fps, this speed is still more than adequate for performing “real-time” operations. For visual effect and debugging purposes, text and image processing overlays were also added to each frame in real-time, as shown in Figure 49.



Figure 49. Truss identification using edge and feature detection algorithms.

Once the line detection algorithms detected our truss, we used the ORB-FLANN feature descriptor matching algorithms (now optimized from previous tests) to locate the truss segment that the robot gripper will attempt to use to pick up and manipulate the truss, as shown in Figure 50.

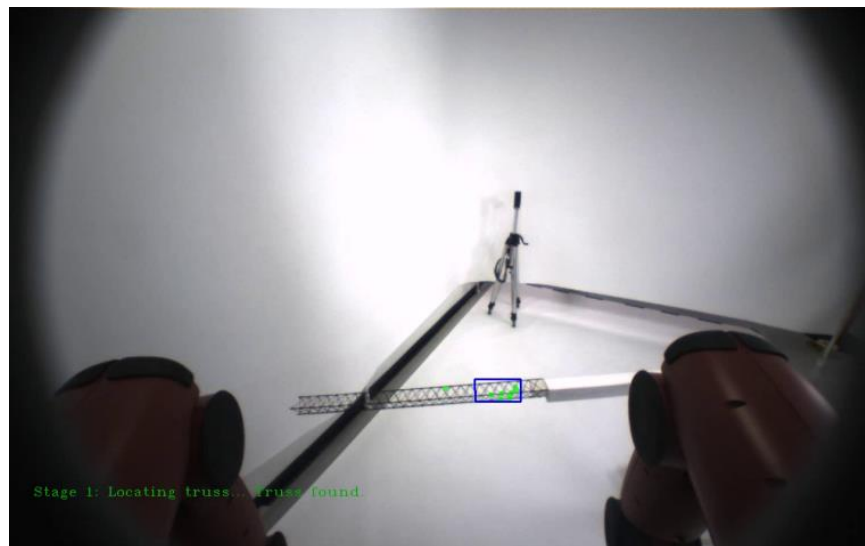


Figure 50. Truss location approximation using homography algorithms.

2.2.6.2 Stage 2 –Truss Alignment and Grasping

Stage two required Baxter to grasp and pick up the truss. This was the most challenging portion on the demo due to the high degree of precision required to align the grippers to pick up the truss and also the lack of precise movement capabilities by Baxter. Given our truss pickup point, and using standard x, y, z coordinates with respect to our gripper cameras (the z coordinates), our grippers has to be aligned with a tolerance of approximately +/- 2 millimeters in the x-plane, +/- 3 millimeters in the y-plane and +/- 3 millimeters in the z-plane. However, before we could begin implementing gripper alignment algorithms, we faced a common, but non-trivial, robotics problem of attempting to specify movements in different frames of reference.

All movement commands sent to Baxter are specified as arrays of joint angles which are generated from an inverse kinematics algorithm using 3-dimensional quaternion coordinates in a “base” frame of reference (where the origin is located at the physical base of the robot). However, when performing the gripper alignment, it is highly desirable to move the grippers using coordinates in the camera’s frame of reference.

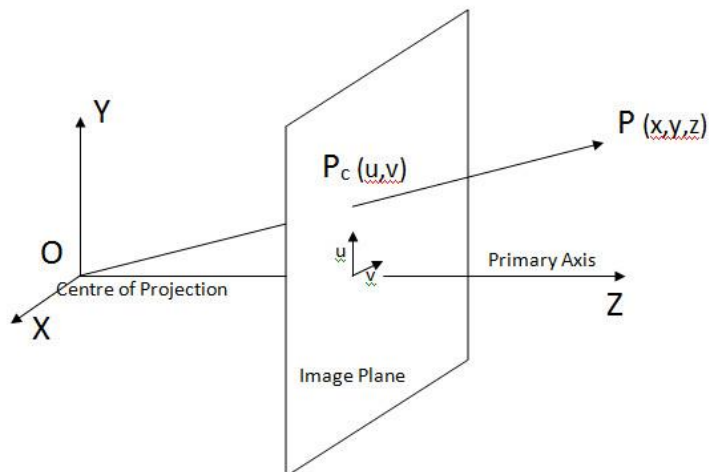


Figure 51. Camera calibration parameters.

Once we could specify coordinates in the camera’s reference frame, and the camera calibration factor was known, aligning the gripper could be solved by

1. Identifying a grasping point on the truss.
2. Determining the location on the truss the gripper is currently aligned to.
3. Creating a feedback loop to correct the gripper angle and x, y, z coordinates until it becomes aligned with our target grasping point.

Feature descriptor detection was used to find our grasping point—which for this test we arbitrarily chose to be the spacing adjacent to the fifth longeron crossing from the end of the truss.



Figure 52. Robot identifying truss grasping point.

The descriptors generated by the ORB feature detection algorithm contains a variety of information—including orientation information that can be used to discern the orientation of the truss in the x, y plane. It should be noted that because the cameras used by Baxter are not stereo vision, it was not possible to determine where the truss was located in the $\pm Z$ direction. That is, we could not determine how far the truss was from the arm camera using only the 2 dimensional images it was generating. This distance information is necessary in order to transform distance measurements from pixels into metric units (i.e. if the gripper is off alignment 20 pixels in the $+X$ direction, we should know how many millimeters in the $-X$ direction to move the robot arm to compensate).

This was a difficult issue to overcome and given our short time frame to complete this demo, we initially decided to use the ultrasonic range sensor located on the robot arm to judge distance. Unfortunately, the data measured by the sensor was often inconsistent due to the lack of solid surfaces on the truss. After many unsuccessful stage 2 attempts, we eventually conceded that we would need to hardcode an expected range in the interest of time--making this one of the few pieces of information that were not generated autonomously by the robot in the demo.

After the distance value was hardcoded to 10-13 centimeters, our algorithms began generating correct gripper adjustment values. Unfortunately, we next ran into an issue with our robot test unit. During our demo, Baxter initially had considerable difficulty executing fine adjustments to the gripper position. The robot would often not respond to commands to move the gripper short distances (which was often less than 3 millimeters) or would overshoot the desired location. Given the small margin for error, this led to very inconsistent grasping attempts. After tweaking the test setup numerous times, we eventually found that gripper movements were much more precise when the robot arm was placed in certain poses during the alignment phase. Once this was taken into account, Baxter was able to complete Stage 1 and 2 with much better consistency.

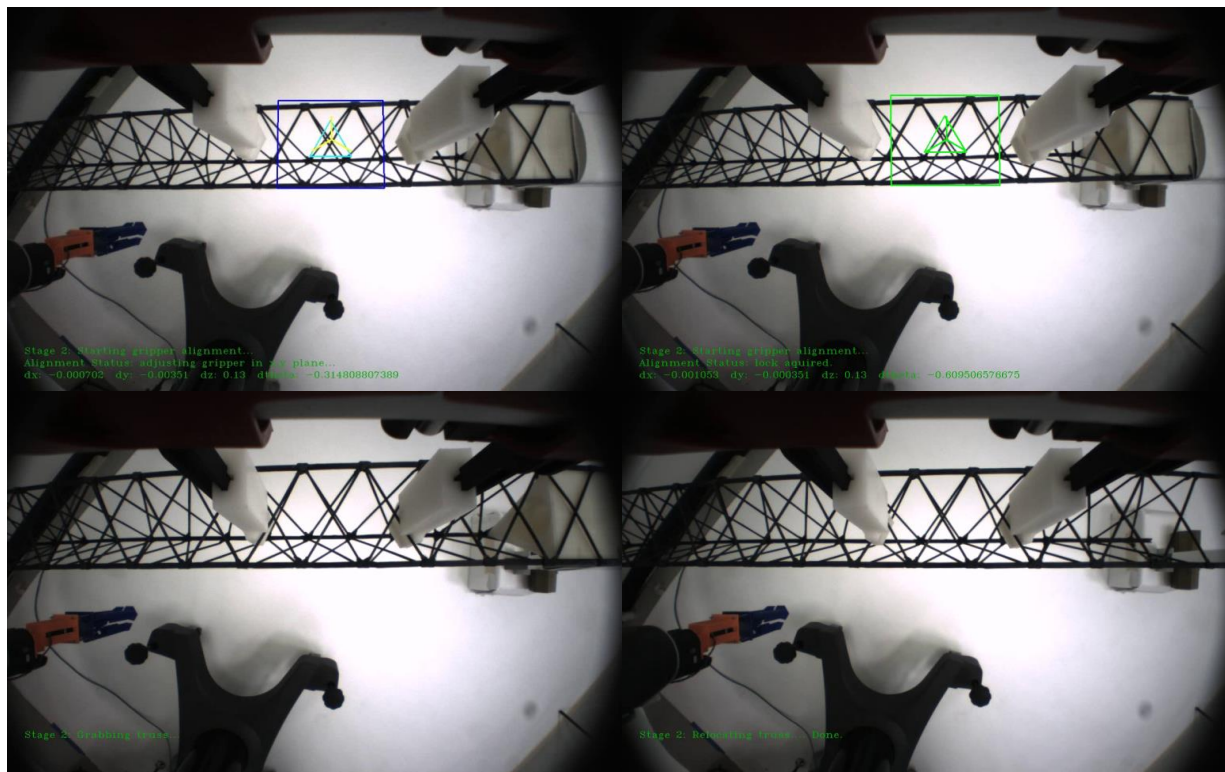


Figure 53. Real-time closed-loop grasping of truss.

2.2.6.3 Stage 3 – Truss Joint Assembly

The final stage required Baxter to maneuver the truss and place it into our 3D printed truss joint, which was designed to be attached to the end of the truss by a custom end-effector.

Since both the end effector truss joint and the truss (assuming it was grabbed in the correct location) are at known locations and dimensions, placing attaching the truss to the joint was simply a manner of aligning both arms such that the two objects could be joined. In the future, this alignment process will be aided by the image processing algorithms using the robot head camera.



Figure 54. Truss-joint and end effector.

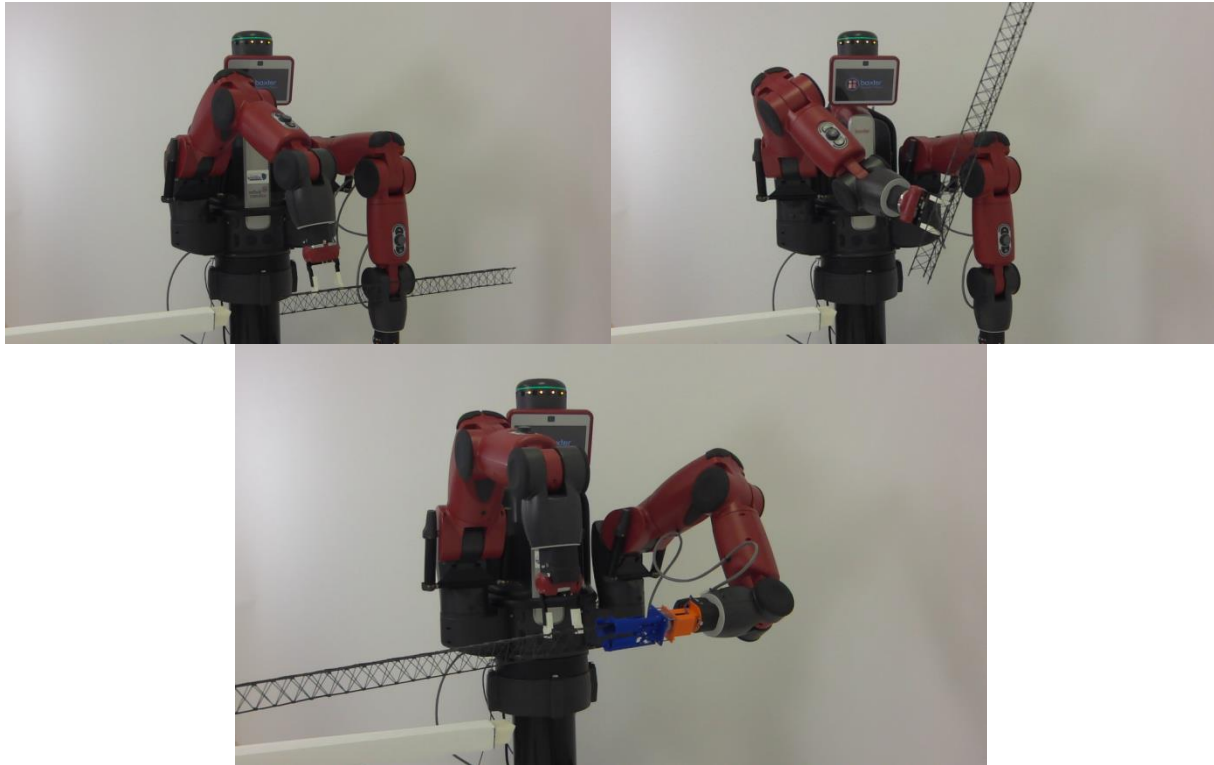


Figure 55. Truss to custom joint end effector assembly.

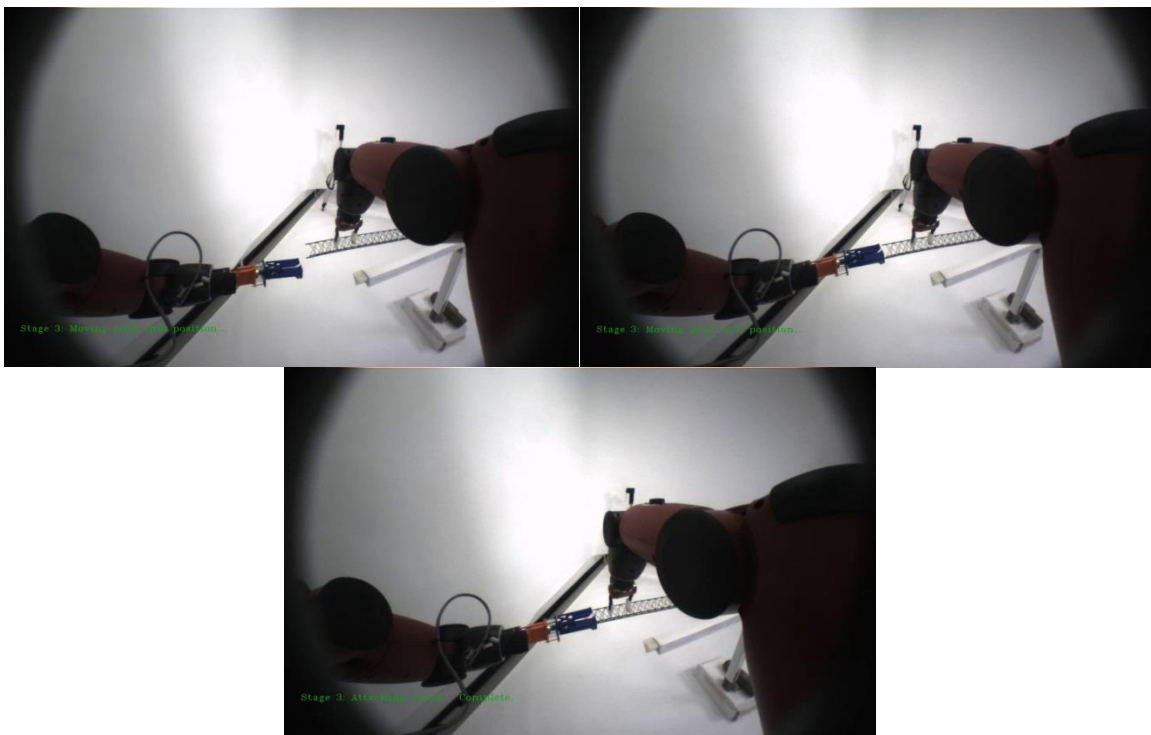


Figure 56. Truss to custom joint end effector assembly (head camera).

2.2.6.4 *Demonstration of Robotic Assembly of Spanner Joints*

Although the joint assembly demonstration described in Section 2.2.6.3 is relatively straightforward and would enable large structures to be assembled using a truss-and-connector method, similar to a ‘tinkertoys’ assembly approach, it has the disadvantage that the mass of the joint connectors will likely dominate the structure mass. A far more efficient structure can be constructed using spanner joints to connect between nodes in the truss, as was discussed in 2.1.1.3. Accordingly, we performed demonstrations using the Baxter robot wielding the Joiner Spinneret described in Section 2.1.4 to validate the feasibility of robotic systems assembling trusses using the highly efficient spanner joint method, as shown in Figure 57.

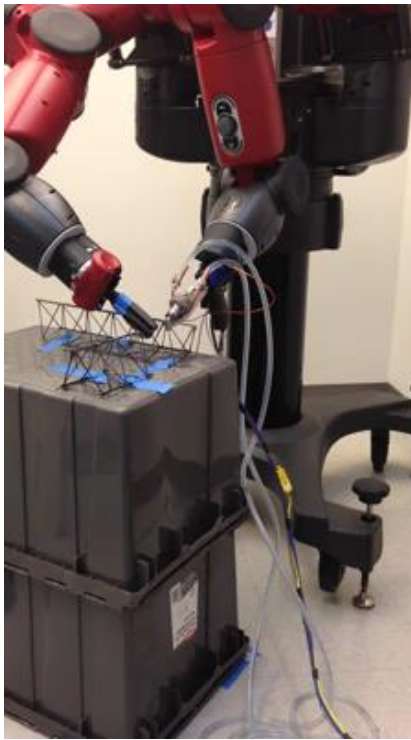


Figure 57. Demonstration of assembly of a spanner joint between perpendicular truss segments using the Joiner Spinneret end-effector on the Baxter robot.

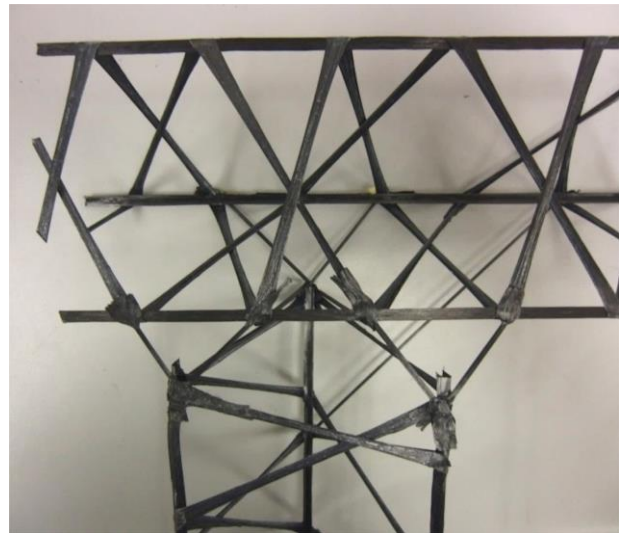


Figure 58. Spanner Joint Geometry. *Highly efficient joints can be formed between truss elements using the Joiner Spinneret to add additional CF/PEEK ligaments between nodes on the truss..*

2.3 DEMONSTRATION MISSION CONCEPT DESIGNS

2.3.1 MakerSat-I: Long-Baseline Sensor Mission Concept

In order to perform a low-cost initial demonstration of the value proposition of in-space manufacture of space structures, TUI is currently designing a CubeSat-based flight demonstration, called MakerSat-I. The primary objectives of MakerSat-I are to demonstrate ISM of a large space structure, characterize its structural performance, and demonstrate the utility of a Constructable structure as part of a long-baseline sensor system.

The preliminary configuration concept for MakerSat-I, shown in Figure 59, is configured as a 6Ux1U CubeSat for compatibility with the NanoRacks deployer aboard the ISS; a 2Ux3U configuration compatible with the CSD and other 6U deployers is also feasible. The MakerSat-I system will integrate our 3U Trusselator system with COTS CubeSat command and data handling (C&DH) and electrical power system (EPS) as well as a HYDROS water-electrolysis thruster and two SWIFT-XTS X-band software defined radios (SDRs), one positioned at and end of the truss system. An optical fiber dispenser derived from TUI’s Underwater Optical Fiber Dispenser will also be integrated into the system, and highly sensitive accelerometers will be integrated at both ends of the system.

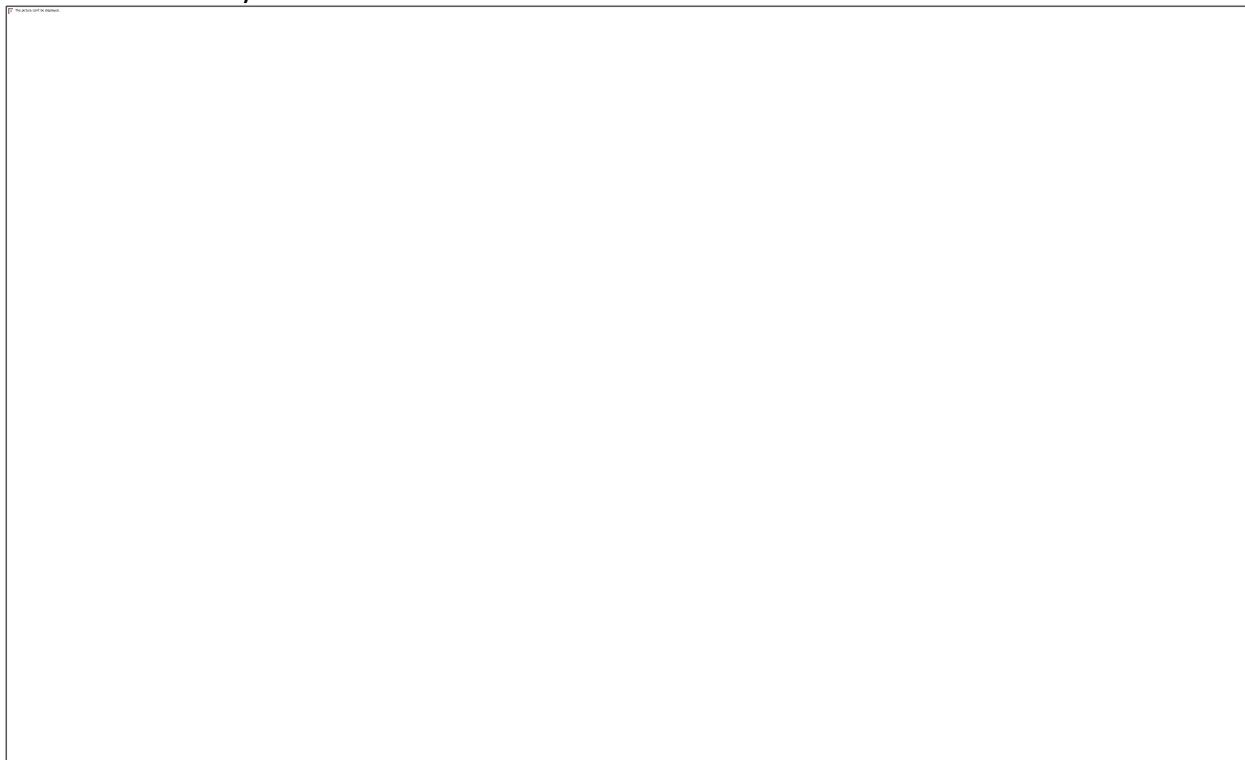


Figure 59. MakerSat-I concept 6U configuration. *The 6U MakerSat-I CubeSat will use a 3U Trusselator system to fabricate a 50m truss in between two X-band software defined radios to demonstrate long-baseline one-pass Interferometric SAR capabilities.*

In the baseline MakerSat-I mission concept, after deployment from the ISS, the system will first deploy its solar panels and antennas. After a delay sufficient to ensure safe separation from the ISS, the satellite will use its HYDROS thruster to move to its desired operational orbit. The system will then activate the Trusselator system, which will additively manufacture a 50m truss. To provide a sense of the scale involved, Figure 60 shows the 50m truss juxtaposed with the

SpaceX Dragon capsule. As the system fabricates the truss, the fiber dispenser will deploy the fiber inside the truss, running from one end of the truss to the other in order to provide high-bandwidth data transfer and sub-ns synchronization between the two SDRs. This timing synchronization will enable the SWIFT-SDRs to operate coherently and provide for phase alignment between the radios. As the system manufactures truss, the truss integrity will be diagnosed by forcing vibrations into the system using thrust impulses provided by the HYDROS thruster and/or small vibratory motors, such as those used in cell phones, and recording the response of the truss structure using the accelerometers positioned at both ends of the system.

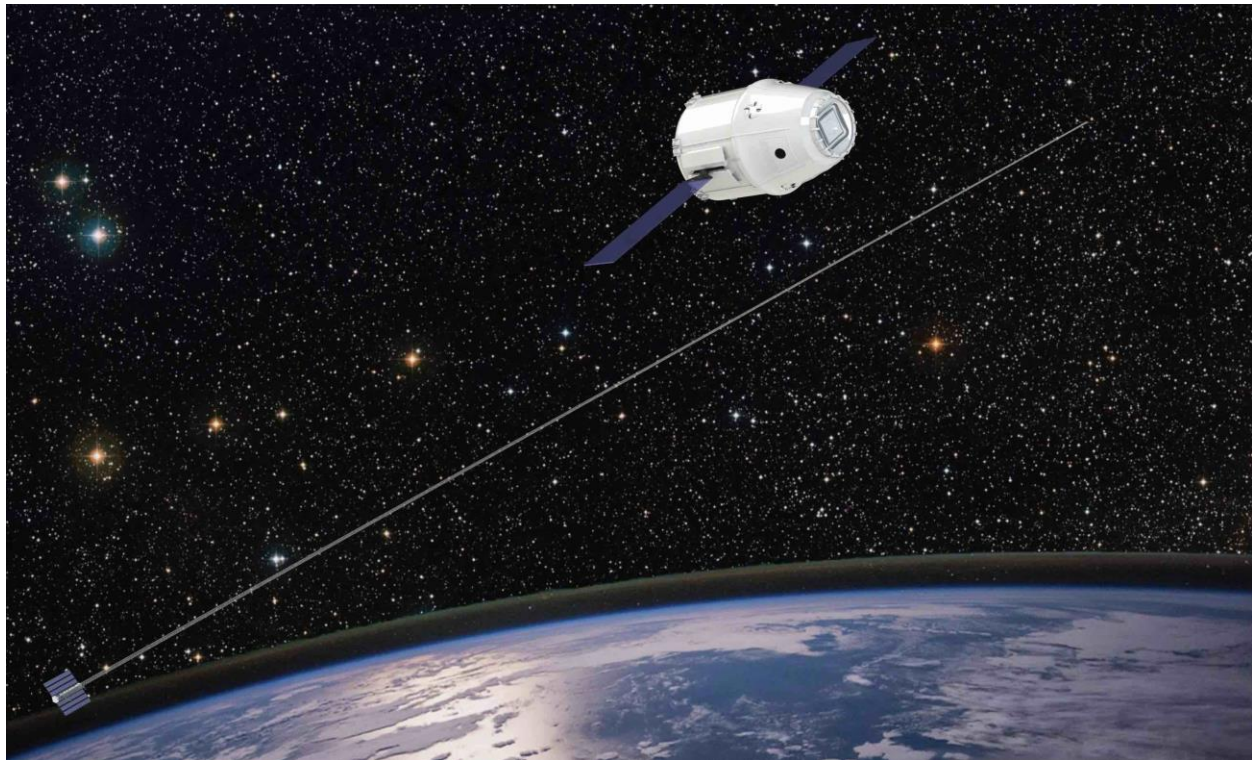


Figure 60. MakerSat-1 “Constructable™” Long-Baseline Sensor. *Dragon capsule shown to provide a sense of scale.*

To demonstrate the utility and value proposition of this Constructable structure, the MakerSat-I mission will then operate the two X-band SDRs as an interferometric synthetic aperture radar (InSAR) or as a long-baseline astronomical interferometer. For InSAR demonstrations, the MakerSat-I system will operate parasitically, relying upon radar transmissions by a much larger satellite. As the truss deploys, gravity gradient forces will tend to orient the system along the local vertical, but off-vertical orientations can be achieved to improve InSAR performance by using the HYDROS thruster to set the system into a cross-plane libration.

The potential performance of this small, low-cost InSAR system can be estimated using the expression for the sensitivity of InSAR height measurements to phase errors:²

$$|\partial h| \approx \frac{\lambda R \cos \psi}{4\pi B \sin(\psi + \beta)} |\partial \phi|, \quad (1)$$

². Richards, M.A., “A Beginner’s Guide to Interferometric SAR Concepts and Signal Processing”, IEEE A&E Systems Magazine, Vol. 22, No. 9 September 2007

where λ is the RF wavelength, ψ is the angle between the local horizontal and the target, β is the angle between the baseline and the local horizontal, B is the baseline length between the receivers, and $\partial\phi$ is the phase measurement error between the receivers. The SWIFT-XTS SDRs are designed to enable coherent operation, and testing under prior efforts has indicated that phase coherency within at least 10 degrees, and potentially as low as 1 degree, is possible. With a baseline length of 50 meters, an operating frequency of 9 GHz, an altitude of 300 km, the truss oriented 45 degrees away from vertical in the cross-plane direction, and a look angle of 45 degrees, we expect the MakerSat-I CubeSat could achieve measurement height accuracy comparable to the 6m demonstrated by the (\$200M+) SRTM experiment flown on the Shuttle *Endeavor* in 2000, and potentially as low as 1 m in a best-case scenario.

2.3.2 MakerSat-II: Constructable™ Antenna Demonstration Mission

The MakerSat-II mission will demonstrate the technical feasibility of combining additive manufacture of RF reflectors with robotic assembly technologies to enable a compact, lightweight payload to perform in-space manufacture (ISM) of large antennas to enable challenging signals intelligence (SIGINT) and satellite communications (SATCOM) missions.

Motivation: Currently, multiple commercial and government efforts are pursuing development of constellations of small satellites in LEO to provide high-bandwidth, low-latency, resilient data services to ground users. Due to the small sizes of the RF apertures these SmallSat systems can deploy, closing the data link requires that the ground users connect to satellite terminals or ‘hotspots’ having antennas at least the size of a laptop computer. This requirement for a bulky and expensive antenna limits the potential market for such a system. A Direct-to-Smartphone broadband (DTSB) service would dramatically increase the utility of a SATCOM system for consumers and military operations. However, closing a broadband (≥ 10 Mbps) data link from LEO to a smartphone carrying an omni antenna and having ~ 33 dBm transmit power will require the satellite use a high gain antenna with diameter on the order of 10-25 meters. Although high-TRL large deployable antennas are available, they have very high recurring costs ($\sim \$500\text{K}/\text{m}^2$), and even when stowed require a large volume within a launch shroud. Consequently, fielding a DTSB SATCOM system using current Deployables technology requires high launch and recurring satellite fabrication costs, making DTSB systems financially untenable unless a more affordable large-antenna technology emerges.

Approach: The MakerSat-II effort will design, prototype, and test a compact “Constructable™ Antenna” payload capable of in-space manufacturing of large antenna reflectors. Figure 61 illustrates a palletized work cell that will fabricate a zero-CTE composite truss support structure and concurrently manufacture and attach reflector segments to assemble a large reflector. To construct a large parabolic dish, the system will first assemble the central portion of the dish and then then build up both the support structure and reflector. Fabrication of the support structure will use the Trusselator™ system developed under NASA SBIR contract NNX14CL06C as well as the real-time vision-based robotics control methods and assembly tools discussed in Section 2.2. A metrology system and adjustable mounting features on the truss will enable closed-loop control to achieve the shape accuracy necessary for the antenna reflector.



Figure 61. Concept for a Constructable™ Antenna payload.

3. OUTREACH AND TRANSITION EFFORTS

3.1 OUTREACH

In addition to our technical work, we have also performed significant efforts to disseminate the results of our NIAC work as well as to identify potential avenues for post-NIAC transition. Below is a list of major outreach efforts performed during the SpiderFab Phase II effort:

- Presented an invited talk on SpiderFab at the Additive Aerospace Summit in Los Angeles, CA on 17 October 2013.
- Presented SpiderFab to the NRC Committee on Space-Based Additive Manufacturing (COSBAM), Irvine CA 12 November 2013. This briefing resulted in the COSBAM report on 3D Printing in Space (http://www.nap.edu/catalog.php?record_id=18871) highlighting “Creation of Structures Difficult to Produce on or Transport from Earth” as one of the more promising potential applications of additive manufacturing in space.
- Presented an invited talk on SpiderFab at the IdTechEx "3D Printing Live!" conference in Santa Clara, CA on 21 November 2013;
- Dr. Hoyt participated as a subject matter expert in an 'industry ecosystem' workshop on 3D printing at Dupont on 2 December 2013;
- Presented invited talk on SpiderFab at the Additive Disruption Summit in San Francisco, 26 March 2014;
- Presented invited talk on SpiderFab at the WA State Joint Center for Aerospace Technology Innovation (JCATI) Symposium at WSU, 21 April 2014;
- Presented invited talk on SpiderFab application to SBSP at the SolarTech Conference, 23 April 2014, in NYC;
- Presented “SpiderFab: Architecture for On-Orbit Manufacture of Large Aperture Space Sys-

tems” FISO Telecon Colloquium, 4 March 2015;

- Presented SpiderFab at the 2015 NASA Tech Day on the Hill event, 29 April 2015;
- NASA 360 TV story on the NIAC SpiderFab effort: <https://goo.gl/996C1F>
- Presented a talk titled “It’s only Science Fiction... Until You DO it!”, featuring SpiderFab, at the “Science Fiction/Science Fact” event at the Museum of Flight, 25 October 2015;
- Presented invited talk on SpiderFab to the Seattle Futurists Society, 12 Dec 2015;
- Presented invited talk on In-Space Additive Manufacturing of Spacecraft Structures at the University of Washington Collaborative Center for Advanced Manufacturing (CCAM), 14 January 2016.

These efforts, along with the (very much appreciated) efforts of Kathy Reilly and others at NIAC to spread the word about our effort have resulted in a large number of positive print and web articles about SpiderFab.

3.2 TRANSITION SUCCESSES

As discussed previously, this NIAC Phase II effort very quickly transitioned to post-NIAC efforts in the NASA/LaRC “Trusselator” SBIR contract.

We believe the results of this NIAC effort also contributed to NASA STMD including in-space manufacturing as a technology of interest in the 2015 Tipping Point Technologies program solicitation. That in turn resulted in TUI teaming with a large prime contractor on a successful proposal to perform a demonstration of in-space manufacture of a key GEO satellite structure, and a contract to begin preparing that flight demonstration is pending.

CONCLUSIONS

In-Space Manufacturing (ISM) of key space system components such as antennas, arrays, and optical systems offers the potential to enable NASA, DoD, and commercial space programs to escape the limitations of rocket shroud volumes and create systems with order-of-magnitude improvements in performance-per-cost relative to current state of the art. The SpiderFab Phase II effort made significant progress in validating the technical feasibility of an ISM architecture in which large apertures will be fabricated *in-situ* using techniques adapted from additive manufacturing (3D printing), automated composite layup, and robotic assembly. The effort developed and demonstrated end-effector tools, vision-based control software, and concepts of operation (CONOPS) to enable robotic systems to assemble composite truss elements manufactured in space to construct large, extremely-high-performance support structures for antennas and other apertures. The effort also developed concepts for several affordable technology demonstration missions that will validate the key technologies in a staged, incremental manner. Most significantly, it has resulted in successful transition to post-NIAC activities, including a SBIR contract to develop system for in-space manufacture of truss structures and a NASA Tipping Point Technologies subcontract effort to demonstrate ISM of a key GEO satellite structure.

APPENDIX A SPIDERFAB JOINER HEAD CONFIGURATION TRADE STUDY

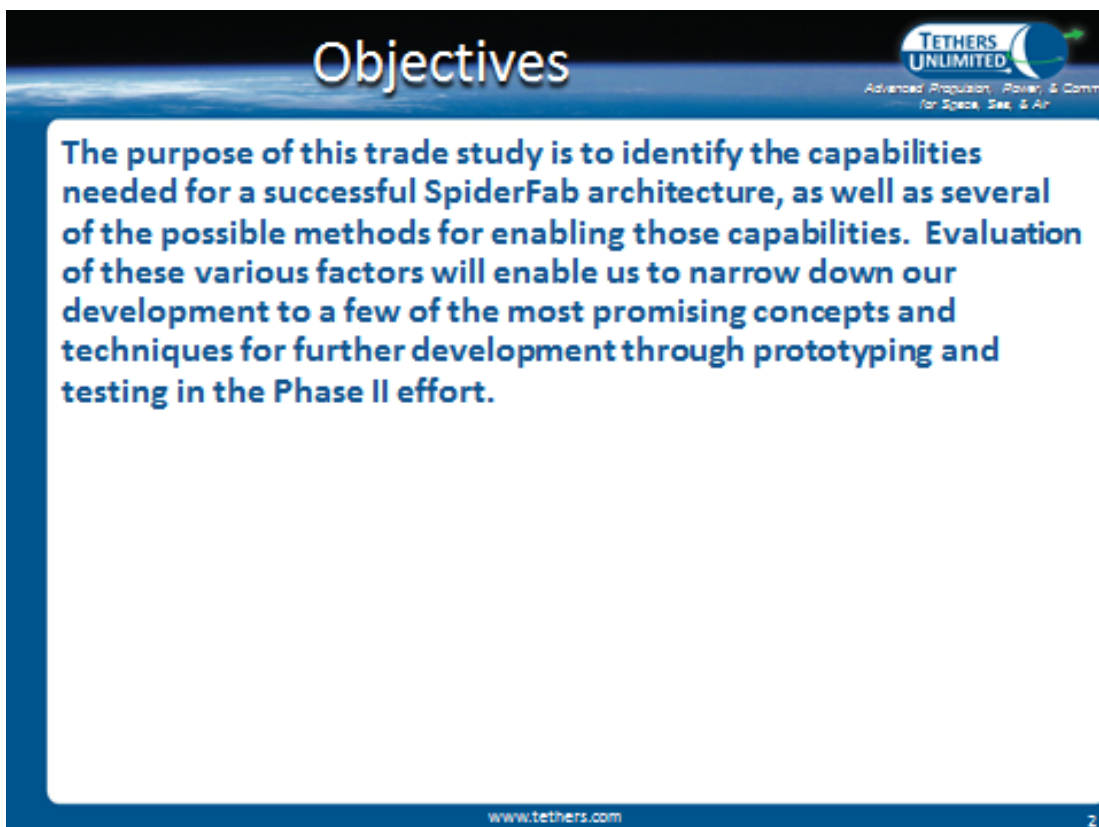


 TETHERS
UNLIMITED
Advanced Propulsion, Power, & Comm.
for Space, Sea, & Air

SpiderFab Joiner Head Configuration Trade Study

Tethers Unlimited, Inc
11711 N. Creek Pkwy S., Suite D113
Bothell, WA 98011
425-486-0100 information@tethers.com

www.tethers.com 1



 TETHERS
UNLIMITED
Advanced Propulsion, Power, & Comm.
for Space, Sea, & Air

Objectives

The purpose of this trade study is to identify the capabilities needed for a successful SpiderFab architecture, as well as several of the possible methods for enabling those capabilities. Evaluation of these various factors will enable us to narrow down our development to a few of the most promising concepts and techniques for further development through prototyping and testing in the Phase II effort.

www.tethers.com 2

Variables Under Consideration



Advanced Propulsion, Power, & Comm
for Space, Sea, & Air

- A. Feedstock Composition**
 - Same as trusses (PEEK) vs Ultem, Fiber Fraction, Carbon vs Boron.
- B. Feedstock Format**
 - Separate Resin and Fiber, Comingled Yarn, Consolidated Tape, Consolidated Rod, Pre-Cut Rods
- C. Heating Methods**
 - Contact (hot plate), Ultrasonic, Laser, Radiative, Microwave, Ohmic
- D. Compaction Methods**
 - Rolling or Sliding or Stationary Contact, Belt vs Wheel, Support back side?
- E. Joint Geometry Scheme**
 - Trusses end at point, Trusses butt together, or Trusses Spaced apart.
- F. Feature Integration Scheme**
 - Fused Filament Fabrication (FFF), Clamp on Fittings
- G. Gripping Mechanisms**
 - Node Grabber vs Truss Grabber, Rigid vs Compliant

www.tethers.com 3

Evaluation Criteria



Advanced Propulsion, Power, & Comm
for Space, Sea, & Air

- Feasibility of Satisfactory Progress during Ph 2
- Expected Performance making Regular 2nd order Truss
- Expected Performance making Arbitrary geometries
- Expected Process Failure Rate
- Expected Production Rate
- Applicability to Trusselator Wrapping Feedheads
- Applicability to Terrestrial Fabrication

www.tethers.com 4

Challenges



Advanced Propulsion, Power, & Comm.
for Space, Sea, & Air

- Avoiding jams, clogs, fuzz, particulates
- Cleaning of feed-heads and compactors if necessary
- Achieving high quality rod members
- Making high quality lamination at joints
- Determining the best structural geometry at each joint
- Fixturing and manipulation
- Any necessary mobility of the robotics
- Accuracy of the assembled 2nd order trusses
- Integrating functional elements, 'payload' (solar blankets, sensors, etc.)

www.tethers.com 3

A. Feedstock Composition



Advanced Propulsion, Power, & Comm.
for Space, Sea, & Air

- 1. PEEK vs. Ultem**
 - a. PEEK matches what was used in the Trusselator and will produce better bonds
 - b. PEEK has higher service temperature and lower outgassing
 - c. PEEK will be selected for use in the present development effort, but Ultem is still a material of interest that may be further investigated
- 2. Fiber Fraction**
 - a. High fiber content is desirable for strength and stiffness
 - b. High resin content is desirable for formability and joining
 - c. The present effort will continue to investigate the optimal ratio of fiber to matrix for various applications of the SpiderFab technologies
- 3. Carbon vs. Boron**
 - a. Boron has higher compressive strength
 - b. Boron may be useful for rad shielding
 - c. Carbon is more readily available and less expensive
 - d. Carbon will be selected for use in the present development effort, but Boron is still a material of interest that may be further investigated

www.tethers.com 6

B. Feedstock Format



Advanced Propulsion, Power, & Comm.
for Space, Sea, & Air

1. Separate resin and dry fiber
2. Comingled Yarn
3. Continuous Consolidated Tape
4. Continuous Consolidated Rod
5. Pre-cut rods

www.tethers.com 7

B. Feedstock Format



Advanced Propulsion, Power, & Comm.
for Space, Sea, & Air

1. Separate resin and dry fiber is combined and formed into rods on orbit
 - a. Could enable dry fiber tension lines, which might allow a more mass-efficient truss
 - b. Might enable resin content to be lower for member lengths, and higher at joints
 - c. Easy to buy resin and fiber components separately
 - d. Wet-out process is entirely performed during final processing, increases mechanical work in process, likely to be challenging to achieve good results with the wet-out process, may drive size, power, and complexity up.
 - e. Potential for tangling or snagging, either on the spool, or in routing, especially if tension is not maintained
 - f. Cannot push fiber material through process train, might be able to push the resin if in a FDM/Bowden-style filament.

NOT SELECTED FOR FURTHER DEVELOPMENT

www.tethers.com 8


Advanced Propulsion, Power, & Comm
for Space, Sea, & Air

B. Feedstock Format

2. Comingled Yarn is formed into rods on orbit

- a. Can be pirn wound
- b. May enable more options in wrapping pattern
- c. Similar to first generation Trusselator, which might allow similarly simple mechanisms.
- d. Might not be suitable to level wind
- e. Potential for tangling or snagging, either on the spool, or in routing, especially if tension is not maintained
- f. Potential for accumulation of frayed fiber bits and excess resin
- g. Wet-out process almost entirely performed during final processing, increases mechanical work in process, likely to be challenging to achieve good results with the wet-out process, may drive size, power, and complexity up.
- h. Not known to be a commercially available material format
- i. Cannot push material through process train

NOT SELECTED FOR FURTHER DEVELOPMENT

www.tethers.com
9


Advanced Propulsion, Power, & Comm
for Space, Sea, & Air

B. Feedstock Format

3a. Consolidated Tape is formed into rod on orbit

- 1. Spools very neatly as a simple spiral wrap
- 2. Very narrow tape would probably enable a level wound spool
- 3. Swappable material canisters may solve reliability issues involving defects in the material
- 4. Low messiness, no loose fiber
- 5. Low potential for tangling or snagging
- 6. Especially suited for converting to tubular members
- 7. Small thickness allows tight spool OD, and tight routing bends in one direction
- 8. Enough rigidity to push through much of the process chain when not yet melted
- 9. Most standard format for uni-directional prepreg feedstock.
- 10. Pre-consolidated Fiber and Matrix minimizes the processing on-orbit
- 11. Battens or diagonals could have a round cross section in the middle of the members.
- 12. Potential for rigidity across the width to limit the routing and wrapping scheme
- 13. Laying compression members in one pass causes some distortion of the fibers when wrapping edges, esp. when changing wrapping direction or angle

SELECTED FOR FURTHER DEVELOPMENT

www.tethers.com
10



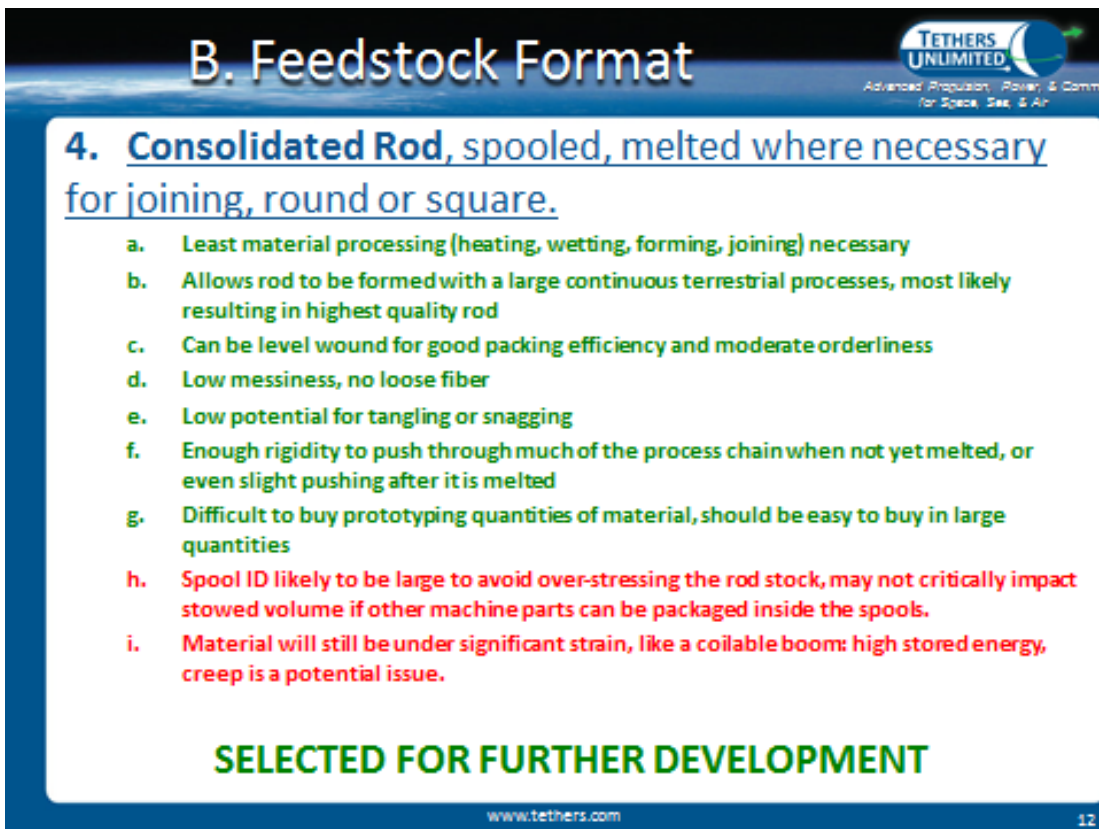
B. Feedstock Format

3b. Consolidated Tape is strung as tension members and laminated into battens on orbit

1. Spools very neatly as a simple spiral wrap
2. Swappable material spools may aid reliability issues due to defects in the material spools.
3. Low messiness, no loose fiber in feedstock, low potential for tangling or snagging
4. Small thickness allows tight spool OD, and tight routing bends in one direction
5. Enough rigidity to push through much of the process chain when not yet melted
6. Most standard format for uni-directional prepreg feedstock.
7. Pre-consolidated Fiber and Matrix simplifies processing
8. Multiple layers of thickness on the compression members increases the uniformity of fiber path length through the thickness, reducing the distortion caused by making turns
9. Can't do a firm or level wind for wide tapes, likely need swappable material canisters, other formats could store *more* material within a given OD limit on a single *long* spool
10. Potential for rigidity across the width to limit the routing and wrapping scheme.
11. Compression Battens will probably have a square, or maybe even rectangular section

SELECTED FOR FURTHER DEVELOPMENT

www.tethers.com 11



B. Feedstock Format

4. Consolidated Rod, spooled, melted where necessary for joining, round or square.

- a. Least material processing (heating, wetting, forming, joining) necessary
- b. Allows rod to be formed with a large continuous terrestrial processes, most likely resulting in highest quality rod
- c. Can be level wound for good packing efficiency and moderate orderliness
- d. Low messiness, no loose fiber
- e. Low potential for tangling or snagging
- f. Enough rigidity to push through much of the process chain when not yet melted, or even slight pushing after it is melted
- g. Difficult to buy prototyping quantities of material, should be easy to buy in large quantities
- h. Spool ID likely to be large to avoid over-stressing the rod stock, may not critically impact stowed volume if other machine parts can be packaged inside the spools.
- i. Material will still be under significant strain, like a coilable boom: high stored energy, creep is a potential issue.

SELECTED FOR FURTHER DEVELOPMENT

www.tethers.com 12

B. Feedstock Format



Advanced Propulsion, Power, & Comm
for Space, Sea, & Air

5. Pre-cut rods are stacked like tooth picks

- a. extra resin can be pre-molded onto the ends of the rods to facilitate joining
- b. No Stored strain energy within the feedstock, might help prevent mishaps
- c. Relatively easy (compared to wrapped diagonals) to align the axes of members
- d. Enables desirable truss geometries not feasible with wraps (“M-Truss”, well balanced, might be less mass efficient though)
- e. Configurable matrix/fiber ratio
- f. High material packing efficiency, likely better than spools if you penalize spools for the empty ID and circularly constrained OD of spools.
- g. High complexity, robotic arm to assemble, basically a miniature version of the higher order truss assembly
- h. Requires new material acquisition & significant pre-processing of feedstock
- i. No reinforcement fibers spanning the joints

NOT SELECTED FOR FURTHER DEVELOPMENT

www.tethers.com

13

C. Heating Methods



Advanced Propulsion, Power, & Comm
for Space, Sea, & Air

1. Contact by a heated plate, roller, or slider
2. Ultrasonic tool such as Branson ultrasonic welder
3. Laser for non-contact heating of very specific areas
4. Radiative Lamp for non-contact general heating
5. Electro-Magnetic for non-contact general heating
6. Ohmic Heating for resistive heating of general areas

www.tethers.com

14

C. Heating Methods



Advanced Propulsion, Power, & Comm.
for Space, Sea, & Air

1. Contact Heating

- May be accomplished by heating outsides of the elements to be joined or by heating surfaces to be joined
- Fairly simple to implement
- Heated element can be small
- Contact may be stationary, sliding, or rolling
- May be possible to also use the heated plate as a cooling compactor
- Build-up of material on the contact heater may be an issue as PEEK tends to stick to the heated block.

SELECTED FOR FURTHER DEVELOPMENT

www.tethers.com 13

C. Heating Methods



Advanced Propulsion, Power, & Comm.
for Space, Sea, & Air

2. Ultrasonic Heating

- Does not require heating of the entire compactor
- The concept may be simple to implement with the Branson tool
- Highly filled composite materials can result in weak joints
- The heating effect varies with the degree of crystallinity of the material

FURTHER INVESTIGATION NEEDED

3. Laser Heating

- Non-contact prevents build-up of material on heating element
- Allows precise targeting of heating zone
- Build-up of material on the contact heater may be an issue

FURTHER INVESTIGATION NEEDED

www.tethers.com 16

C. Heating Methods


Advanced Propulsion, Power, & Comm
for Space, Sea, & Air

4. **Radiative Heating**
 - a. Non-contact of lamp prevents build-up of material on the heater
 - b. Thermally inefficient and does not allow for precise target heating
5. **Microwave Heating**
 - a. Carbon Fiber can act as a conductor
 - b. Heating would not be precisely targeted
 - c. Significant development needed (no reported industrial applications)
6. **Ohmic Heating**
 - a. Carbon Fiber can act as a conductor
 - b. Bench-top tests showed feasibility
 - c. Difficult to control uniformity of heat
 - d. Degradation of electrodes over time may be an issue

METHODS NOT SELECTED FOR FURTHER DEVELOPMENT

www.tethers.com 17

G. Gripping Mechanisms


Advanced Propulsion, Power, & Comm
for Space, Sea, & Air

1. **Node Gripper vs. Truss Gripper**
 - a. Gripping nodes allows for more precise knowledge of location
 - b. Gripping of truss prevents rotation of the truss during joining processes
 - c. Solution should combine best of both (gripping entire truss, with features that locate the truss axially according to the nodes)
 - d. Robotic arm must have adequate precision, or locating features must self-align the truss
2. **Rigid vs. Compliant**
 - a. Rigid mechanisms would provide more precise knowledge of location and resistance during joining process, whereas a compliant mechanism would not
 - b. Rigid mechanisms would require force-feedback sensors to prevent damage to trusses, whereas a compliant mechanism would not
 - c. Solutions should combine the best of both

ALL SELECTED FOR FURTHER DEVELOPMENT

www.tethers.com 21

E. Joint Geometry Scheme


Advanced Propulsion, Power, & Comm
for Space, Sea, & Air

- 1. Trusses terminate in a point**
 - a. Point allows trusses to be in pure compression or tension, not bending.
 - b. Trusses can be joined together at any angle
 - c. Torsional rigidity of joint would be minimal
- 2. Trusses butt together**
 - a. Nodes of one truss directly fused to nodes of the other truss
 - b. High structural rigidity
 - c. May be difficult to align nodes, particularly with triangular trusses
 - d. Would only allow for joining of trusses at specific angles
- 3. Trusses spaced apart**
 - a. Rods span the gaps from the nodes of one truss to the nodes of the other, and are attached through SpiderFab process.
 - b. Can accommodate any desired geometry

ALL 3 SELECTED FOR FURTHER DEVELOPMENT

www.tethers.com 19

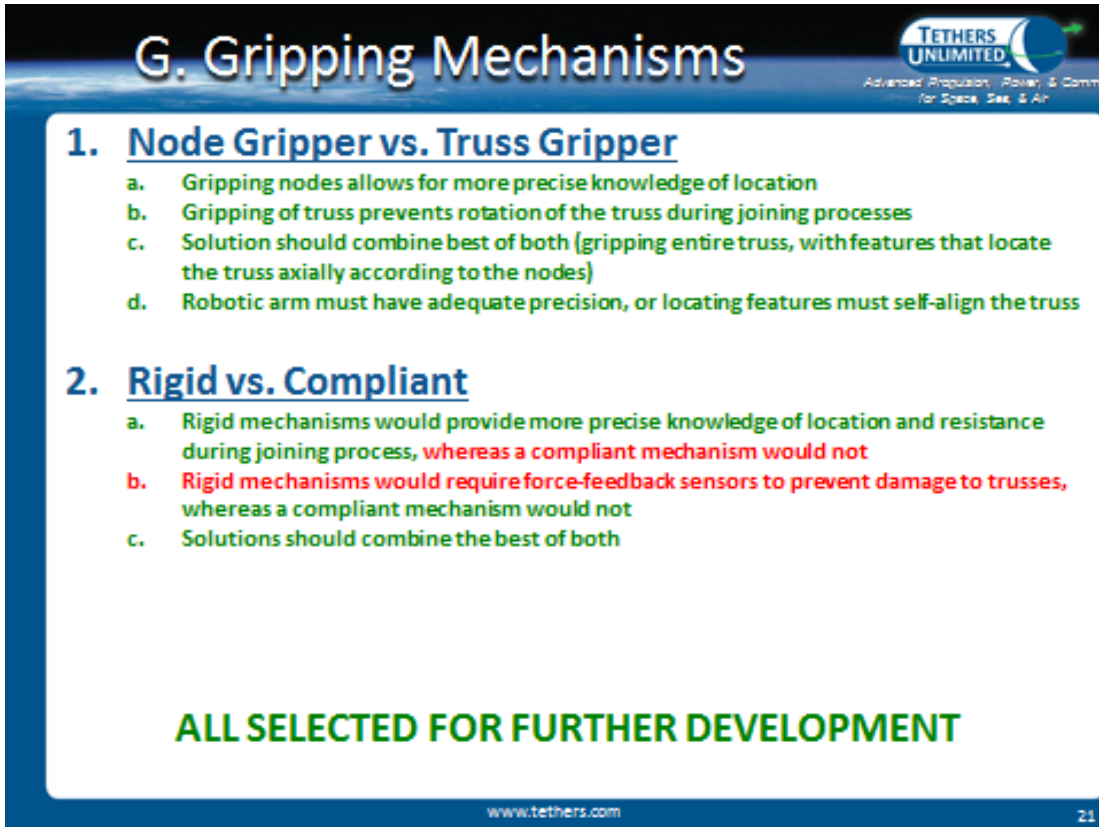
F. Feature Integration Scheme


Advanced Propulsion, Power, & Comm
for Space, Sea, & Air

- 1. Fused Filament Fabrication (FFF)**
 - a. Allows strategic integration of features or attachment of components
 - b. Can be joined to truss at any point with moderate resolution
 - c. Could be fabricated directly on truss, or separately formed then bonded to structures via SpiderFab processes
 - d. Typical drawbacks to 3D Printing include clogging and cleaning of the nozzle
- 2. Clamp-on Fittings**
 - a. Can be used for high-precision componentry
 - b. Contrary to the basic premise of SpiderFab but may be a stop-gap solution

ALL SELECTED FOR FURTHER DEVELOPMENT

www.tethers.com 20



G. Gripping Mechanisms

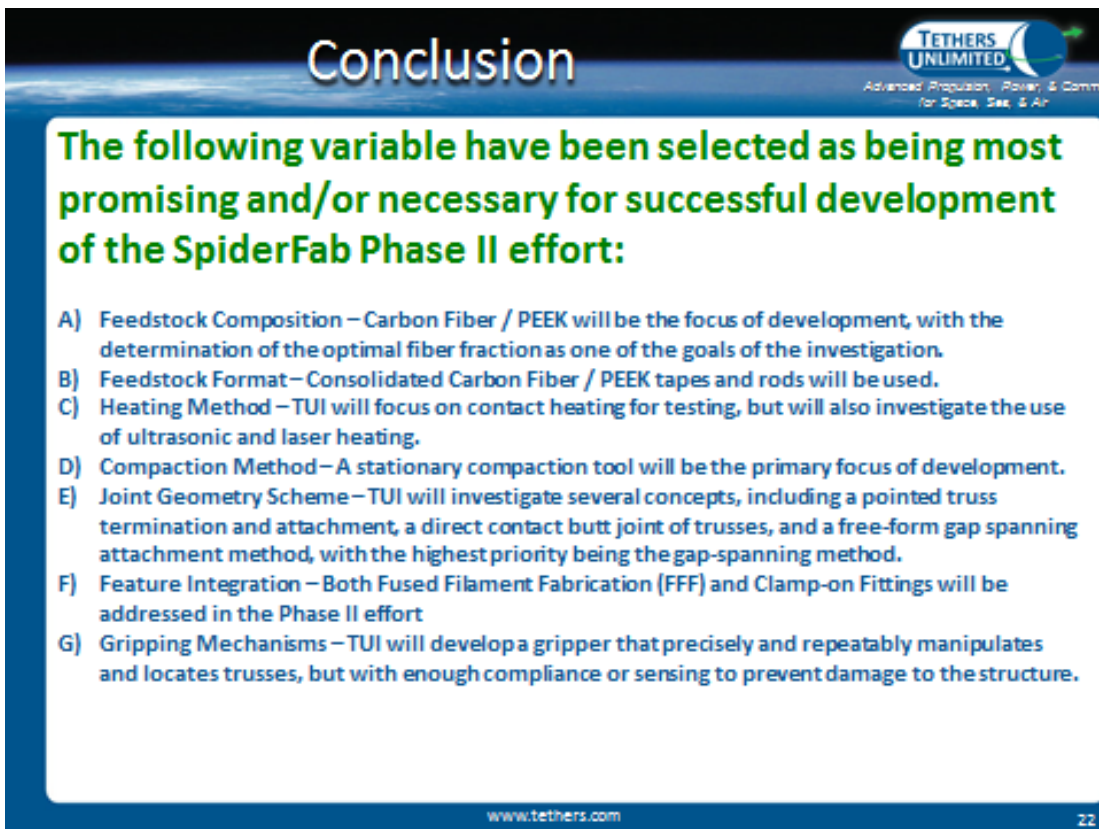

Advanced Propulsion, Power, & Comm
for Space, Sea, & Air

- 1. Node Gripper vs. Truss Gripper**
 - a. Gripping nodes allows for more precise knowledge of location
 - b. Gripping of truss prevents rotation of the truss during joining processes
 - c. Solution should combine best of both (gripping entire truss, with features that locate the truss axially according to the nodes)
 - d. Robotic arm must have adequate precision, or locating features must self-align the truss

- 2. Rigid vs. Compliant**
 - a. Rigid mechanisms would provide more precise knowledge of location and resistance during joining process, whereas a compliant mechanism would not
 - b. Rigid mechanisms would require force-feedback sensors to prevent damage to trusses, whereas a compliant mechanism would not
 - c. Solutions should combine the best of both

ALL SELECTED FOR FURTHER DEVELOPMENT

www.tethers.com 21



Conclusion


Advanced Propulsion, Power, & Comm
for Space, Sea, & Air

The following variable have been selected as being most promising and/or necessary for successful development of the SpiderFab Phase II effort:

- A) Feedstock Composition – Carbon Fiber / PEEK will be the focus of development, with the determination of the optimal fiber fraction as one of the goals of the investigation.
- B) Feedstock Format – Consolidated Carbon Fiber / PEEK tapes and rods will be used.
- C) Heating Method – TUI will focus on contact heating for testing, but will also investigate the use of ultrasonic and laser heating.
- D) Compaction Method – A stationary compaction tool will be the primary focus of development.
- E) Joint Geometry Scheme – TUI will investigate several concepts, including a pointed truss termination and attachment, a direct contact butt joint of trusses, and a free-form gap spanning attachment method, with the highest priority being the gap-spanning method.
- F) Feature Integration – Both Fused Filament Fabrication (FFF) and Clamp-on Fittings will be addressed in the Phase II effort
- G) Gripping Mechanisms – TUI will develop a gripper that precisely and repeatably manipulates and locates trusses, but with enough compliance or sensing to prevent damage to the structure.

www.tethers.com 22

APPENDIX B

SpiderFab: An Architecture for Self-Fabricating Space Systems

Robert P. Hoyt,³ Jesse I. Cushing,⁴ Jeffrey T. Slostad,⁵ Greg Jimmerson,⁴ Todd Moser,⁴ Greg Kirkos,⁴ Mark L. Jaster,⁴
Nestor R. Voronka⁶
Tethers Unlimited, Inc., Bothell WA, 98011, USA

On-orbit fabrication of spacecraft components can enable space programs to escape the volumetric limitations of launch shrouds and create systems with extremely large apertures and very long baselines in order to deliver higher resolution, higher bandwidth, and higher SNR data. This paper will present results of efforts to investigate the value proposition and technical feasibility of adapting several of the many rapidly-evolving additive manufacturing and robotics technologies to the purpose of enabling space systems to fabricate and integrate significant parts of themselves on-orbit. We will first discuss several case studies for the value proposition for on-orbit fabrication of space structures, including one for a starshade designed to enhance the capabilities for optical imaging of exoplanets by the proposed New World Observer mission, and a second for a long-baseline phased array radar system. We will then summarize recent work adapting and evolving additive manufacturing techniques and robotic assembly technologies to enable automated on-orbit fabrication of large, complex, three-dimensional structures such as trusses, antenna reflectors, and shrouds.

Nomenclature

ρ = material mass density
 D = beam diameter
 E = material modulus
 l = beam length
 m = the mass per unit length of a beam

I. Introduction

THE SpiderFab effort, funded by NASA's Innovative Advanced Concepts (NIAC) program, has investigated the value proposition and technical feasibility of radically changing the way we build and deploy spacecraft by enabling space systems to fabricate and integrate key components on-orbit. Currently, satellites are built and tested on the ground, and then launched aboard rockets. As a result, a large fraction of the engineering cost and launch mass of space systems is required exclusively to ensure the system survives the launch environment. This is particularly true for systems with physically large components, such as antennas, booms, and panels, which must be designed to stow for launch and then deploy reliably on orbit. Furthermore, the performance of space systems are largely determined by the sizes of their apertures, solar panels, and other key components, and the sizes of these structures are limited by the requirement to stow them within available launch fairings. Current State-Of-the-Art (SOA) deployable technologies, such as unfurlable antennas, coilable booms, and deployable solar panels enable apertures, baselines, and arrays of up to several dozen meters to be stowed within existing launch shrouds. However, the cost of these components increases quickly with increased size, driven by the complexity of the mechanisms required to enable them to fold up within the available volume as well as the testing necessary to ensure they deploy reliably on

³ CEO & Chief Scientist, 11711 N. Creek Pkwy S., D113, Bothell WA 98011, and AIAA Member.

⁴ Aerospace Engineer 11711 N. Creek Pkwy S., D113, Bothell WA 98011.

⁵ V.P. & Chief Engineer, 11711 N. Creek Pkwy S., D113, Bothell WA 98011.

⁶ V.P. & Chief Technologist, 11711 N. Creek Pkwy S., D113, Bothell WA 98011.

orbit. As a result, aperture sizes significantly beyond 100 meters are not feasible or affordable with current technologies.

On-orbit construction and 'erectables' technologies can enable deployment of space systems larger than can fit in a single launch shroud. The International Space Station is the primary example of a large space system constructed on-orbit by assembling multiple components launched separately. Unfortunately, the cost of multiple launches and the astronaut labor required for on-orbit construction drive the cost of systems built on the ground and assembled on-orbit to scale rapidly with size.

A. The SpiderFab™ Solution

The SpiderFab architecture seeks to escape these size constraints and cost scaling by adapting additive manufacturing techniques and robotic assembly technologies to fabricate and integrate large space systems on-orbit. The vision that has motivated this effort is that of creating a satellite 'chrysalis', composed of raw material in a compact and durable form, 'software DNA' assembly instructions, and the capability to transform itself on-orbit to form a high-performance operational space system. Fabricating spacecraft components on-orbit provides order-of-magnitude improvements in packing efficiency and launch mass. These improvements will enable NASA, DoD, and commercial space missions to escape the volumetric limitations of launch shrouds to create systems with extremely large apertures and very long baselines. **Figure 62** provides a notional illustration of the value proposition for SpiderFab relative to current state of the art deployable technologies. The larger antennas, booms, solar panels, concentrators, and optics created with SpiderFab will deliver higher resolution, higher bandwidth, higher power, and higher sensitivity for a wide range of missions. Moreover, on-orbit fabrication changes the cost equation for large space systems, enabling apertures to scale to hundreds or even thousands of meters in size with providing order-of-magnitude improvements in system performance-per-cost.

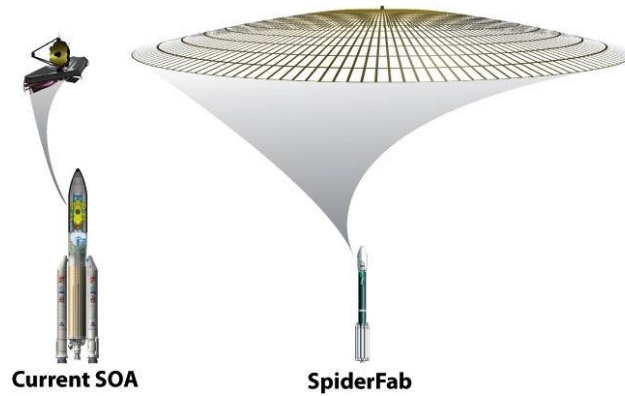


Figure 62. SpiderFab Value Proposition. *On-orbit fabrication of spacecraft components enables higher gain, sensitivity, power, and bandwidth at lower life-cycle cost.*

In this paper we will first describe a concept architecture for a system designed to fabricate and integrate large spacecraft components on-orbit. We call this architecture "SpiderFab" because it involves a robotic system that builds up large, sparse structures in a manner similar to that in which a spider spins its web: by extruding high-performance structural elements and assembling them into a larger structure. We will then evaluate the value proposition of this on-orbit fabrication architecture for several classes of spacecraft components, including antennas and starshades. Next, we will detail concept solutions for the technical capabilities required to realize the proposed architecture, and describe proof-of-concept testing performed to establish technical feasibility of these solutions. Finally, we will describe an incremental development approach to enable maturation of these capabilities to mission readiness.

II.SpiderFab Architecture

On-orbit construction has been investigated as a way to deploy large space systems for several decades, but aside from the on-orbit assembly of the International Space Station (ISS), which required many launches and many hours of astronaut labor to complete, it has not been used in other operational missions because the potential benefits did not outweigh the attendant risks and costs. However, the recent rapid evolution of additive manufacturing processes such as 3D printing and automated composite layup, as well as the advancement of robotic manipulation and sensing technologies, are creating new opportunities to extend the on-orbit construction concept from simply assembly in space to a full in-space manufacturing process of fabrication, assembly, and integration. These additive manufacturing technologies can enable space programs to affordably launch material for spacecraft in a very compact and durable form, such as spools of yarn, filament, or tape, tanks of liquid, bags of pellets, or even solid blocks of material, and then process the material on-orbit to form multifunctional 3D structures with complex, accurate geometries and excellent structural performance.

These capabilities can enable a radically different approach to developing and deploying spacecraft, one in which we verify, qualify, and launch the process, not the product.

A. The Self-Fabricating Satellite

In developing a process for on-orbit fabrication of space systems, we have focused upon implementations that will enable a space system to create and integrate its own components, so that it is self-fabricating. We call this the 'satellite chrysalis' approach, because each space system is launched with the material and tools needed to transform itself on-orbit into an operational system. An alternative approach is the 'orbital factory' approach, where a set of fabrication tools are launched to an orbital facility, such as the ISS, and this facility uses the same tools repeatedly to produce many space systems. We have chosen to focus upon the more challenging 'chrysalis' approach because although a factory can possibly achieve better economies of scale, launch mass, and reliability through repetition, the economics of the factory approach suffer from the transportation costs imposed by orbital dynamics. Specifically, the ΔV required to transfer satellites produced at an orbital facility to operational orbits with different inclinations is extremely high, and the resulting launch mass penalty can easily exceed the satellite's mass. As a result, we believe that in the near term, the factory approach will only be competitive in two applications: producing systems that will operate at or near the ISS, and in producing systems in geostationary orbit, where transfer ΔV 's are relatively small. A self-fabricating capability that is economically competitive with conventional technologies will be competitive in any orbit. Moreover, the capabilities required for a factory are a subset of those required for a self-fabricating system, so if we can successfully implement a self-fabricating 'satellite chrysalis', then implementing an orbital satellite factory will be straightforward.

B. Architecture Components

On-orbit fabrication of spacecraft components will require (1) Techniques for Processing Suitable Materials to create structures, (2) Mechanisms for Mobility and Manipulation of Tools and Materials, (3) Methods for Assembly and Joining of Structures, (4) Methods for Thermal Control of Materials and Structures, (5) Metrology to enable closed-loop control of the fabrication process, and (6) Methods for Integrating Functional Elements onto structures built on-orbit.

3.2.1 Material Processing and Suitable Materials

The self-fabricating satellite will require a capability to process raw material launched in a compact state into high-performance, multifunctional structures. Additive manufacturing processes such as Fused Filament Fabrication (FFF, also known under the trademark of Fused Deposition Modeling, or FDM®), Selective Laser Sintering (SLS), Electron Beam Melting, and Electron Beam Free-Form Fabrication (EBF3) are highly advantageous for this capability because they enable raw materials in the form of pellets, powders, or ribbons of filament to be melted and reformed to build up complex 3D geometries layer by layer, with little or no wasted material. **Figure 64** shows a photo of one of our developmental FFF machines printing a small sparse truss structure.

Working in the space environment presents both challenges and advantages for these additive manufacturing processes. The foremost is the microgravity environment in space. Most terrestrial additive manufacturing processes rely upon gravity to facilitate positioning and bonding of each material layer to the previous layers, and in the microgravity environment we will not be able to rely upon this advantage. However, the lack of gravity also presents a very interesting opportunity in that it enables structures to be built up in any direction without concern for distortions due to gravity. In 3D printers on the ground, gravity causes unsupported elements to slump, so structures with overhanging elements or large voids must be supported by additional materials that are removed after printing. In space, these support materials will not be required, and a 3D printer could 'print' long, slender elements, drawing a sparse structure in 3D like a spider spins its web, or build up a solid structure in concentric spherical layers, like an onion. **Figure 63** shows several example sparse structures fabricated in the lab using ABS and PEEK thermoplastics. Slumping due to gravity in the lab limited the free-standing lengths of the elements to roughly a centimeter, but in zero-g the element lengths would be limited only by the reach of the fabrication tool.

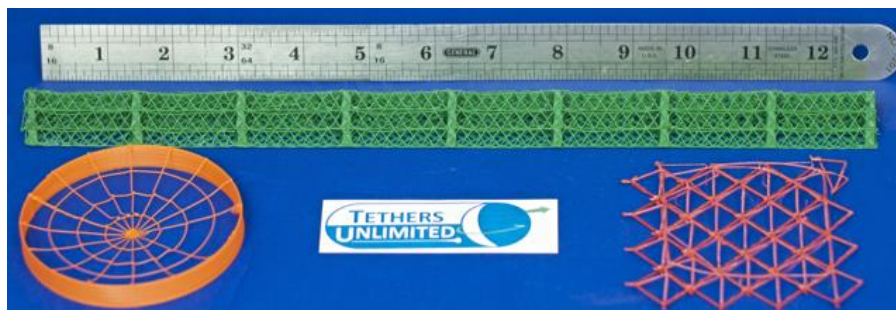


Figure 63. Samples fabricated using FFM. On Earth, slumping due to gravity limits the element dimensions of sparse structures to centimeter scales, but this limit will not be present in microgravity.

A second technical challenge for on-orbit additive manufacturing is the vacuum and thermal environment of space. Our preliminary testing of FFF processes in vacuum has indicated that the lack of an atmosphere is likely not an impediment, but the absence of conductive and convective cooling will require careful design of any process that involves thermal processing of materials so that printed structures cool and solidify in the desired manner. Furthermore, temperatures and temperature gradients can vary greatly depending upon the solar angle and sunlit/eclipse conditions, and methods for controlling these temperatures will be necessary to prevent undesired stresses from distorting structures under construction.

Although current 3D printing processes such as FFF can now handle a wide range of thermoplastics, and EBF3 can work with metals, the structural performance of these materials is still not optimal for large sparse space structures. If we are to pursue the construction of kilometer-scale systems, we must utilize materials with the highest structural performance available. Additionally, the speed of current 3D printing processes are not suitable for creating large space systems. A typical FFF machine requires an entire afternoon to print an object the size of a coffee mug. For these reasons, we are pursuing an approach that fuses the flexibility of FFF with the performance and speed of another additive manufacturing process: automated fiber layup. Essentially, we are working to develop a capability to rapidly '3D print' composite structures using high-performance fiber-reinforced polymers. This method will enable a robotic space system to build up very large, sparse structures in a manner similar to that in which a spider spins a web, extruding and pultruding structural elements and assembling them in 3-dimensional space to create large apertures and other spacecraft components. For this reason, we have termed this method the "SpiderFab™" process. The incorporation of pultrusion into the 3D printing process is particularly important, because it enables structural elements to be fabricated with high-modulus, high-tenacity fibers aligned in directions optimal for the service loads the structure must sustain.

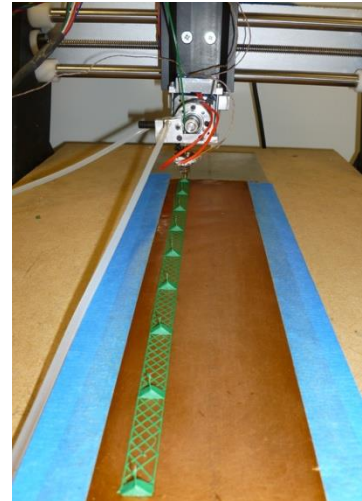


Figure 64. TUI's FFF machine printing a sparse truss structure.

The materials used in this process must be suitable for the space environment. In particular, they must be able to withstand the temperature extremes, UV light, radiation, and atomic oxygen that may be present in their operational orbit. Furthermore, low outgassing characteristics are necessary to prevent outgassed volatiles from contaminating optics, solar panels, and other components. In this work, we have focused on the use of Carbon Fiber reinforced Polyetheretherketone (PEEK) thermoplastics. These CF/PEEK composites have excellent structural performance, very high temperature tolerance, and very low outgassing characteristics. Although these materials are challenging to process due to the high melting temperature of PEEK, in this and other parallel efforts we have made excellent progress in developing techniques to perform thermoforming, pultrusion, and Fused Filament Fabrication with these materials. Although our work to date has focused on CF/PEEK composites, we should note that the SpiderFab process is readily adaptable to other composite choices, and we have also performed initial development with fiber-glass-PET composite materials.

3.2.2 *Mobility & Manipulation*

In order for a robotic system to fabricate a large structure, it will require means to move itself relative to the structure under construction, as well as to distribute the raw materials from the launch volume to the build area on the structure. Additionally, it will require the capability to manipulate structural elements to position and orient them properly and accurately on the structure. There are multiple potential solutions for both requirements. In developing the SpiderFab architecture, we have focused on the use of highly dexterous robotic arms because, serendipitously, under a separate contract effort we are currently developing a compact, dexterous robotic arm for nanosatellite applications. In our concept implementations, one or more such robotic arms will be used to position fabrication heads, translate the robot across the component under construction, and position structural elements for assembly.

3.2.3 *Assembly & Joining*

Once the robot has created a structural element and positioned it properly on the spacecraft structure, it will require means to bond the element to the structure. This bonding could be accomplished using welding, mechanical fasteners, adhesives, and other methods. Because our SpiderFab efforts have focused upon the use of fiber-reinforced thermoplastics, we can take advantage of the characteristics of thermoplastics to accomplish fusion-bonding using a combination of heat and pressure.

3.2.4 *Thermal Control*

A significant challenge for fabricating precise structural elements, managing structural stresses in the elements, and reliably forming fusion bonds between the elements will be managing the temperature of the materials in the space environment, where both mean temperatures and temperature gradient vectors can vary dramatically depend-

ing upon the direction to the sun and the position in orbit. In the SpiderFab implementations we propose to use additives or coatings in the fiber-reinforced thermoplastics to cold-bias the materials and minimize their thermal fluctuations under different insolation conditions, and use contact, radiative, and/or microwave heating to form and bond these materials.

3.2.5 *Metrology*

Automated or tele-robotic systems for constructing large components will require capabilities for accurately measuring the component as it is built. This metrology will be needed at two scales: macro-scale metrology, to measure the overall shape of the component to ensure it meets system requirements, and micro-scale metrology, to enable accurate location of material feed heads with respect to the local features of the structure under construction. Technologies currently in use in terrestrial manufacturing processes, such as structured-light scanning and stereo-imaging, can be adapted to provide these functionalities.

3.2.6 *Integration of Functional Elements*

Once the SpiderFab system has created a base structure, it will also require methods and mechanisms to integrate functional elements such as reflective membranes, antenna panels, solar cells, sensors, wiring, and payload packages into or onto the support structure. Because most of these components can be packaged very compactly, and require high precision in manufacture and assembly, in the near term it is likely to be most effective to fabricate these components on the ground and integrate them on-orbit. In the long-term, it may be possible to implement additive manufacturing methods capable of processing many materials so that some of these components could be fabricated *in-situ*, but nonetheless it will only be advantageous to do so if on-orbit fabrication provides a significant improvement in launch mass or performance. The techniques for automated integration of functional elements onto a space structure will depend upon the nature of the element. Reflective membranes and solar cells can be delivered to orbit in compact rolls or folded blankets and unrolled onto a structure using thermal bonding, adhesives, or mechanical fasteners to affix them to the structure. Sensors, payloads, and avionics boxes can be integrated onto the structure using mechanical fasteners. Wiring can be unspooled and clipped or bonded to the structure, and attached to payload elements using quick-connect plugs.

C. Concept Implementations

1. SpiderFab Truss-Fabricator for Large Solar Array Deployment

Figure 65 illustrates a concept for on-orbit fabrication of support structures for large solar arrays. In this concept, three SpiderFab "Trusselator" heads will extrude continuous 1st order trusses to serve as the longerons, and a fourth fabrication head on a 6DOF robotic arm will fabricate and attach cross-members and tension lines to create a truss support structure with 2nd-order hierarchy. As it extends, the support structure will tension and deploy a foldable/rollable solar array blanket prepared on the ground. To create the structural elements forming the truss-of-trusses, this system will process a "Continuous Fiber Reinforced Thermoplastic" (CFRTP) yarn consisting of high-modulus fibers co-mingled with thermoplastic filaments. This yarn can be wound in a highly compact spool for launch and then processed to create stiff composite structures. Figure 66 shows a proof-of-concept demonstration of a 'Trusselator' mechanism creating long truss structures. The spool shown on the left of Figure 66 holds enough yarn to fabricate a 100m long, 2m diameter trussed beam.

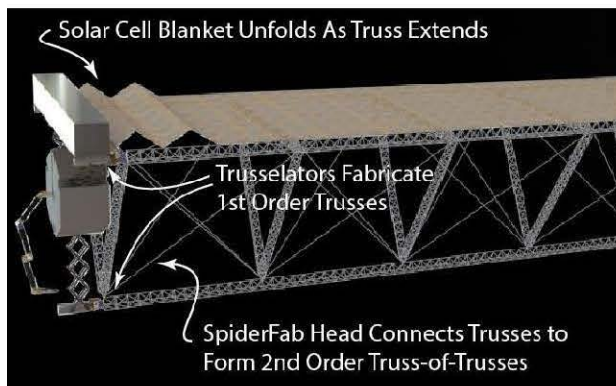


Figure 65. Concept Method for Fabrication of Large, High-Performance Truss Structures to Support Solar Arrays.



Figure 66. First-Generation SpiderFab "Trusselator" Process.

2. SpiderFab Bot for Assembly of Large Apertures

For other applications such as antenna reflectors, solar concentrators, solar sails, and structures for manned habitats, it will be desirable to implement a SpiderFab system able to create large two-dimensional or three-dimensional structures. A flexible fabrication capability could be enabled by a mobile "SpiderFab Bot" that uses several robotic arms for both mobility with respect to the structure under construction as well as for precise positioning of structural elements as it assembles the overall structure. To fabricate the structural elements, it uses two specialized 'spinneret' fabrication tools. One is an "Extruder Spinneret" used to convert spools of wound yarn or tape into high-performance composite tubes or trusses, as illustrated in **Figure 67**. It then uses a high-dexterity 'Joiner Spinneret' tool that adapts 3D printing techniques to create optimized, high-strength bonds between the structural elements, as illustrated in **Figure 68**, building up large, sparse support structures. **Figure 69** illustrates the concept of the SpiderFab Bot building a support structure for an antenna or starshade onto a host satellite bus. Metrology systems for both micro-scale feature measurement and macro-scale product shaping enable the system to accurately place and bond new elements as well as ensure the overall structure achieves the desired geometry. Once the support structure is complete, the system uses its robotic manipulators and bonding 'spinneret' to traverse the structure and apply functional elements such as reflectors, membranes, meshes, or other functional components to the support structure, as illustrated notionally in **Figure 70**. These capabilities will enable a SpiderFab Bot to create large and precise apertures to support a wide variety of NASA, DoD, and commercial missions.

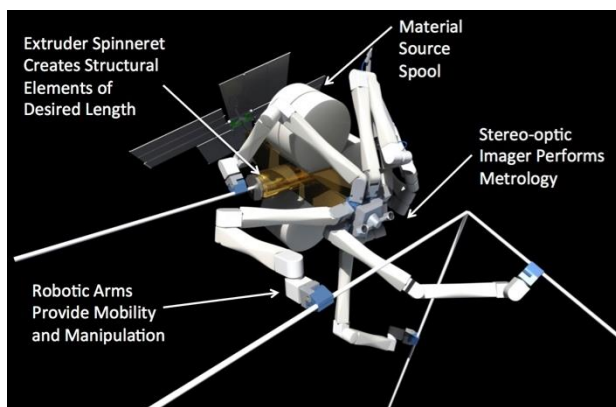


Figure 67. The SpiderFab Bot creates structural elements and adds them to the structure.

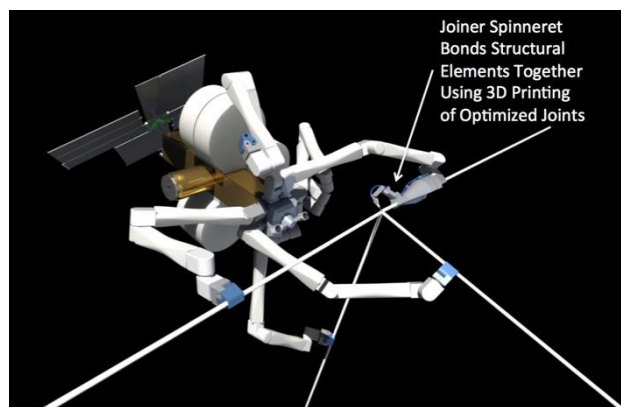


Figure 68. The SpiderFab Bot uses a 6DOF 3D printing tool to bond structural elements with joints optimized for the service loads.

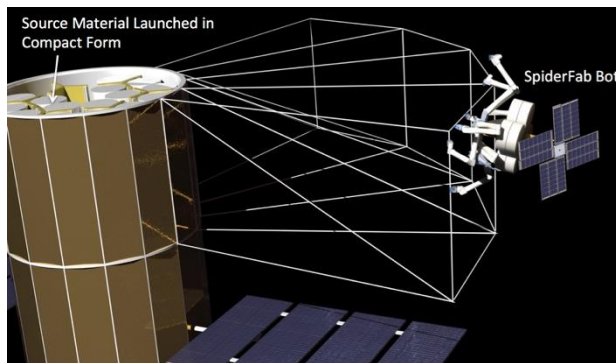


Figure 69. Concept for a "SpiderFab Bot" constructing a support structure onto a satellite.

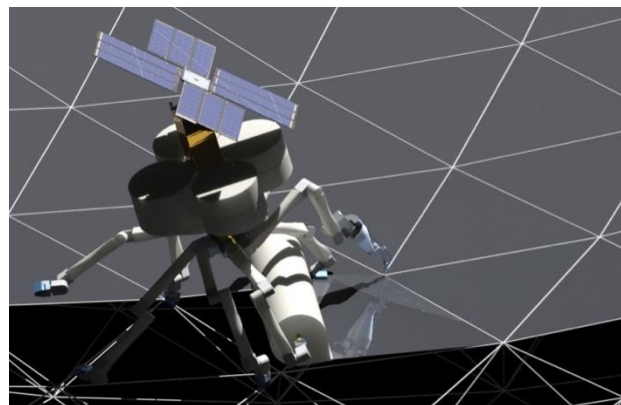


Figure 70. The SpiderFab Bot then applies functional elements, such as reflective membranes, to the support structure.

III.Value Proposition for On-Orbit Fabrication

The Phase I effort evaluated the value proposition for on-orbit fabrication of space systems using the SpiderFab architecture, by first considering the trade-offs between building components on the ground versus building them on orbit, and identifying two key advantages that on-orbit fabrication can provide. We then reviewed NASA's Technology Roadmaps to identify Technology Areas and future NASA missions where SpiderFab could provide signifi-

cant advantages. Then we developed performance metrics to quantify the potential advantages that SpiderFab could provide for several space system components, including high-power solar arrays, phased array radars, optical occulter, and antenna reflectors. In each case, we found that SpiderFab can enable order-of-magnitude improvements in key performance metrics; in this proposal we will present the value proposition analyses for optical occulter and antenna reflectors, and refer the reviewer to our Phase I final report for details on the other case studies.

A. Build-on-Ground vs. Build-on-Orbit

On-orbit fabrication of a space system can free the system design from the volumetric constraints of launch vehicles and reduce the mass and engineering costs associated with designing the system to survive launch. Additionally, an on-orbit fabrication capability enables repair and reconfiguration after launch, reducing risks due to design errors and increasing mission flexibility. However, these advantages must be traded against the additional cost and complexity of enabling these components to be fabricated and integrated in an automated manner in the space environment. Furthermore, whereas in the conventional approach components are fabricated, integrated, and tested prior to launch, a program using on-orbit fabrication must commit and expend the costs associated with launch before these parts are created and integrated. Consequently, although our far-term goal is to enable fabrication and integration of essentially all of a spacecraft on-orbit, we must approach this goal incrementally, focusing initial investment on classes of components where our current technology capabilities can provide a significant net benefit. Satellites and other spacecraft are typically composed of a number of subcomponents, ranging from bulk structures to actuated mechanisms to complex microelectronics. All of these components could, in theory, be fabricated on-orbit, but investing in developing the capability to do so can only be justified if on-orbit fabrication can provide a dramatic net improvement in performance-per-cost. On-orbit fabrication can provide benefits primarily in two ways: launch mass reductions, and packing efficiency improvements.

B. Mass Optimization

Fabricating a space structure on-orbit can reduce system mass because the design of structural components can be optimized for the microgravity loads they must sustain in the space environment, not for the 100's of gravities shock and vibrations they would experience during launch. Additionally, large structures built on-orbit do not require the hinges, latches, and other complex mechanisms needed by deployable structures, reducing the 'parasitic' mass of the structure and enabling it to be fully optimized for its design loads. Building a structure on-orbit, rather than designing it for deployment, also enables its geometry to be varied and/or tapered in an optimal manner throughout the structure, which for very large structures supporting well-defined loads can result in significant mass savings. Furthermore, it enables creation of structures with cross-sections that would be too large to fit in a launch shroud, taking advantage of geometric optimizations that can provide large improvements in structural performance. For example, the bending stiffness of a longeron truss increases as the square of its diameter D :

$$\frac{EI}{m} = \frac{1}{8} \frac{E}{\rho \Sigma} D^2, \tag{1}$$

where ρ is the material mass density, m is the mass per unit length of the beam, E is the material modulus, and Σ is a constant accounting for battens, cross members, and joints.¹ Whereas a deployable truss designed to stow within a launch shroud will typically have a maximum diameter on the order of a meter, trusses fabricated on orbit can readily be built with diameters of several meters or more, providing an order of magnitude improvement in stiffness per mass. Moreover, large structures can be built with 2nd or higher-order hierarchical geometry, enabling an additional 30-fold increases in structural performance.²

C. Packing Efficiency Improvements

The second manner in which on-orbit fabrication can enable significant improvements is the packing efficiency of large components. **Figure 71**, adapted from Reference [1], compares the packing efficiency of deployable trusses (flown) and erectable trusses (proposed). Existing deployable technologies fall one to two orders of magnitude short of ideal packing efficiency (ie - 95% to 99% of their stowed volume is "wasted"). Proposed erectable technologies, in which individual structural elements such as longerons and struts are launched in tightly packed bundles and then assembled on-orbit to fabricate large sparse structures, may be able to improve the packing efficiency somewhat, 'wasting' only about 90% of their stowed volume. On-orbit fabrication with the SpiderFab process, which uses materials that can be launched as tightly wound spools of yarn, tape, or filament, as pellets, or even as solid blocks of feedstock, can enable packing efficiencies approaching unity. **Figure 71** notes the regime we project SpiderFab on-orbit fabrication can enable space trusses to achieve - diameters of multiple meters to take advantage of the geometric advantages expressed in Eqn (1), and reducing wasted launch volume down to 50%-10%. This improvement in packing efficiency will be particularly advantageous for components that are by nature very large, sparse, and/or gossamer, such as antennas, trusses, shrouds, and reflectors.

D. Relevance to NASA Technical Roadmap

With the parameters that SpiderFab will be most advantageous for space systems that require very large, sparse, or gossamer components, we reviewed the 2012 NASA Technology Roadmaps and identified a number of technology areas where on-orbit fabrication with SpiderFab could provide the size and/or performance improvements required to enable future missions NASA has identified as high priority. **Table 1** summarizes the results of this review, and demonstrates that SpiderFab has strong relevance across a wide range of NASA Science and Exploration missions.

Table 1. Relevance of SpiderFab On-Orbit Fabrication to NASA Needs and Missions. *On-orbit fabrication can enable the large systems required to accomplish many future NASA missions.*

Technology Area	Need	Example Mission/Program	Reference
Starshade (occulter)	30-100m, 0.1m shape accuracy	New Worlds Observer	2012 TA08 Roadmap: Table 7
Large Deployable Antennas	10-14m 20 Gbps from 1AU	SWOT, ONEP, ACE, SCLP Mars-28, Mars 30	2012 TA08 Roadmap: Table 3 2012 TA05 Roadmap: Table 7
Deployable Boom/Mast	20-500m	Structure-Connected Sparse Aperture; TPF-I; SPECS	2012 TA08 Roadmap: Fig 4
High Power Solar Array	30-300kW 0.5-1 kW/kg	HEOMD Solar-EP Missions	2012 TA03 Roadmap
Radiators	multi-MW	HEOMD Nuclear-Electric Missions	2012 TA14 Roadmap
Large Solar Sail	>1000 m ² 1 g/m ²	Solar Sail Space Demo, Interstellar Probe	2012 TA02 Roadmap: 2.2.2
Solar Concentrator	85-90% concentrator efficiency	LEO Cargo Tug; LEO-GEO Tug;	2012 TA02 Roadmap: 2.2.3
Large Aperture Telescope	50m ² aperture	Extremely Large Space Telescope (EL-ST), TPF-C	2012 TA08 Roadmap: Table 7

E. Value Proposition for Exoplanet Imaging

One of the most exciting potential applications of SpiderFab is the creation of very large apertures or optics to enable imaging of exoplanets. To evaluate the value proposition of SpiderFab for large optical systems, we considered the deployment of the starshade proposed for the New Worlds Observer (NWO) mission.³ Illustrated in **Figure 72**, the NWO mission would deploy a large starshade in between a telescope and a distant star in order to attenuate light from that star so that the telescope could image and obtain interferometric measurements of Earth-like planets within the habitable zone of the star. The NWO mission concept originated in a 2005 NIAC project led by Professor Webster Cash of the University of Colorado, and it presented an excellent case study for SpiderFab because the NWO team developed and documented a detailed concept for deploying a starshade using SOA deployable structures.

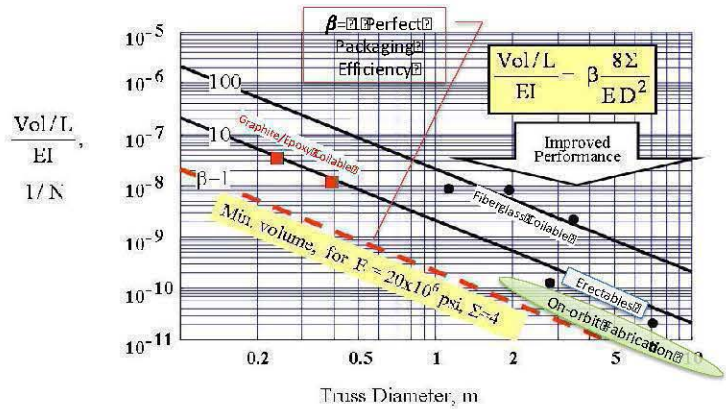


Figure 71. Truss Packing Efficiency. *On-orbit fabrication enables packing efficiencies approaching ideal values.*

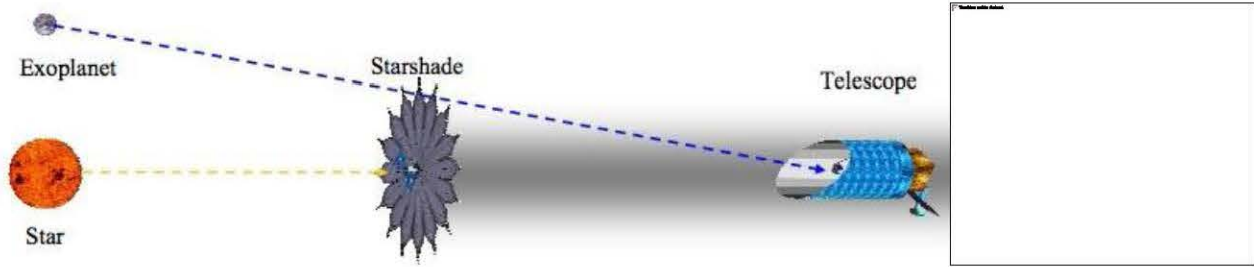


Figure 72. New Worlds Observer starshade concept. A starshade positioned between a distant star and a telescope attenuates light from the star to allow the telescope to image planets orbiting that star. [Images from Ref 3]

The NWO starshade spacecraft designed by the NWO team, illustrated in **Figure 73**, uses several radially-deployed booms to unfurl an opaque metalized Kapton® blanket with folded rigid edge pieces. Using the largest available Delta-IVH launch shroud, this SOA deployable design could enable a starshade with a diameter of 62 m. The mass of the starshade component of the system (not including the spacecraft bus), was estimated by the NWO team to be 1495 kg.

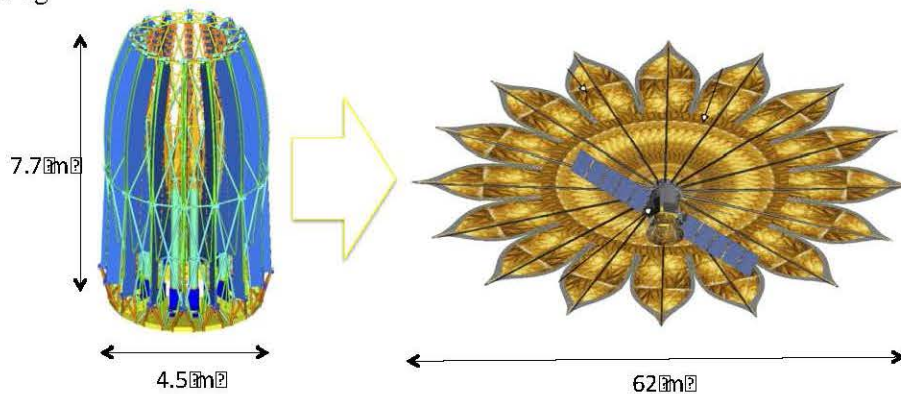


Figure 73. SOA Deployable NWO Starshade Design. The NWO Starshade design folds to fit a 62m diameter structure within the largest available launch shroud. [Figures adapted from Ref 3]

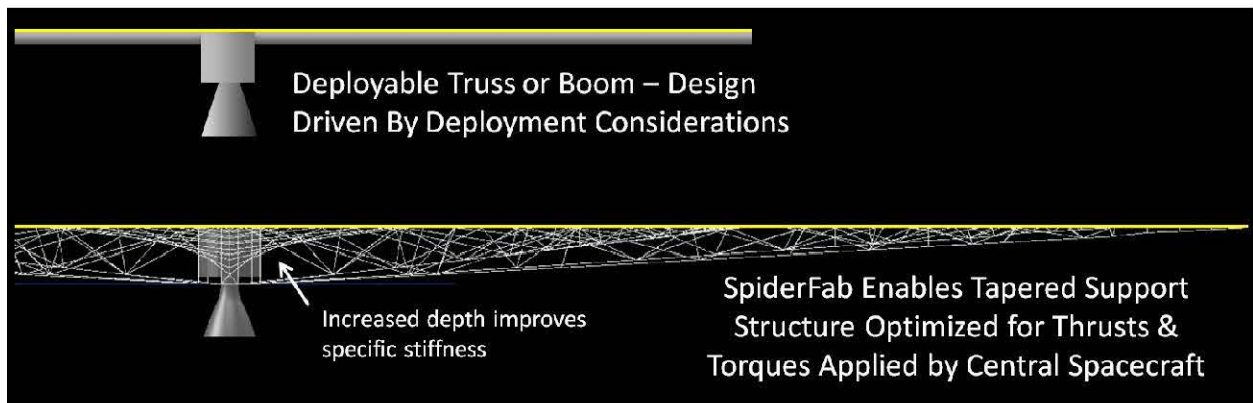


Figure 74. Notional Comparison of Support Structures of the NWO Deployable Starshade and a SpiderFab Starshade. On-orbit fabrication enables creation of structures with variable dimensions and geometries optimized to the operational loads in the microgravity environment.

Figure 74 presents a notional comparison between the NWO deployable starshade's structural design and the structures enabled by SpiderFab on-orbit fabrication. The NWO starshade's opaque membrane is deployed and supported by 16 radial spoke telescoping booms made of glass-reinforced polymer composite. The diameter of these booms is limited by packaging concerns to be less than a meter. Once deployed, these booms must support the opaque membrane against thrusts and torques applied by the central spacecraft. The lower half of **Figure 74** illustrates the kind of structure made possible by SpiderFab. We created this structure using ANSYS tools, using estimates of the torques and thrusts the structure must support and assuming the use of high-performance carbon fiber composites. Freed from the constraints of launch shroud dimensions and the requirement for a structure to be un-

foldable or unfurlable, the support structure for the starshade could be made with a variable cross-section and variable geometry. The structure could be several meters deep in the middle and taper out towards the periphery, and the concentration and geometry of the structural elements can be varied so as to optimize its strength to the operational loads. As illustrated in **Figure 75**, our analyses indicate that with the same amount of mass allocated for the SOA deployable starshade, a SpiderFab process could create a starshade structure of twice the diameter - four times the area. In this case the SpiderFab starshade mass estimate included an allocation of 250 kg + 150 kg margin for the robotic system required to fabricate the support structure (based upon the mass of our KRAKEN robotic arm and estimates derived from past experience on the Mars Polar Lander mission), and for the opaque membrane, we assumed the same total thickness of Kapton film (125 μm) used in the NWO design. In addition to increasing the size of the starshade that could be deployed with a given launch mass, SpiderFab also enables a 30-fold reduction in stowed volume, from 120 m^3 for the SOA deployable approach down to 4 m^3 for the on-orbit fabrication approach. This volume estimate assumed an 80% packing efficiency for the carbon fiber composite source material for the support structure (readily achievable with yarns or flat tapes) and included 2 m^3 allocated for the SpiderFab robotic system) This reduction in stowed volume could enable the Starshade component of the NWO mission to launch on a Falcon-9 rather than a Delta-IVH, reducing its launch cost by a roughly a third.

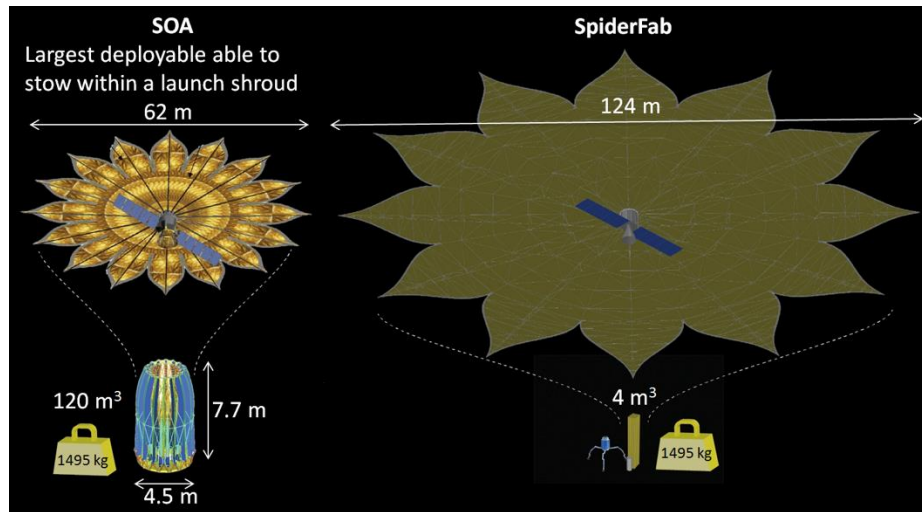


Figure 75. Size increase achievable with SpiderFab. SpiderFab enables dramatic increases in aperture size with equal launch mass and significantly smaller stowed volume.

Doubling the size of the starshade would enable the NWO telescope to resolve planets 2 times closer to a star.⁴ This closer inspection would increase the number of potential Earth-like targets within the star's habitable zone by a factor of 8. Additionally, doubling the occulter size would double the maximum wavelength at which the starshade would provide sufficient attenuation, from 1 μ to 2 μ . This larger wavelength window would bring the system into the range where the James Webb Space Telescope (JWST) can operate, potentially enabling the JWST to be used as part of the NWO system, or at least as part of a pathfinder demonstration of the NWO architecture. By reducing the number of launches required to deploy a NWO system from two Delta-IV Heavies to one Falcon-9, and by increasing the number of planets the system could resolve, the SpiderFab approach could enable a net benefit of providing a 16-fold increase in the number of Earth-like planets the NWO mission could discover per life-cycle cost. More succinctly, SpiderFab enables NASA to discover 16X more Earth-like planets per dollar.

F. Value Proposition for Large Antenna Reflectors

Fundamentally the majority of NASA, DoD, and commercial space systems deliver one thing to their end-users: data. The net quality of this data, whether it is the resolution of imagery, the bandwidth of communications channels, or the signal-to-noise of detection systems, is largely driven by the characteristic size of the apertures used in the system. Deployable antenna reflectors therefore represent a very important potential market for application of on-orbit fabrication technologies.

We can compare the potential performance of SpiderFab for large antenna reflectors by comparing it with state-of-the-art deployable antennas such as the Astromesh reflectors produced by Northrop Grumman's Astro Aerospace subsidiary, and the unfurlable antennas produced by Harris Corporation. The Astromesh reflectors use a tensegrity design in which a hoop-shaped truss deploys to spread open a conductive mesh, and a system of tension lines strung across the hoop serve to hold the mesh in the desired parabolic configuration. The Harris antennas typically use

several radial spokes that unfold like an umbrella to spread apart and shape a conductive mesh. These tensegrity-based SOA deployables are exceptionally efficient in terms of mass, and we believe it is unlikely that an on-orbit fabrication approach can provide a significant improvement in launch mass. However, these deployables are not optimum from the perspective of stowed volume and cost, and therefore there is substantial opportunity for an on-orbit fabrication architecture such as SpiderFab to provide significant capability improvements by enabling much larger apertures to be deployed within the constraints of existing shrouds.



Figure 76. Mass and Cost Scaling of Deployable Antenna Reflectors. *On-orbit fabrication of antenna apertures using SpiderFab can change the cost equation for apertures, enabling deployment of very large apertures at lower cost than conventional deployable technologies.*

Figure 76 plots the mass and estimated cost of current SOA deployable antennas.⁵ The size of the antenna images used in the plot indicate the relative size and/or performance of the antenna. The plot demonstrates that the cost of these deployables increases rapidly with the size of the aperture reaching costs on the order of several hundred million dollars for apertures of a few dozen meters. The cost scaling is exponential with size due to the complexity of the additional folding mechanisms required as well as the facility costs needed to assemble and qualify very large components. Furthermore, because these deployable antennas are limited in terms of how compactly they can fold up, the largest aperture that can be deployed with these SOA technologies is on the order of several dozen meters. SpiderFab changes the cost equation for large antennas. For an antenna fabricated on-orbit, the cost will primarily be driven by the cost of building, launching, and operating the robotic system needed to construct it. In this analysis, we have estimated the recurring cost of such a robotic system at \$25M-\$75M, based upon use of an ESPA-class microsat bus such as the ~\$20M Space Test Program Standard Interface Vehicle (STP-SIV) as well as estimates for the robotic systems based upon the Mars Polar Lander (MPL) robotic arm and the DARPA Phoenix mission. This 'base' cost may make SpiderFab non-competitive for small apertures. However, once that robotic system is paid for, the incremental cost for creating a larger antenna is primarily the cost for launching the required material and operating the robotic system for a longer duration. In particular, we can eliminate the facility costs for assembling and testing very large antennas. As a result, the antenna life cycle cost will scale much more gently with aperture size, making antennas with diameters of hundreds of meters affordable.

IV. SpiderFab Technical Feasibility

These SpiderFab concepts require capabilities for: (1) Processing Suitable Materials to Create Space Structures, (2) Mechanisms for Mobility and Manipulation of Tools and Materials, (3) Methods for Assembly and Joining of Structures, (4) Methods for Thermal Control of Materials and Structures, (5) Metrology to enable closed-loop control of the fabrication process, and (6) Methods for Integrating Functional Elements onto structures built on-orbit.

A. Processing Suitable Materials to Create Space Structures

Creating satellite components with scales on the order of hundreds or thousands of meters will require the use of extremely high structural performance materials in order to achieve affordable launch masses. Additionally, creating such large structures within an acceptable schedule will require techniques capable of processing these materials

in a rapid fashion. To enable the maximal structural efficiency desired, we have focused upon materials and techniques for producing high-performance composite structures.

Materials: In space applications, structural elements will be fabricated using a material composed of a thermoplastic and a high-performance fiber, such as polyetheretherketone (PEEK) and Carbon Fiber (PEEK/CF) composite. The carbon fiber will supply high tensile strength, stiffness, and compressive strength, and the PEEK will supply shear coupling between the fibers. PEEK is a thermoplastic with high melting temperature, high service temperature, and low outgassing characteristics that has been used successfully on prior space flight missions. To minimize degradation of the PEEK polymer by UV radiation and to minimize thermal variations of the structure on-orbit, the PEEK thermoplastic can be doped with titanium dioxide.

In our initial efforts, we investigated two different material feedstock formats for use in the SpiderFab process. The first is a Continuous Fiber Reinforced Thermoplastic (CFRTP) yarn consisting of high-modulus fibers co-mingled with thermoplastic filaments. The second form of feedstock is tape of continuous fibers pre-impregnated with a polymer matrix, similar to that used in laminate style composite fabrication. In the SpiderFab architecture, these source materials will be launched in compact spools and then processed on-orbit to form structural elements such as trussed beams, tubes, lattices, and solid surfaces.

Processes: To validate the feasibility of creating large, sparse composite structures with these materials, we developed a hand-held 'SpiderFab' CFRTP pultrusion tool; this tool can be thought of as like a glue gun that extrudes thin, stiff composite elements. **Figure 78** shows the tool, examples of structures we fabricated with the tool, and a demonstration of their strength.

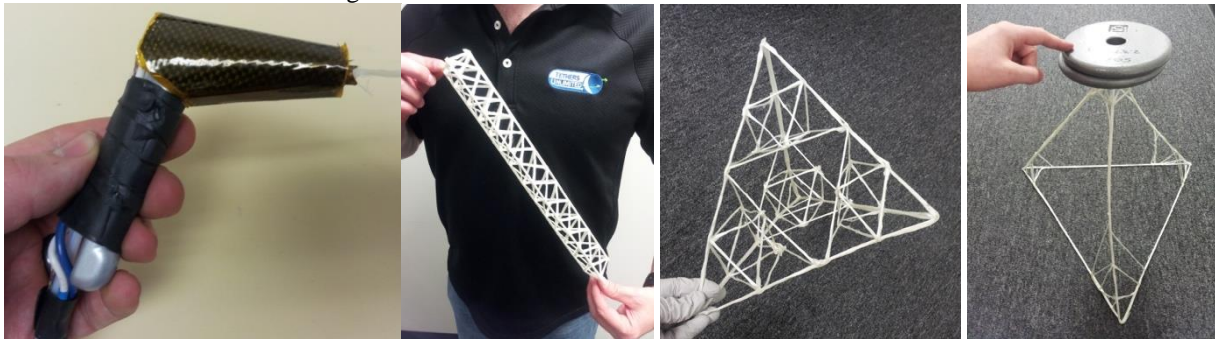


Figure 78. Handheld 'SpiderFab' tool and samples of composite lattice structures fabricated with the tool. Pultrusion of CFRTP elements can enable free-form fabrication of large, sparse composite structures with excellent structural performance.

Additionally, we performed proof-of-concept demonstration of thermoforming a tape composed of unidirectional carbon fiber with a PEEK prepreg matrix into a composite tube using pultrusion/extrusion through a set of heated dies. This PEEK/CF tape is flexible and can readily be wound into compact spools, but after thermoforming into tubes can approach the performance of the best available structural technologies.

B. Mobility and Manipulation:

Both the Trusselator system illustrated in **Figure 65** and the SpiderFab Bot illustrated in **Figure 67** will require robotic manipulators and automated control software to provide mobility of the fabrication tool with respect to the structure as well as for positioning and joining structural elements together. A number of robotic arms designed for space operation exist that could serve this function, including the SU-MO robotic arm developed by NRL and MDA that is planned to be tested on the DARPA PHOENIX mission and the robotic arms used in the Robonaut system. In our concept designs, we have baselined the use of the compact, high-dexterity "KRAKEN™" robotic arm that we have developed for nanosatellite servicing and assembly applications. A developmental model of the 7DOF KRAKEN arm is shown in with a notional SpiderFab feed head mounted on a 3DOF 'carpal-wrist' gimbal.



Figure 77. KRAKEN Robotic Arm Prototype. The KRAKEN is a 7DOF robotic arm with 1m reach. Two KRAKEN arms will stow within a 3U volume.

C. Assembly & Joining

To enable a robotic system to construct complex sparse lattice structures, we developed a concept design for a specialized “Joiner Spinneret” end effector that uses Fused Filament Fabrication (FFF) techniques to join tubular truss elements. This tool, illustrated in **Figure 79**, is designed to approach the new tubes to be joined from the side (radially), clamp onto the tube, and then use a rotary stage to reach 360 degrees around the end of the tube, while allowing the end effector to approach and retract radially from the side of the tube. As illustrated in **Figure 79**, a ‘finger’ with 3 independently cable-driven joints allows the spinneret print head to reach every spot and every angle needed to print a uniformly filleted joint, even when it requires reaching between tubes at tightly angled orientations to each other. The smaller scale motion stages built into the finger allow the new tube to be fixtured by the same robotic arm that is performing the joining, which simplifies the accuracy and obstacle avoidance schemes required in generating the tool paths. **Figure 80** shows a multi-element joint fabricated with optimized geometry using 3D printing, assembled with carbon composite tubes. The joiner spinneret can also be used to add brackets, bolt-holes, and other features to enable mounting of payloads and functional elements, as illustrated notionally in **Figure 81**.

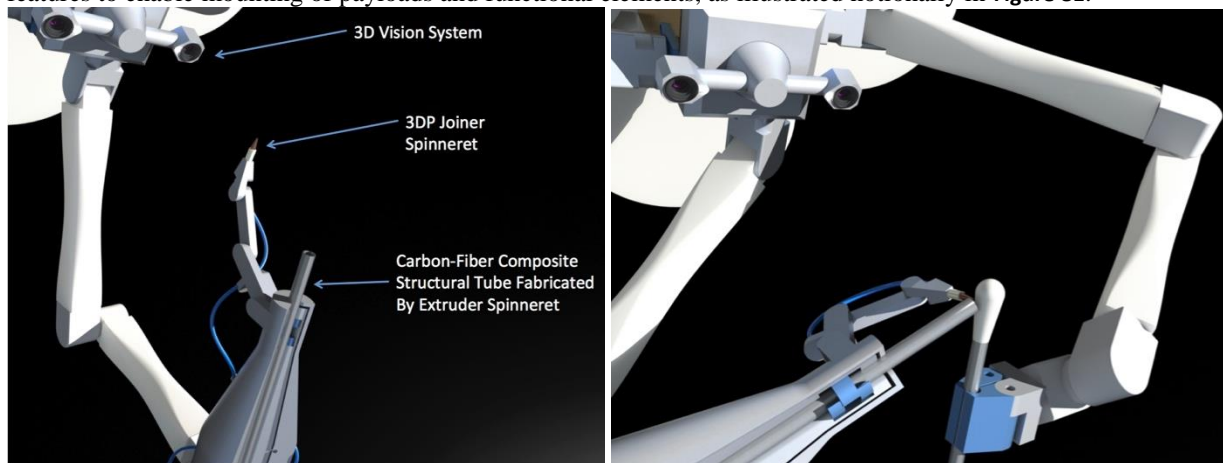


Figure 79. Conceptual Tube-Joining Process Using Fused Filament Fabrication. *The Spinneret uses a FFF head on the joining tool to fashion a joint between the element and the existing structure.*



Figure 80. Prototype 3D-Printed Optimized Joint. *Use of 3D-printing techniques with a highly dexterous print head can enable fabrication of joints optimized for the service loads, maximizing structural efficiency.*



Figure 81. SpiderFab Bot Printing Mounting Feature onto Truss Node. *Mounting interface features can be printed onto the joints after completion of the truss structure, enabling fine-tuning of placement of mirrors or other functional elements.*

D. Thermal Control

Thermoforming and bonding of fiber-reinforced thermoplastics requires control of the temperature of both the material being processed and the structure it is being applied to in order to ensure reliable bonding and minimize stresses and distortions in the structure. This will be a significant challenge in the space environment, as temperatures and thermal gradients can vary dramatically depending upon solar angle and eclipse/sunlit conditions. Terrestrial high-precision FDM 3D printing machines typically house the entire workspace and material processing tools within a

thermally-controlled enclosure to minimize warping of parts due to coefficient of thermal expansion (CTE) behavior. This solution will not be practical for building very large space structures. To address this challenge, we propose to pursue a method combining low-CTE material combinations, surface coatings to minimize temperature variations, and local spot-heating to ensure the temperatures necessary for reliable bonding. To ensure a joint is at the proper temperature to enable reliable fusing of new material to it, we can use spot-heating with IR radiators, lasers, RF heaters, or conductive-contact heaters. **Figure 82** illustrates a concept approach to using an IR laser pre-heating areas onto which the tool will 3D print material, and **Figure 83** shows a photo of an initial test of using a high-power IR laser to spot-heat a section of a 3D-printed joint. The initial testing indicated that this approach is feasible, but further work will be required to develop a reliable and controllable process. An additional method that may be feasible would be for the SpiderFab Bot to use positionable shades (such as the gimbaled solar panel shown in **Figure 70**) and/or reflectors to control insolation conditions within the work volume

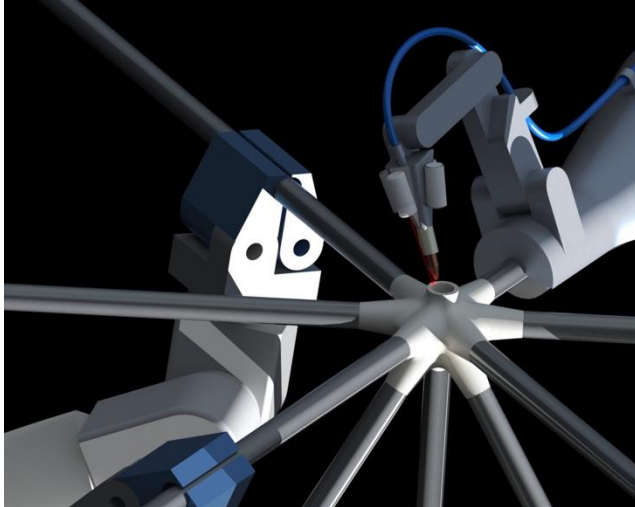


Figure 82. Concept for laser pre-heating of joint material. *Low equilibrium temperatures may necessitate pre-heating of the joint surfaces prior to fusing additional material onto previously printed parts.*

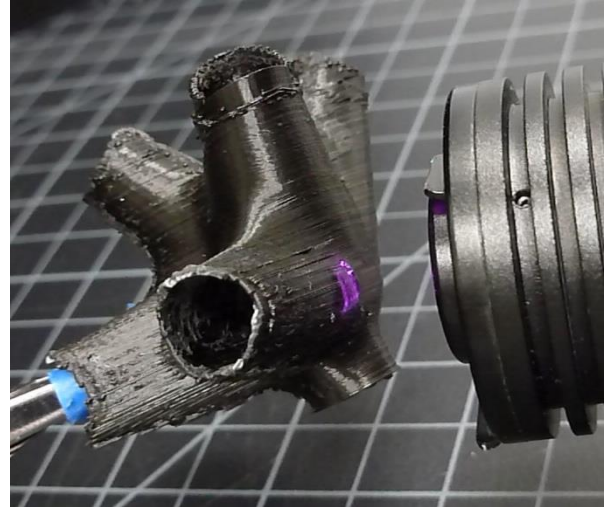


Figure 83. Testing of Plastic Joint Surface Pre-Heating with 700mw IR Laser. *We have experimented with non-contact methods of heating the joint material to bring cold parts into the processable range.*

E. Metrology

On-orbit construction of large space system components in an automated or telerobotic manner will require capabilities for measuring the component as it is built in order to ensure its final form meets the requirements for it to perform its functions. This metrology will be required on both the global scale to measure overall shape quality, for instance to ensure a parabolic antenna dish has the required surface quality, and on the local scale, to enable the fabrication tool to position itself and new components relative to the structure under build. A number of technologies currently in use in the manufacturing and construction industries are applicable to this challenge, including structured light mapping, LIDAR, and imaging photogrammetry. Each has relative advantages and disadvantages. In order to establish the basic feasibility of the required metrology capabilities, we worked with a vendor of a structured light scanner technology, GOM Systems, and performed a test in which we used a GOM scanner to measure the as-built shape of a truss fabricated in the lab with the an early version of our Trusselator mechanism. We then used this as-built data to design and 3D print a notional mounting bracket shaped to mate perfectly with the truss. This exercise was a relatively simplistic demonstration, but establishes a basic proof-of-concept for metrology-based control of the SpiderFab fabrication process.

V. Technology Maturation Plan

In our Phase I NIAC effort, we formulated a concept architecture for on-orbit fabrication and assembly of spacecraft components, identified potential solutions for the key capabilities required, and performed proof-of-concept level testing of these solutions to establish the technical feasibility of the concept. These proof-of-concept demonstrations have matured the SpiderFab concept to TRL-3. Maturing the SpiderFab technology to flight readiness will require developing, integrating, and validating hardware implementations for: material processing to create structural elements; robotic manipulators and software for both fabricator mobility and positioning of structural element; tools and methods for assembling and joining these elements to create the desired structure; metrology tools to ena-

ble closed-loop-control of the build process; and methods for integrating functional elements onto the support structure.

Fortunately, the many potential applications of the SpiderFab architecture make it well suited for an incremental development program, as illustrated in **Figure 84**. In this staged development concept, a currently-funded NASA SBIR effort to develop the Trusselator implementation described in Section I.A.1 and proposed follow-on NIAC SpiderFab efforts will develop key technology components for fabrication of truss elements, assembly of higher-order structures, and integration of functional components such as membranes. In particular, a Phase II NIAC effort will address key risks to the proposed fabrication techniques in the thermal-vacuum environment of space. These NIAC and SBIR efforts will mature the core technologies for SpiderFab to a level at which they will be suitable for NASA's Game Changing Development and Small Spacecraft Technology Programs to demonstrate them on low-cost platforms such as CubeSats and hosted payloads. An initial flight test could demonstrate fabrication of a several-dozen meter long truss from a 6U CubeSat platform, and 1U payloads positioned at both ends of the truss could demonstrate a mission capability requiring a long baseline, such as radio interferometry.



Figure 84. SpiderFab Capability Maturation Plan. *Implementation of the SpiderFab systems is amenable to an incremental development program, with affordable CubeSat and hosted demonstrations building capabilities towards demonstrating construction of large apertures and eventually a fully self-fabricating space system.*

A follow-on mission flown as a secondary payload on an upper stage or other suitable platform could integrate robotic assembly techniques developed by DARPA's Phoenix program to demonstrate fabrication and assembly of a higher-order structure to support a functional membrane. This second mission could demonstrate construction of a large-area spacecraft component, such as a 30x30m reflectarray, as illustrated in **Figure 85**. With these fundamental capabilities matured to high TRL, we can then implement a full "SpiderFab Bot" construction system, integrating additional additive manufacturing techniques for digital printing of circuitry and application of specialized coatings. We will demonstrate this system by fabricating a very large, complex spacecraft component, such as an Arecibo-sized antenna reflector, and integrating it with a host spacecraft to enable applications such as high-bandwidth communications with Mars and asteroid missions. This third demonstration would establish the SpiderFab capability at TRL 7+, readying it for infusion into the critical path of NASA Science and Exploration missions. Moreover, by

accomplishing flight validation of a re-usable space system fabrication *process*, rather than just a space system *product*, this development and demonstration program would enable a wide variety of future missions to be deployed with lower NRE cost and lower technical risk.

VI. Conclusion

The SpiderFab effort has investigated the value proposition and technical feasibility of radically changing the way we build and deploy spacecraft by enabling space systems to fabricate and integrate key components on-orbit. We began by developing an architecture for a SpiderFab system, identifying the key capabilities required to fabricate large spacecraft components on-orbit, and developed two concept implementations of this architecture, one specialized for fabricating support trusses for large solar arrays, and the second a more flexible robotic system capable of fabricating many different spacecraft components, such as antenna reflectors and optical occulter. We then performed several analyses to evaluate the value proposition for on-orbit fabrication of spacecraft components, and in each case we found that the dramatic improvements in structural performance and packing efficiency enabled by on-orbit fabrication can provide order-of-magnitude improvements in key system metrics. To establish the technical feasibility, we identified methods for combining several additive manufacturing technologies with robotic assembly technologies, metrology sensors, and thermal control techniques to provide the capabilities required to implement a SpiderFab system. We performed lab-based, proof-of-concept level testing of these approaches, in each case demonstrating that the proposed solutions are feasible, and establishing the SpiderFab architecture at TRL-3. Further maturation of SpiderFab to mission-readiness is well-suited to an incremental development program. A pair of initial low-cost flight demonstrations can validate key capabilities and establish mission-readiness for modest applications, such as long-baseline interferometry. These affordable small demonstrations will prepare the technology for full-scale demonstration in construction of more ambitious systems, such as an Arecibo-scale antenna reflector. This demonstration mission will unlock the full game-changing potential of the SpiderFab architecture by flight qualifying and validating an on-orbit fabrication and integration *process* that can be re-used many times to reduce the life-cycle cost and increase power, bandwidth, resolution, and sensitivity for a wide range of NASA Science and Exploration missions.

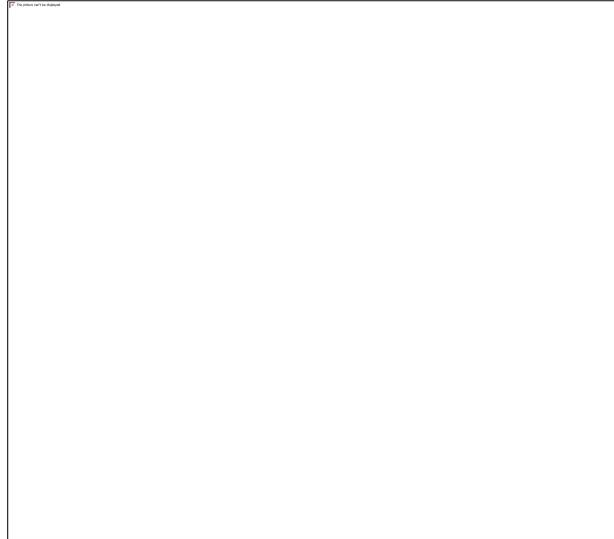


Figure 85. Concept for demonstration of on-orbit construction of a large planar RF aperture. SpiderFab can be validated on affordable secondary payload platforms prior to use in operational missions.

The SpiderFab effort has investigated the value proposition and technical feasibility of radically changing the way we build and deploy spacecraft by enabling space systems to fabricate and integrate key components on-orbit. We began by developing an architecture for a SpiderFab system, identifying the key capabilities required to fabricate large spacecraft components on-orbit, and developed two concept implementations of this architecture, one specialized for fabricating support trusses for large solar arrays, and the second a more flexible robotic system capable of fabricating many different spacecraft components, such as antenna reflectors and optical occulter. We then performed several analyses to evaluate the value proposition for on-orbit fabrication of spacecraft components, and in each case we found that the dramatic improvements in structural performance and packing efficiency enabled by on-orbit fabrication can provide order-of-magnitude improvements in key system metrics. To establish the technical feasibility, we identified methods for combining several additive manufacturing technologies with robotic assembly technologies, metrology sensors, and thermal control techniques to provide the capabilities required to implement a SpiderFab system. We performed lab-based, proof-of-concept level testing of these approaches, in each case demonstrating that the proposed solutions are feasible, and establishing the SpiderFab architecture at TRL-3. Further maturation of SpiderFab to mission-readiness is well-suited to an incremental development program. A pair of initial low-cost flight demonstrations can validate key capabilities and establish mission-readiness for modest applications, such as long-baseline interferometry. These affordable small demonstrations will prepare the technology for full-scale demonstration in construction of more ambitious systems, such as an Arecibo-scale antenna reflector. This demonstration mission will unlock the full game-changing potential of the SpiderFab architecture by flight qualifying and validating an on-orbit fabrication and integration *process* that can be re-used many times to reduce the life-cycle cost and increase power, bandwidth, resolution, and sensitivity for a wide range of NASA Science and Exploration missions.

VII. Acknowledgments

This work was supported by NASA Innovative Advanced Concepts (NIAC) Grant NNX12AR13G.

References

1. Mikulas, M.M., *et al.*, "Truss Performance and Packaging Metrics," NASA Technical Document 20060008916.
2. Murphey, T.W., Hinkle, J.D., "Some Performance Trends in Hierarchical Truss Structures," AIAA-2--3-1903.
3. Cash, W., *et al.*, "Astrophysics Strategic Mission Concept Study: The New Worlds Observer," 24 April 2009.
4. Cash, W., *personal commun.*, 4Feb2013.
5. Data extracted from DARPA/TTO Phoenix Program Industry Day Briefing, 11Feb13.

APPENDIX C

IN-SPACE MANUFACTURING OF CONSTRUCTABLE™ LONG-BASELINE SENSORS USING THE TRUSSELATOR™ TECHNOLOGY

Robert P. Hoyt,⁷ Jeffrey T. Slosad,⁸ Todd J. Moser,⁹ Jesse I. Cushing,³ Greg J. Jimmerson,¹⁰ Rachel L. Muhlbauer,¹¹
Andrew J. Conley,³ Steven R. Alvarado,³ Robert Dyer³
Tethers Unlimited, Inc. Bothell, WA 98011

Under funding from NASA’s SBIR and NIAC programs, TUI has been developing technologies to enable in-space manufacturing of large space system components such as antennas, solar arrays, and optical systems. In this paper, we present recent progress in development and testing of a system for in-situ additive manufacturing and assembly of high performance composite structures, discuss results of testing and analysis of the thermal and space environment survivability of these structures, and describe an affordable nanosatellite-based mission to demonstrate in-space manufacture of a large space structure.

THE mission performance of many space systems is driven by the size of their apertures. The dimensions of the antennas, optics, and arrays used by the satellite determines key performance metrics such as power, sensitivity, bandwidth, and resolution. With current state-of-the-art deployable technologies, these apertures must be designed to fold up and stow within the available launch volume, which for primary payloads is the launch shroud volume, and for secondary payloads is an envelope such as the ESPA secondary payload volume or a P-POD deployer volume. This stowage requirement limits the size and performance of the apertures that space systems can deploy. Under funding from NASA’s Innovative Advanced Concepts (NIAC) and Small Business Innovation Research (SBIR) programs, TUI has been developing capabilities for In-Space Manufacturing (ISM) of key satellite components to enable space programs to escape these volumetric limitations and create space systems with dramatically higher-performance apertures. Under the NIAC “SpiderFab” program, TUI has developed an architecture for ISM of large apertures such as antennas and starshades, and has successfully demonstrated tools and methods to enable automated fabrication and assembly of such large structures using robotic systems.⁶ Under the NASA/LaRC “Trusselator” SBIR, TUI has developed and tested a system that uses additive manufacturing processes to fabricate high-performance composite truss structures.⁷ In this paper, we first summarize recent progress in integrating and testing a Trusselator systems and methods for robotic assembly of truss structures. We will then present results of testing and analysis of composite truss material thermal and space environmental effects (SEE) characteristics, which are key to applicability to many space missions. Finally, we will describe the preliminary design of a CubeSat-based experiment, called MakerSat, that is intended as a low-cost initial demonstration of in-space manufacture of a “Constructable™” long-baseline sensor system.

The SpiderFab architecture envisions ISM of large antennas, solar arrays, and optical systems by using additive manufacturing tools to process raw materials, such as spools of carbon fiber composite, into linear structural elements such as tubes and trusses, and then using robotic manipulators to assemble these structural elements into larger 2D and 3D structures. The same robotic systems will then integrate functional elements, such as reflective meshes, membrane antennas, photovoltaic blankets, and sensor payloads, onto the support structures. Under the Trusselator SBIR effort, TUI has worked to demonstrate the key initial step of this process by developing a system that transforms spools of carbon fiber composite material into high-performance carbon fiber trusses. In the Phase I of the SBIR effort, we built a proof-of-concept prototype, shown in Figure 86, and used it to demonstrate fabrication of

⁷ CEO & Chief Scientist, 11711 N. Creek Pkwy S., D113, Bothell WA 98011, AIAA Member.

⁸ Chief Operating Officer.

⁹ Aerospace Engineer

¹⁰ Chief Engineer

¹¹ Additive Manufacturing and Materials Group Leader

multiple 10+ meter segments of truss. Shown on the right in Figure 86 is a 10 m segment, which had a mass of just 340 grams, and had more than sufficient strength to be self-supporting in 1 gee, as illustrated in Figure 8. We then used these first-order trusses to construct a 2nd-order truss – a truss-of-trusses – shown in Figure 87. This 3-meter long 2nd order truss sample, which has a mass of 540 grams, was assembled manually using an end-effector tool designed for use with a robotic arm, with the intent of identifying the methods and requirements necessary to enable a robotic system to assemble 2nd-order truss structures.



Figure 86. Demonstration of long truss fabrication using Phase I prototype. *The 10m segments had a mass of 340 g, with more than sufficient strength to be self-supporting in 1-g.*



Figure 87. Truss-of-Trusses assembled using truss elements made with the Phase I prototype.



Figure 88. 16m Truss sample, with semi trailer shown for scale.

Currently, we are in the process of integrating and testing an advanced prototype of the Trusselator system. The new prototype is designed to fit within a 3U CubeSat volume in order to enable affordable flight validation of this key ISM technology on a nanosatellite platform. This 3U Trusselator implements an improved truss fabrication process that enables the geometry of the truss to be varied during fabrication. This capability will enable each structural element of a 2nd-order structure to be optimized for the loads and torques it will experience in operation in order to maximize the structural efficiency of the system.

In order to advance the technical maturity of the Trusselator system and evaluate the utility of the truss structures it produces to space system applications, we have performed testing of the 3U Trusselator prototype in a vacuum environment, tested the structural performance of the truss samples fabricated using the older Phase I prototype, measured the coefficient of thermal expansion (CTE) of the materials used by the system, and performed analysis of the effects of atomic oxygen on the service lifetime of these materials.

7. VACUUM TESTING

We integrated the truss forming mechanism and feedstock cartridge subsystem together in a preliminary configuration for initial testing in a vacuum environment, as illustrated in Figure 89. We performed a short test of operation of the prototype in a rough vacuum (~0.5 mTorr), forming one bay of the truss. Figure 90 shows a video frame capture from the testing. For this video, the IR filter was removed from the camera lens to allow for better imaging of the thermal behavior of the prototype. This initial testing was intended to identify any critical problems and scope the need for active cooling within the system. No significant challenges were observed in the test, and the system worked well without active cooling. However, without active cooling the system has a slower than desired production rate, so we are continuing to investigate active cooling approaches primarily to optimize production rate.

In this vacuum test, the prototype drew an average of 103 W during operation, with peak draw of 310W. A total of 117 kJ was required to produce one 5.5 cm long bay of the truss.

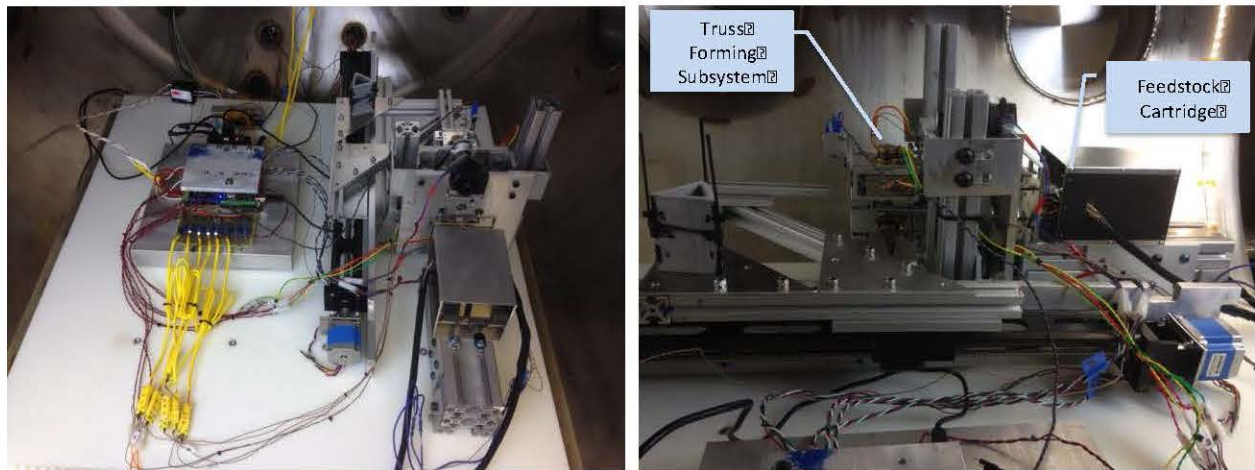


Figure 89. Trusselator Vacuum Test Setup.



Figure 90. Vacuum testing of the Trusselator Prototype.

8. TRUSS STIFFNESS TESTING

To evaluate the potential structural performance of the truss, we tested samples produced by the Phase I prototype to determine bending stiffness, and compared them to existing deployable truss technologies using a metric that compensates for the effects of differing diameters and different linear masses of each truss.

We tested the bending stiffness of our truss sample using the setup shown in Figure 91. The length of the cantilevered truss segment was 0.5842 m, and a load of 1.96 N was applied. The Moment of Inertia of the truss, calculated using a CAD model, was 9279 mm⁴. The applied load resulted in a deflection of 0.3 mm. This measurement indicates a bending stiffness of 434 Nm².

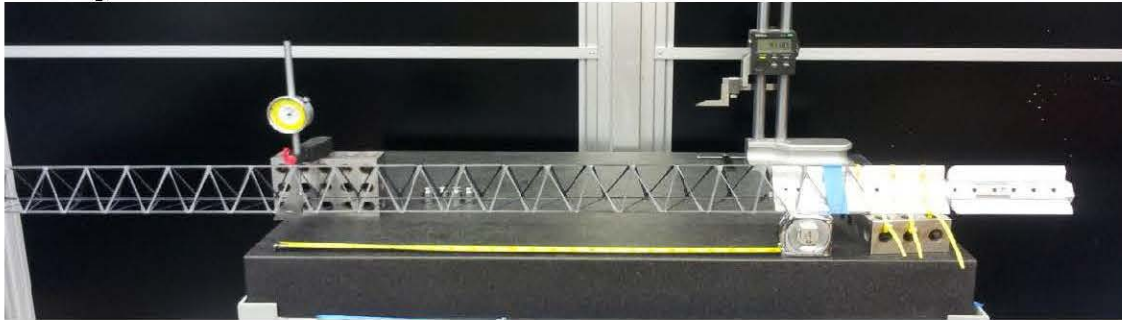


Figure 91. Bending Stiffness Test Setup.

To enable comparison of this result to other truss designs, we normalized the bending stiffness EI by the linear mass and Diameter² for this truss and a number of deployable truss technologies that have flown previously, including the FastMast used on the ISS, the SRTM mast flown on the Shuttle, and the Northrop Grumman AstoMast. This metric expresses the efficiency with which the truss extracts bending stiffness out of a given amount of mass and given diameter. Figure 92 plots the values of this metric for the truss samples and the SOA deployables. *The Phase I Trusselator samples achieved better ‘bending stiffness efficiency’ than all of the previously flown deployable mast technologies.* We anticipate that the improved truss geometry enabled by the revised mechanism design implemented in the 3U Trusselator will provide further increases in truss efficiency.

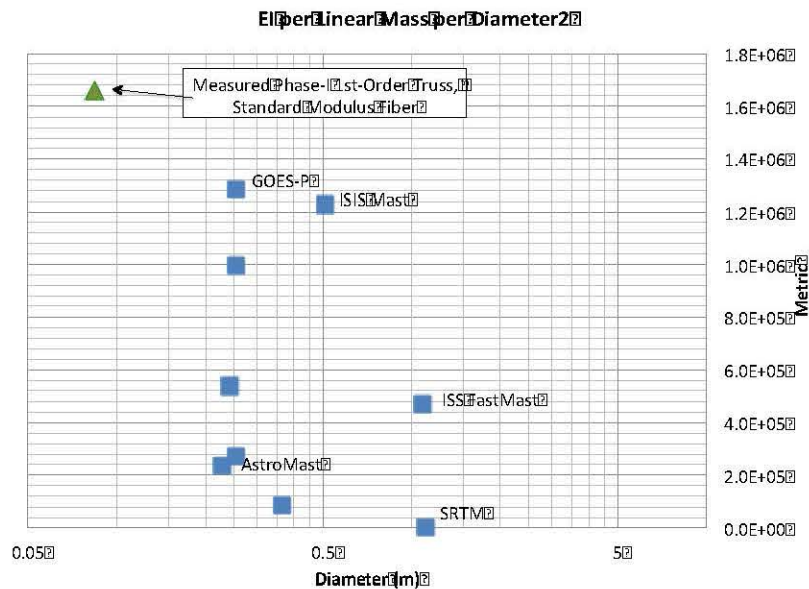


Figure 92. “Bending Stiffness Efficiency” for the Trusselator Samples and SOA Deployables.

9. CTE TESTING OF TRUSS MATERIALS

Because the truss will experience thermal events during which rapid heating and cooling may occur, it is important to understand the thermal expansion characteristics of the truss materials in order to engineer around any deflection, bending, or degradation which may occur as a result. The thermal behavior of the truss structure is dependent upon the geometry of the truss as well as the materials used to form the truss. The four different truss materials being considered for the Trusselator design were cut into 2 cm long sections and polished to a flattened edge, as shown in Figure 14. Figure 14A shows the cross-section of the V-log, the main component of the longerons, which

is made of a PEEK matrix with continuous AS4 carbon fibers. Figure 14B shows the cross-section of a rod made with the same materials system. The composites shown in figures 14C and 14D are made by Plasticomp and use a PEEK matrix with carbon fibers T800 (Toray) and HM63 (Hexcel), respectively.

Using dilatometry, the coefficient of thermal expansion (CTE) was measured for the four different truss composites from the range of room temperature to 300°C (300 K to 573 K). A positive CTE denotes material expansion is occurring while a negative CTE describes material contraction. The CTE upon heating is shown in Figure 15 which plots CTE (E-6/K) vs. temperature (K). The CTE of the V-Log composite is slightly positive across the temperature range showing only a slight increase in CTE as temperature increases. The rod composite made of the same materials, however, has a negative but increasing CTE for the entire range of temperatures. The rods made with the T800 carbon fiber and the HM63 carbon fiber both show a relaxation type curve shape between 400 and 450 K before which the CTE is decreasing and after which the CTE is increasing. This temperature range holds the glass transition temperature of PEEK.

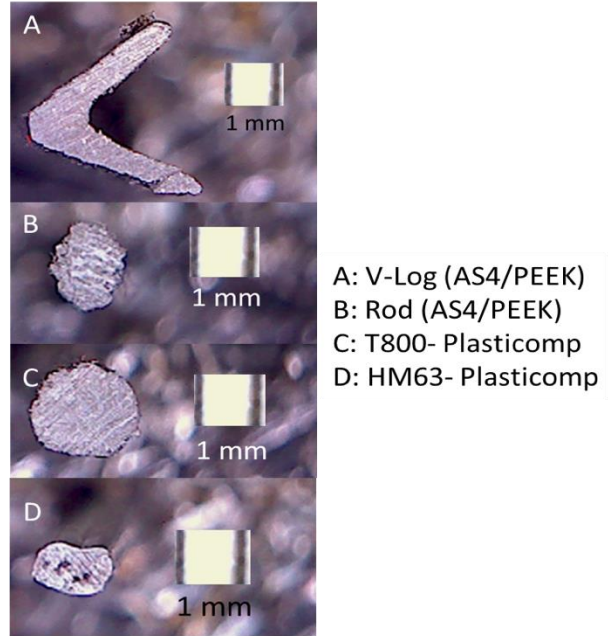


Figure 93. Cross-sections of truss composites being evaluated for the Trusselator design.

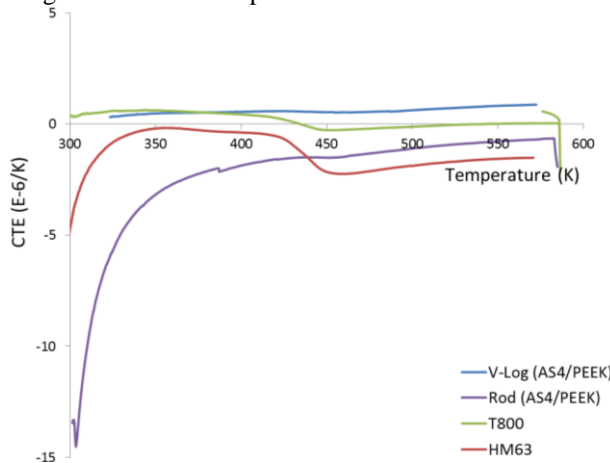


Figure 15. CTE vs. Temperature for the four different truss composites.

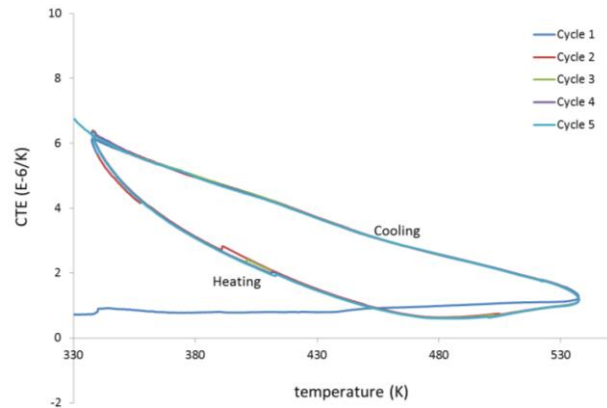


Figure 16. CTE vs. Temperature for the four different truss composites.

Since the V-log composite will be the backbone of the truss structure, its CTE was tracked over 5 thermal cycles (75°C to 250°C), as shown in Figure 16. The behavior of the cooling/heating curves is constant after the initial heating event is over. All subsequent cooling and heating cycles do not cause the material to change. This data suggests that the first heating event will be the most impactful on the properties of the truss, after which it will reach a steady state behavior. Further cyclic thermal testing is planned at a lower temperature range (75°C to 150°C) to better assess the behavior of the truss material in space conditions within the limits of the dilatometer.

10. ATOMIC OXYGEN SERVICE LIFE LIMIT ANALYSIS

In order to help guide the applications of the PEEK/CF materials currently being used with the Trusselator, we calculated service life estimates for unshielded PEEK/CF structures. For LEO missions, flight experiments have shown that atomic oxygen (AO) erosion dominates the surface material degradation for polymer composites, so that is the only factor considered in the lifetime estimates graphed below. We can augment this later with analyses of MMOD, UV, Thermal Cycling, and radiation damage. As we did not find references in the public literature for AO reaction efficiency measurement for CF/PEEK composites, we estimate, based on available data for graphite, plain

PEEK, and other CF composites (from LDEF and MISSE reports), the erosion rate for CF/PEEK will be approximately 2×10^{-24} cm³/atom. We defined a service life limit of 20% mass loss, and estimated AO flux as a function of orbit altitude using the MSISE-90. Figure 94 plots the predicted service life as a function of truss structural member thickness and operational altitude.

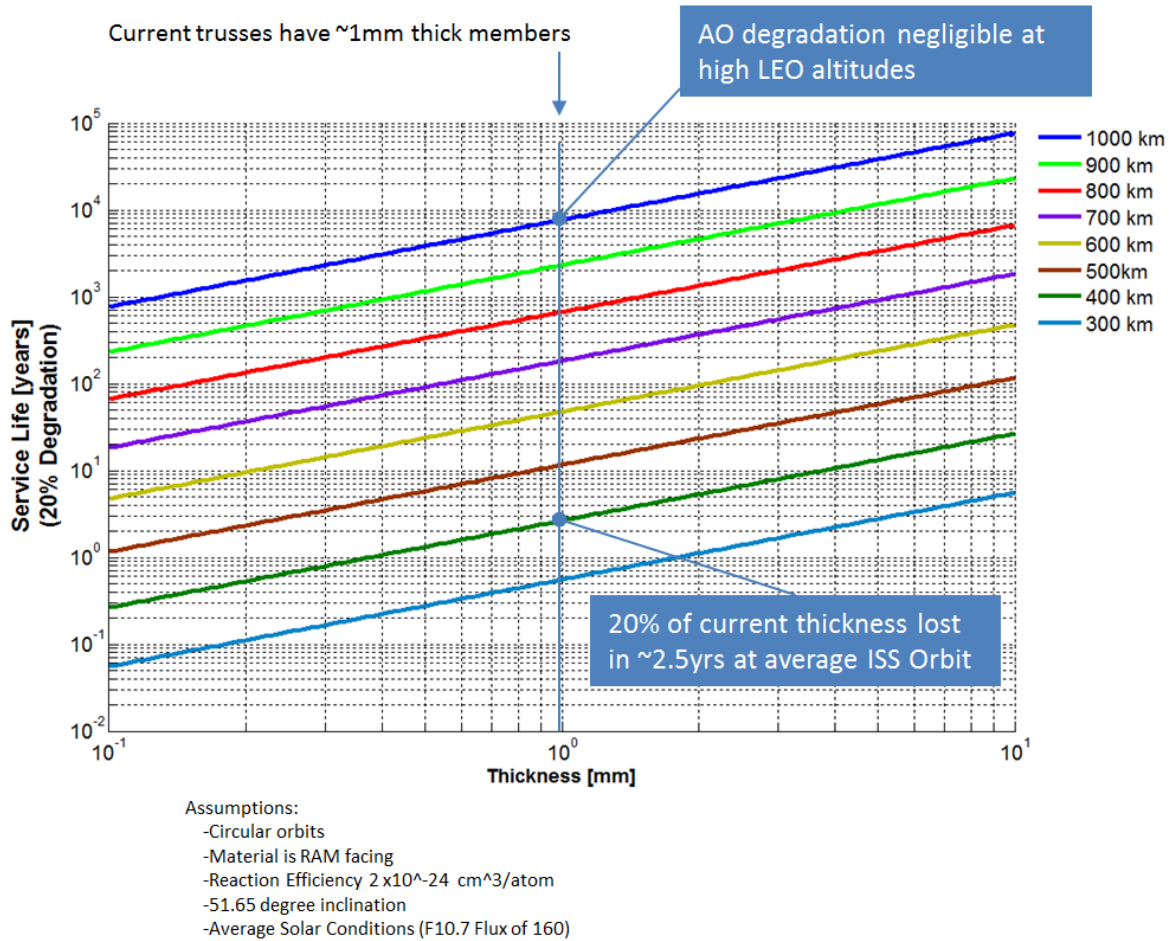


Figure 94. Lifetime Analysis in the LEO Atomic Oxygen Environment.

The results suggest that some mitigation would likely be needed for low LEO missions lasting more than 24 months. This mitigation could be a resistant shield of silica or TiO₂, or simply using thicker truss members. However, the AO erosion rate is likely to be tolerable for unshielded CF/PEEK in some ~1yr low LEO missions, and should not be a significant issue for missions at altitude in high LEO and above.

The SpiderFab architecture for in-space manufacture of large space system components, such as 10+m antenna apertures and multi-MW solar arrays, involves the use of robotic systems to first assemble multiple 1st-order truss elements fabricated by the Trusselator to form larger 2D and 3D structures, and then to integrate functional elements such as photovoltaic blankets and reflective membranes onto the support structure. Doing so in the space environment will require highly autonomous control of the robotic systems used to assemble the structure. In order to demonstrate the feasibility of such autonomous assembly processes, TUI acquired a research-model Baxter Robot from Rethink Robotics, and has used it as a platform for development and testing of robotic end effectors and vision-based algorithms for closed-loop control of robotic assembly of truss structures. Figure 95 shows a sequence of stills from a demonstration of the closed loop control, in which the robot successfully located the truss using feature matching algorithms, positioned a gripper precisely, and then captured and manipulated the truss.

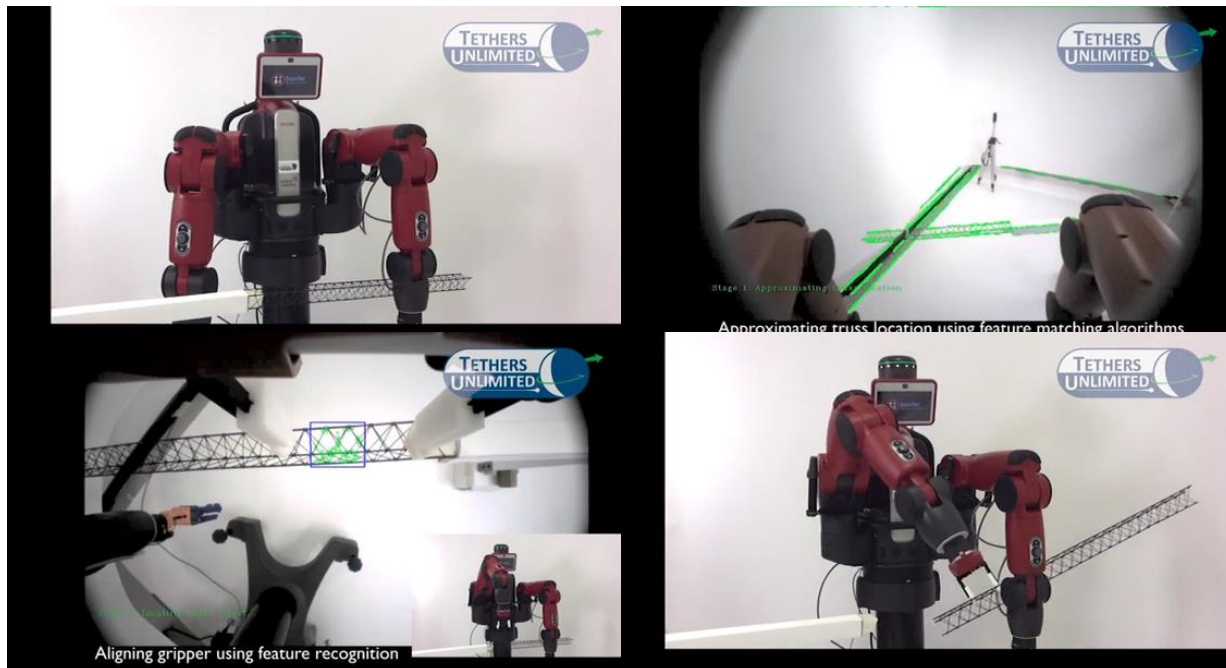


Figure 95. Video capture sequence from a demonstration of closed-loop control of robotic truss manipulation using real-time video processing algorithms.

In order to perform a low-cost initial demonstration of the value proposition of in-space manufacture of space structures, TUI is currently designing a CubeSat-based flight demonstration, called MakerSat-I. The primary objectives of MakerSat-I are to demonstrate ISM of a large space structure, characterize its structural performance, and demonstrate the utility of a Constructable structure as part of a long-baseline sensor system.

The preliminary configuration concept for MakerSat-I, shown in Figure 59, is configured as a 6Ux1U CubeSat for compatibility with the NanoRacks deployer aboard the ISS; a 2Ux3U configuration compatible with the CSD and other 6U deployers is also feasible. The MakerSat-I system will integrate our 3U Trusselator system with COTS CubeSat command and data handling (C&DH) and electrical power system (EPS) as well as a HYDROS water-electrolysis thruster and two SWIFT-XTS X-band software defined radios (SDRs), one positioned at and end of the truss system. An optical fiber dispenser derived from TUI's Underwater Optical Fiber Dispenser will also be integrated into the system, and highly sensitive accelerometers will be integrated at both ends of the system.

In the baseline MakerSat-I mission concept, after deployment from the ISS, the system will first deploy its solar panels and antennas. After a delay sufficient to ensure safe separation from the ISS, the satellite will use its HYDROS thruster to move to its desired operational orbit. The system will then activate the Trusselator system, which will additively manufacture a 50m truss. To provide a sense of the scale involved, Figure 60 shows the 50m truss juxtaposed with the SpaceX Dragon capsule. As the system fabricates the truss, the fiber dispenser will deploy the fiber inside the truss, running from one end of the truss to the other in order to provide high-bandwidth data transfer and sub-ns synchronization between the two SDRs. This timing synchronization will enable the SWIFT-SDRs to operate coherently and provide for phase alignment between the radios. As the system manufactures truss, the truss integrity will be diagnosed by forcing vibrations into the system using thrust impulses provided by the HYDROS thruster and/or small vibratory motors, such as those used in cell phones, and recording the response of the truss structure using the accelerometers positioned at both ends of the system.

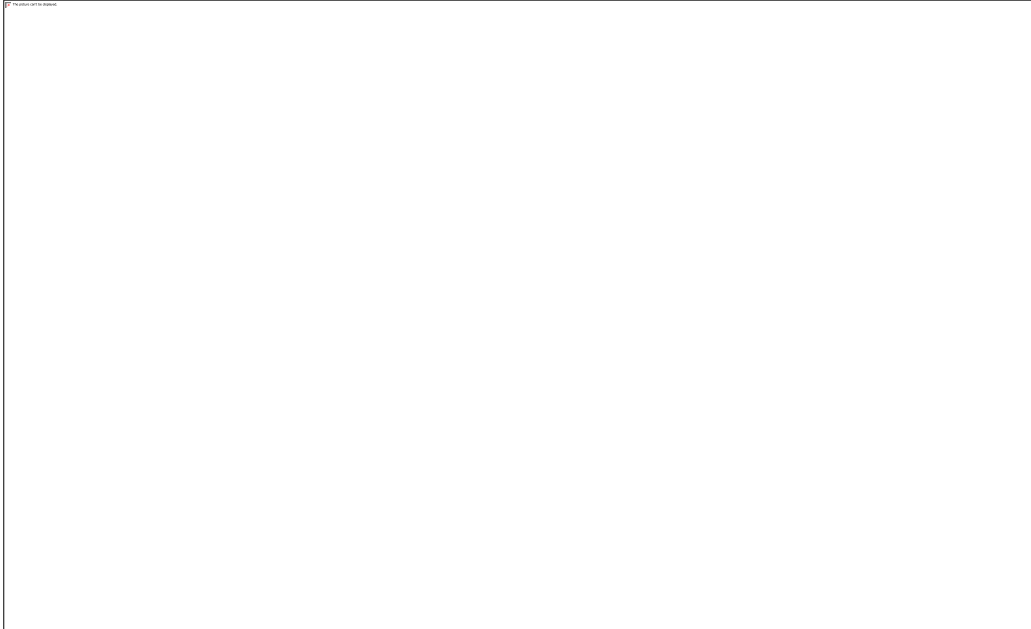


Figure 96. MakerSat-I concept 6U configuration. *The 6U MakerSat-I CubeSat will use a 3U Trusselator system to fabricate a 50m truss in between two X-band software defined radios to demonstrate long-baseline one-pass Interferometric SAR capabilities.*

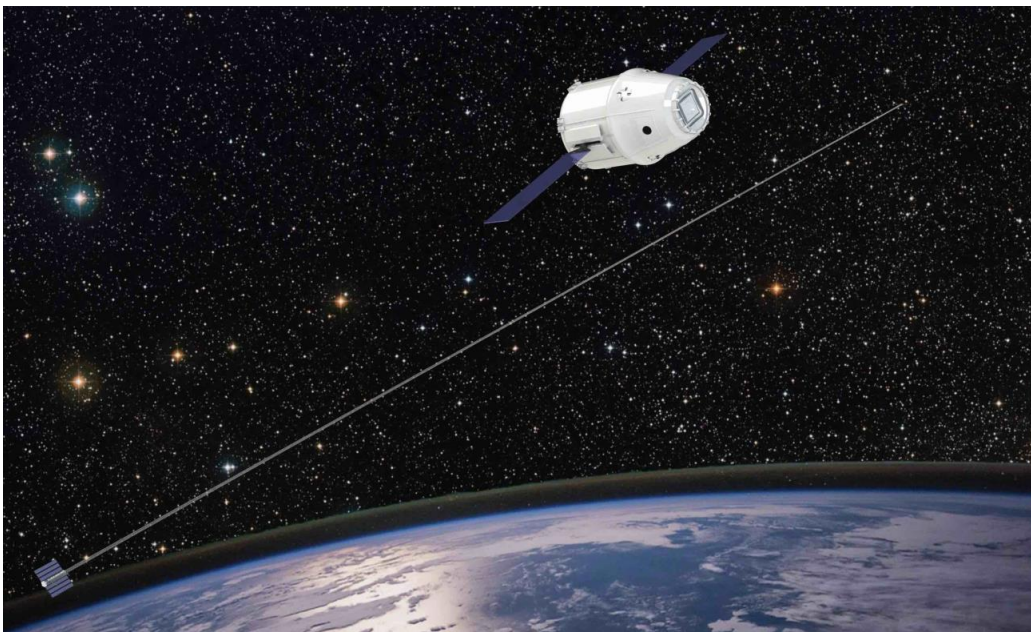


Figure 97. MakerSat-1 “Constructable™” Long-Baseline Sensor. *Dragon capsule shown to provide a sense of scale.*

To demonstrate the utility and value proposition of this Constructable structure, the MakerSat-I mission will then operate the two X-band SDRs as an interferometric synthetic aperture radar (InSAR) or as a long-baseline astronomical interferometer. For InSAR demonstrations, the MakerSat-I system will operate parasitically, relying upon radar transmissions by a much larger satellite. As the truss deploys, gravity gradient forces will tend to orient the system along the local vertical, but off-vertical orientations can be achieved to improve InSAR performance by using the HYDROS thruster to set the system into a cross-plane libration.

The potential performance of this small, low-cost InSAR system can be estimated using the expression for the sensitivity of InSAR height measurements to phase errors:⁸

$$|\partial h| \approx \frac{\lambda R \cos \psi}{4\pi B \sin(\psi + \beta)} |\partial \phi|, \quad (1)$$

where λ is the RF wavelength, ψ is the angle between the local horizontal and the target, β is the angle between the baseline and the local horizontal, B is the baseline length between the receivers, and $\partial \phi$ is the phase measurement error between the receivers. The SWIFT-XTS SDRs are designed to enable coherent operation, and testing under prior efforts has indicated that phase coherency within at least 10 degrees, and potentially as low as 1 degree, is possible. With a baseline length of 50 meters, an operating frequency of 9 GHz, an altitude of 300 km, the truss oriented 45 degrees away from vertical in the cross-plane direction, and a look angle of 45 degrees, we expect the MakerSat-I CubeSat could achieve measurement height accuracy comparable to the 6m demonstrated by the (\$200M+) SRTM experiment flown on the Shuttle *Endeavor* in 2000, and potentially as low as 1 m in a best-case scenario.

The NIAC and NASA SBIR funded SpiderFab and Trusselator efforts have investigated the feasibility of in-space manufacturing to create key components that determine the performance of space systems, including long-baseline sensors and antenna apertures. Development and testing of the Trusselator prototypes has demonstrated a capability for *in-situ* fabrication of very high performance carbon fiber composite trusses. Testing and analysis of these trusses indicate strong potential for providing the low-CTE performance and SEE-survivability required for many long-baseline and aperture applications. Preliminary testing with a commercial robotics platform has demonstrated the feasibility of closed-loop control to enable autonomous assembly of truss structures. Although substantial further research and development is required to fully implement a capability for in-space manufacture of large space systems, we have identified and begun to design an affordable CubeSat-based mission that will validate the feasibility fabricating large structures on-orbit, as well as demonstrate the value proposition of the ISM approach by using this Constructable Truss to perform InSAR sensing at a cost nearly two orders of magnitude lower than prior systems.

Acknowledgements

The effort was funded by a Phase II NASA/LaRC SBIR contract titled “Trusselator”, number NNX13CL35P as well as by a NIAC Phase II Grant titled “SpiderFab”, number NNX13AR26G.

6. Hoyt, R.P., “SpiderFab: An Architecture for Self-Fabricating Space Systems,” AIAA Paper 2013-5509, [AIAA SPACE 2013 Conference and Exposition](#), Pasadena CA, Sept. 2013.
7. Hoyt, R.P., Cushing, J.I., Slostad, J.T., Jimmerson, G.J., “TRUSSELATOR: On-Orbit Fabrication of High-Performance Composite Truss Structures,” AIAA Paper 2014-4337, AIAA Space 2014 Conference and Exposition, San Diego CA, Aug. 2014.
8. Richards, M.A., “A Beginner’s Guide to Interferometric SAR Concepts and Signal Processing”, IEEE A&E Systems Magazine, Vol. 22, No. 9 September 2007



APPENDIX D SPIDERFAB PRESENTATION